Landform-regolith patterns of Northwestern Africa: Deciphering Cenozoic surface dynamics of the tropical cratonic geosystem

Dominique Chardon

Earth-Science Reviews 242 (2023) 104452

Contents lists available at ScienceDirect

Earth-Science Reviews

journal homepage: www.elsevier.com/locate/earscirev

Landform-regolith patterns of Northwestern Africa: Deciphering Cenozoic surface dynamics of the tropical cratonic geosystem

Dominique Chardon *

GET, IRD, Université de Toulouse, CNRS, UPS, CNES, Toulouse, France

ARTICLE INFO

Keywords:
Laterite
Catena
Pediment
Glacis
Pediplain
Etchplain
Landform evolution processes
Epeirogeny

ABSTRACT

The tropical cratonic geosystem encompasses non-orogenic continental domains of the tropical belt that developed and preserved Cenozoic lateritic regolith mantles (i.e., the products of intense rock weathering). These domains represent a significant part of the continental landsurface contributing to regulate global biogeochemical cycles. Here I address the surface evolution mechanisms of the tropical cratonic geosystem based on a comprehensive review and an original map of the landform-regolith associations (combinations of reliefs and regolith mantles of specific nature and age) of Northwestern Africa, an archetype of the tropical cratonic geosystem. The landform-regolith pattern is a composite record of long-term climate variability modulated by the composition of the bedrock. Relictual, pan-tropical associations attest to (i) very intense, greenhouse-driven weathering starting in the Late Cretaceous and culminating at the Early Eocene thermal maximum, (ii) intense Late Oligocene weathering driven by seasonally humid climate, (iii) dry erosional climate during the Early and Late Miocene, with a return to moderate weathering-prone, seasonally dry climate around the Miocene climatic optimum (18–11 Ma) and at the End-Miocene (7–6 Ma). Post Miocene functional landform-regolith associations are latitudinally zoned, reflecting installation of the modern climatic zonation in the tropics. Modern regional susceptibility to erosion has to be partitioned among the functional landform-regolith associations, which tend towards pedoclimatic equilibrium, and relict associations, which are mostly fossil. Moreover, results show that (i) past etchplains and pediplains ("paleo-surfaces") are unreliable topographic gauges of mantle-driven deformation, (ii) staircase patterns of successive etchplains or pediplains attributed to positive epeirogenic pulses are invalid and (iii) low-temperature thermochronology fails to document final rock exhumation paths in cratonic contexts.

1. Introduction

Large portions of the non-orogenic continental surface in the tropical belt are blanketed by lateritic regolith i.e., an unconsolidated or secondarily indurated cover that derives from intense weathering of the fresh bedrock enhanced by high tropical rainfalls and temperatures. Such mantles, also called weathering profiles, are typical of the cratons, shields or platform of Africa, South America, India and Australia. Lateritic regolith mantles underlay the tropical and equatorial ecosystems, among which the rainforests. They set the nature and distribution of soils and host considerable groundwater resources. They prevent access to the bedrock and its mineral resources but may also concentrate ore deposits. They are enriched in metals and their excavation and storage generate environmental hazards. Understanding the nature, distribution and history of lateritic regolith covers has therefore important implications for sustainable development challenges (e.g., Thomas, 1988).

Given the strong mutual interactions among slope processes, groundwater flow and lateritic weathering that concur to generate and regulate regolith mantles, tropical landforms and their underlying regolith are intimately linked. They may therefore be conveniently described and mapped using the landform-regolith association concept developed for economic geology purposes (e.g., Pain, 2008). Shield regions are by definition not submitted to tectonic deformation but to slow and limited long-wavelength vertical deformation (epeirogeny) and, conversely, to limited erosion. In the tropical belt, this allowed for the preservation of landform-regolith associations dating back to at least the Early Cenozoic, which coexist with younger and functional associations. Given the specificity of both the geodynamic setting and tropical morphoclimatic context of shield terrains of the southern continents, the

* Corresponding author.
E-mail address: Dominique.chardon@ird.fr.

https://doi.org/10.1016/j.earscirev.2023.104452
Received 8 February 2023; Received in revised form 10 April 2023; Accepted 13 May 2023
Available online 18 May 2023

concept of tropical cratonic geosystem is here introduced.

Relict lateritic landform-regolith associations constitute archives of past landscapes and weathering periods of the tropical cratonic geosystem. Weathering loosens fresh bedrock to produce clayey sediments (i.e., regolith) and leaches elements that are exported via groundwater flow to rivers. Thus, regolith mantles are significant sediment reservoirs available to erosion (Fairbridge and Finkl, 1980; Millot, 1983). The spatial distribution of dated landform-regolith associations may therefore be exploited to characterize paleogeographies and erosion processes over large drainages feeding continental margin basins with clastic sediments and the world ocean with solute erosion products (e.g., Beauvais and Chardon, 2013; Grimaud et al., 2015, 2018). Dilation of the intertropical zone during greenhouse climatic periods of the Phanerozoic also produced lateritic regolith mantles over high-latitude continental platforms (e.g., Bárdossy and Aleva, 1990; Retallack, 2010). The last of these periods even led to the concept of Early Cenozoic "tropicoid paleoearth" (Büdel, 1982). Tropical weathering also consumes CO_2, especially during such periods, so that regolith and soil mantles constitute carbon sinks over geological timescales. Finally, generations of landform-regolith associations set the boundary conditions to the environments that permitted the great diversification of tropical terrestrial flora and fauna during the Cenozoic (e.g., Couvreur et al., 2021), and specifically hominids in Africa (e.g., deMenocal, 2004; see also, for instance, Lihoreau et al., 2021).

Continental-scale map integration of landform-regolith systematics should be useful to interpret surface dynamics of the tropical cratonic geosystem as a component of the evolving earth system. More specifically, such an integration should provide clues on (i) the current state of the non-orogenic continental tropical surfaces, how they evolved through geological time and what may be their susceptibility to global change, (ii) whether and how climate, epeirogeny or other geological factors influenced the production and preservation of landform-regolith associations and (iii) whether current approaches to the long-term evolution of non-orogenic (tropical) continental surfaces need refining.

Here I characterize and interpret the nature, distribution and history of the landform-regolith associations at the scale of Northwestern Africa, a region with the best documented extensive lateritic regolith cover in the world. This contribution builds on the production of original landform-regolith chart and map and a comprehensive integration of the available documentation. To be representative of the tropical cratonic

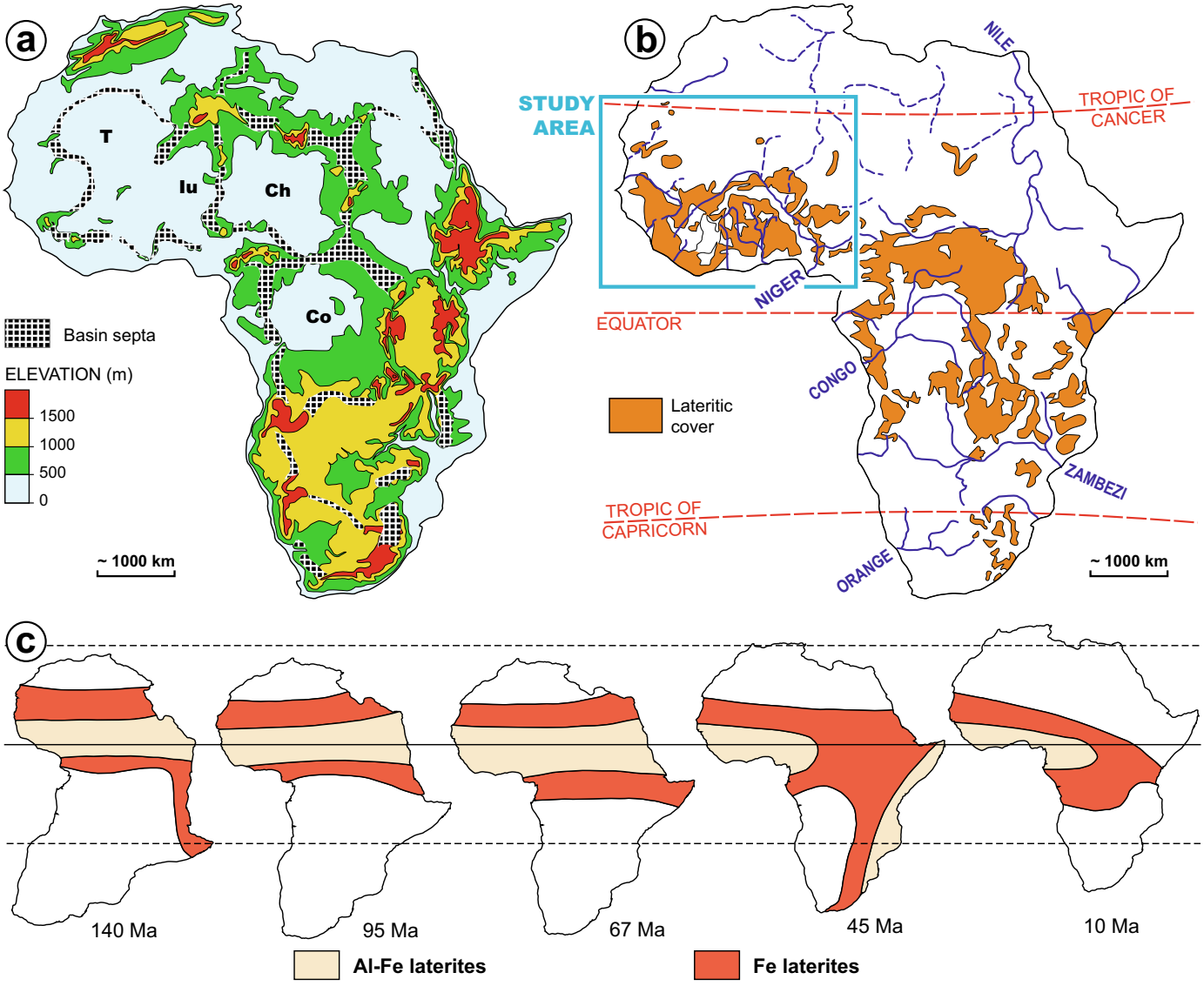

Fig. 1. (a) Topography of Africa showing continental scale basin-and-swell relief pattern. Ch: Chad basin; Co: Congo basin; Iu: Iullemmeden basin; T: Taoudenni basin (Modified after Chardon et al., 2016). (b) African lateritic cover (Al- and Fe-duricrusts and their reworked products i.e., lateritic gravels) showing the main river systems (simplified after Beauvais, 1991). (c) Evolving position of Africa relative to the equator and the tropics and potential lateritic weathering zonation from the Early Cretaceous to the Late Miocene (after Tardy and Roquin, 1998; Vrielynck and Bouysse, 2003).

geosystem, the size of the map area is large (~2800 × 1800 km), in order to encompass the climatic zonation of the inner tropical belt as well as several continental-scale drainage basins and large-scale topographic features, and a diversity of geological substrates (Fig. 1a and b). This work has first-order implications on how the tropical cratonic geosystem responded to, and kept record of, long-term global climate change and latitudinal climatic zonation as a function of bedrock lithologies. The results further call for a methodological reappraisal of long-term surface evolution of shields by showing, for instance, that mantle-driven epeirogenic deformation models of the African topography are over-simplified and that "paleo-landsurfaces" (i.e., ancient landform-regolith associations of continental extent) are biased epeirogenic gauges. Finally, it is shown that low-temperature thermochronology fails to document final rock exhumation paths in cratonic contexts.

2. Geological and geomorphic background

2.1. Morpho-climatic and geological context

The study area belongs to "low Africa", defined by contrast with "high Africa" forming the eastern and southern part of the continent (Doucouré and de Wit, 2003; Fig. 1a). The mapping area covers the continental ground south of 24°N and west of 12°E (Fig. 2) and encompasses, from South to North, the forest, Guinean, Soudanian, Sahelian and Saharan vegetation/climatic zones, which roughly mimic the current rainfall pattern (Fig. 3). The topography consists of plainlands of very-low regional slope (<1.5 ‰), rarely exceeding 400 m in elevation, and studded with high plains, dissected plateaux and cuestas (Fig. 2). The main regional topographic massifs do not exceed 1500 m a.s.l., except the Cameroon Rise, where Cenozoic volcanic reliefs of the Cameroon volcanic line culminate between ~2000 and 3000 m a.s.l. and the Hoggar massif, culminating in the Attakor mountain, where ~1000 m thick Cenozoic volcanic traps are studded with volcanic edifices that attain 2918 m a.s.l. (Figs. 2 and 4). The Guinean Rise, (divided here in two: Fouta Djalon and Southeastern Guinean Rise) is prolonged to the NE by the Mandingue plateau. Together with the Banfora and Bandiagara plateaus, these massifs constitute the High Niger River watershed region (Fig. 2). High plains, dissected plateaus and cuestas are mostly controlled by tabular sandstones and siltstones of the cratonic cover (Fouta Djalon, Mandingue and Banfora-Bandiagara plateaus, Tagant, Adrar, Tanezrouft, Iullemmeden basin, Southern Volta basin) and areas of Jurassic dolerite sill clusters or Cenozoic volcanics (Southeastern

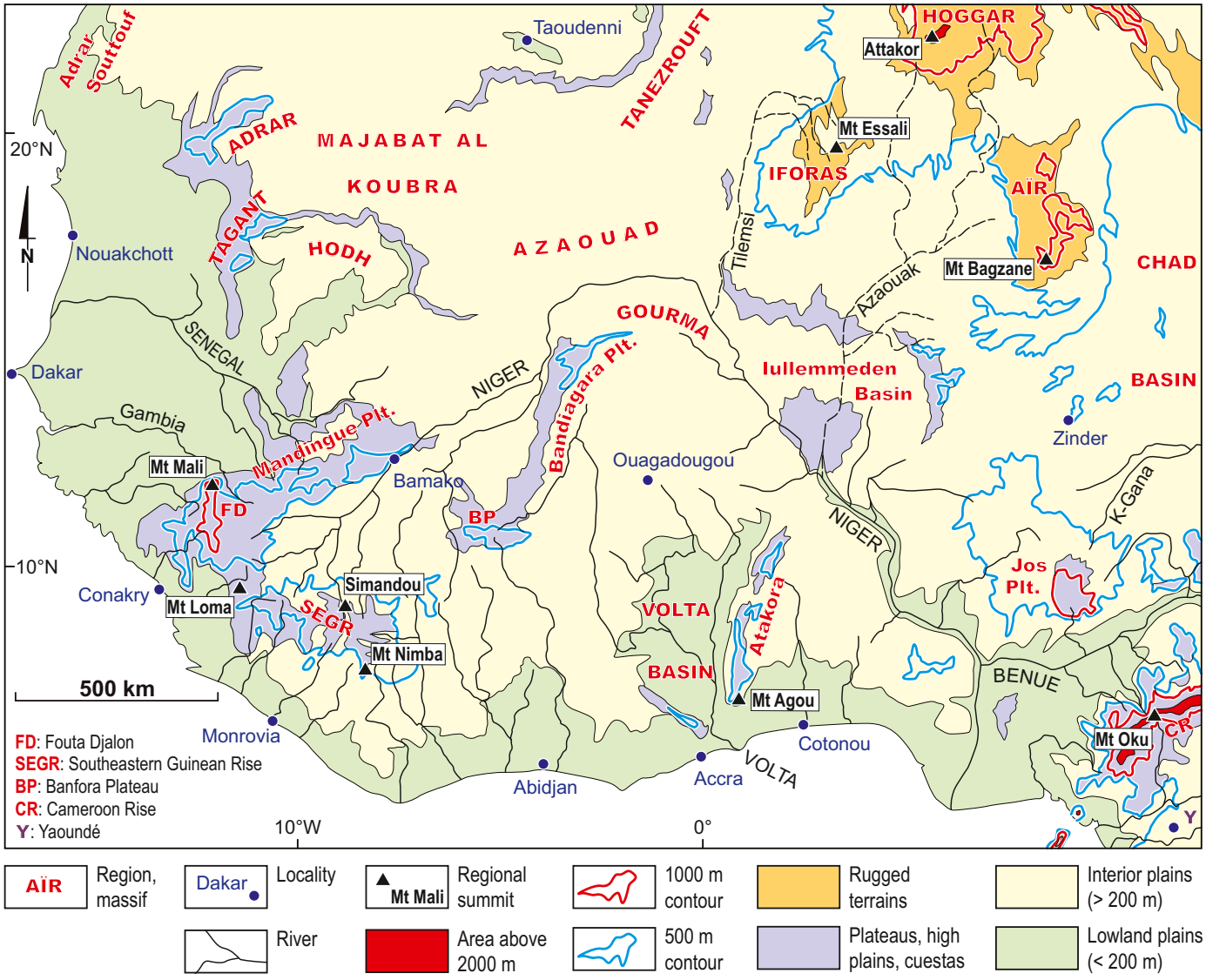

Fig. 2. Main physiographic elements of Northwestern Africa. Elevation of summits (a.s.l.): Attakor (Mount Tahat): 2918 m; Mount Agou: 986 m; Mount Bagzane: 2022 m; Mount Essali: 890 m; Mount Loma: 1948 m; Mount Mali: 1515 m; Mount Nimba: 1752 m; Mount Oku: 3011 m; Simandou: 1658 m.

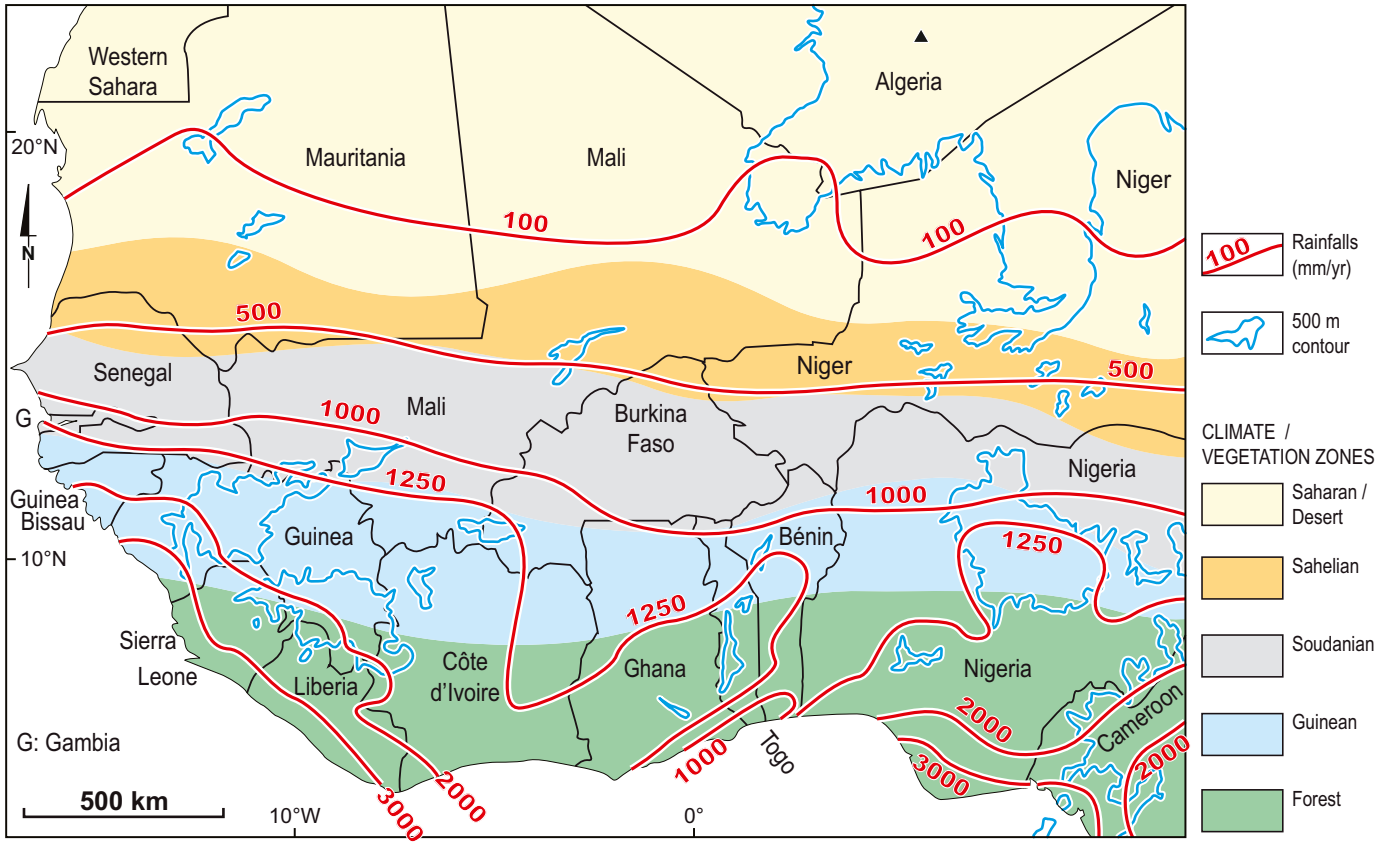

Fig. 3. Climate / vegetation zones and rainfall pattern of Northwestern Africa. International borders and country names are in black. Savannas typically encompass the Guinean and Soudanian zones.

Guinean Rise, high Senegal drainage, Jos Plateau, Cameroon Rise; Figs. 2 and 4). An exception is the Atakora range, which is armed by steeply folded Neoproterozoic quartzites (Figs. 2 and 4).

Neoproterozoic and Phanerozoic platform cover occupies nearly two third of the map area (Fig. 4). That cover is compartmentalized among the Taoudenni and Iullemmeden intracratonic basins (Figs. 1a and 4). The Senegalo-Mauritanian basin is an onshore extension of the Central Atlantic Ocean divergent margin, whereas the Benue through and adjoining Bida basin are aborted extensions of the Cretaceous rift system that led to the opening of the Equatorial Atlantic Ocean. Narrow Meso-Cenozoic sedimentary embayements are preserved along the coast between Conakry and Yaoundé (Fig. 4). The crystalline basement of the West African craton crops out in the Leo-Man shield, in the South and in the Reguibat shield, in the North (Fig. 4). The Tuareg shield is a large outcrop of Panafrican basement forming the Hoggar massif and its two digitations i.e., the Iforas and Aïr massifs (Figs. 2 and 4). Panafrican basement is also exposed in the Benino-Nigerian shield and is reworked in the Mauritanides belt (Fig. 4).

2.2. *The West African morpho-climatic sequence: definition and age constraints*

A unique specificity of sub-Saharan West Africa is the preservation of five successive benchmark duricrust-capped type landforms i.e., the West African morphoclimatic sequence, whose relicts are widely and densely distributed (Michel, 1973a; Gunnell, 2003; Burke and Gunnell, 2008; Beauvais and Chardon, 2013). The present work reveals a more complex map pattern than just an assemblage of these landform-regolith associations. However, the West African morphoclimatic sequence has provided a reference frame for defining a majority of the map units, which somehow derive from the benchmark landform-regolith associations or the combination or degradation thereof. The West African morphoclimatic sequence is therefore summarized below (Fig. 5).

Bauxitic duricrusts cap most reliefs of sub-Saharan West Africa, defining a regional topographic envelop for the region (Egbogah, 1975; Boulangé and Millot, 1988; Grimaud et al., 2014, 2018; Chardon et al., 2016). They seal an ancient mantled etchplain i.e., a low relief landsurface of continental extent underlain by a very thick (>80 m) weathering profile (Thomas, 1989a), which has now been partly eroded. That etchplain was ascribed by Boulangé (1984), Boulangé and Millot (1988) and Valeton (1991) to the African Surface, originally defined by King (1948) as a pan-African, supposedly flat landscape formed near sea-level elevation and achieved in the Paleogene. Another striking element of West African landscapes are ubiquitous relics of lateritic pediments (glacis in French) i.e., low-sloping erosional and transportation slopes linking the foot of an escarpment or a smoothed interfluve to the neighboring river drain. Three successive pediment systems of regional extent have been recognized, namely the High, Middle and Low glacis systems (Brammer, 1956; Tricart et al., 1957; Michel, 1959, 1969, 1973a; Vogt, 1959; Grandin, 1976; Chardon et al., 2018). Over some parts of the region, High and Middle glacis systems are preserved as relict pediplains i.e., plains of regional extent made of coalescent pediments (Chardon et al., 2018).

Paleo-landscape remnants capped by a very distinctive class of Al—Fe duricrusts and ferricretes (i.e., iron duricrusts) have been systematically documented below relicts of the bauxitic etchplain and above the relics of the pediment systems. Because of their relative geomorphic position in the sequence and the regional consistency of their geomorphic patterns and capping duricrusts, these remnants were used to define the Intermediate Surface or Intermediate Relief (Michel, 1959, 1973a and references therein; Grandin, 1976; Boulangé, 1984; Boulangé and Millot, 1988; Chardon et al., 2016). The Intermediate

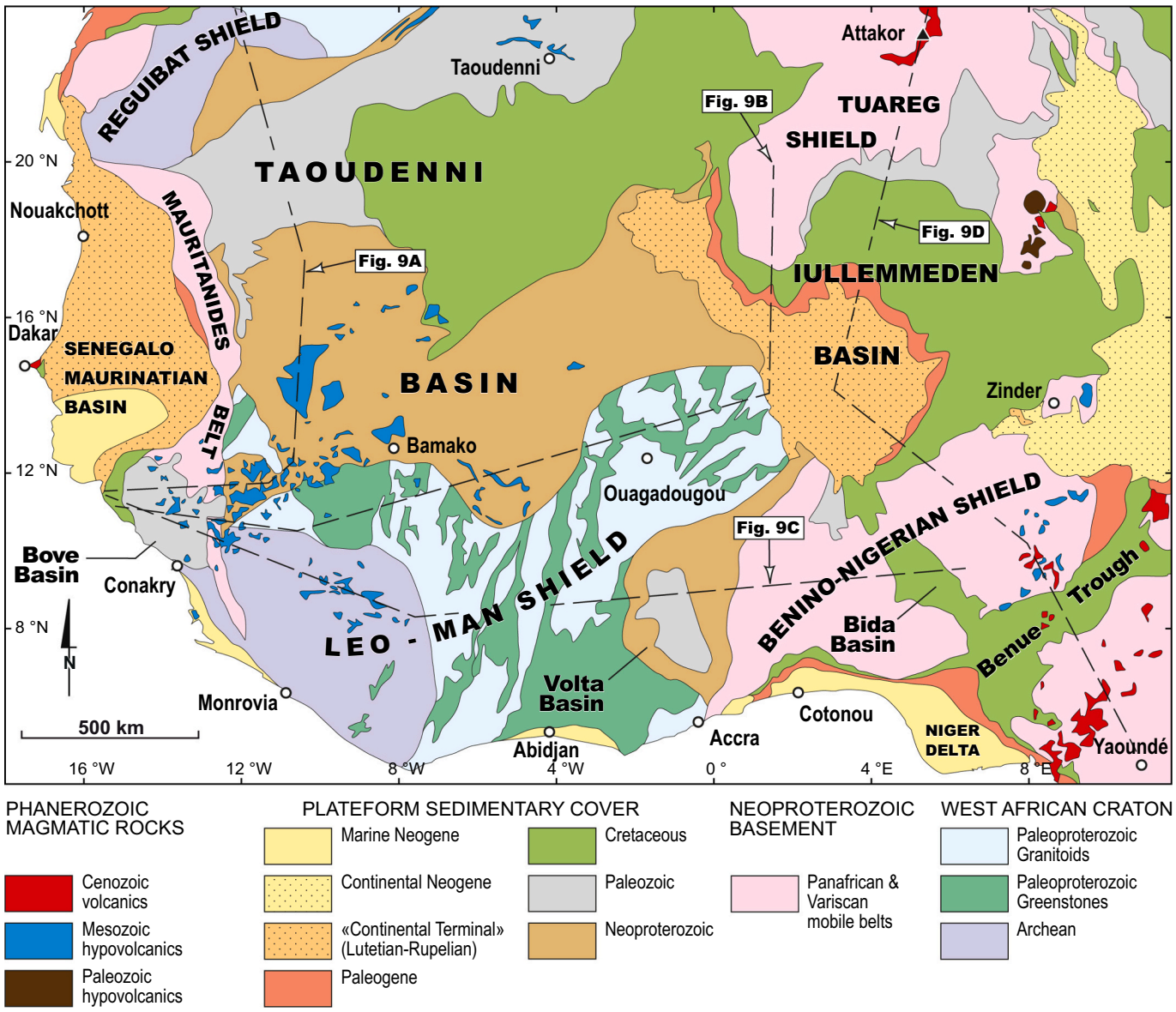

Fig. 4. Bedrock geology of Northwestern Africa (modified after Choubert and Faure-Muret, 1988; Ye et al., 2017). Mesozoic magmatic occurrences of the western half of the map are dolerite sill complexes from the Central Atlantic Magmatic Province (CAMP) emplaced around 200 Ma. Dashed lines are the traces of the cross-sections shown in Fig. 9.

landscape fossilizes an early dissection stage of the bauxitic etchplain. It is also underlain by a weathering profile several tens of meters thick. It is therefore also a mantled etchplain, but studded in some areas with reliefs preserving relics of the bauxitic etchplain.

Age constraints on the West African morphoclimatic sequence were provided by Ar—Ar dating of cryptomelane, a potassium-bearing Mn-oxide produced by advanced weathering in laterites, particularly in duricrusts formed on Mn-rich bedrock (Colin et al., 2005; Beauvais et al., 2008; Beauvais and Chardon, 2013; Fig. 5). The High, Middle and Low glacis systems were shaped essentially during the 24–18 Ma, 11–7 Ma and 6–3 Ma intervals, respectively (Fig. 5b). They were weathered and ultimately duricrusted during the 18–11 Ma, 7.2–5.8 Ma and 3.4–3 Ma intervals, respectively (Fig. 5b). Bauxites developed on all pre-Eocene rocks in West Africa (Millot, 1970) and are overlain by the Lutetian (<48 Ma) to Oligocene (>29 Ma) «Continental Terminal» Fm of the Iullemmeden basin (Radier, 1959; Greigert, 1966; Colin et al., 2005; Chardon et al., 2016; Fig. 4). The pre-Lutetian stratigraphic age of the bauxitic etchplain is consistent with Ar—Ar ages of bauxitization, mostly between 59 and 45 Ma, with a late main cluster between 50 and 45 Ma (Fig. 5b). The main, late duricrusting period of the Intermediate Surface is constrained between 29 and 24 Ma, which has ended a ~ 15 My period of partial dissection of the bauxitic etchplain (Fig. 5b). Ar—Ar ages obtained on Alunite and Jarosite minerals (Vasconcelos et al., 1994), although signing lower weathering intensities than cryptomelanes, are consistent with the Ar—Ar chronogram. They further indicate that weathering took place during morphogenesis of the Intermediate Surface between 40 and 29 Ma and suggest the weathering period having produced the bauxites started as early as in the Early Paleocene (Fig. 5b).

2.3. *Historical outline*

We owe to Daveau (1962) the first and sole regional systematics of Sub-Saharan West African landscapes. She distinguished three main types: (i) the dominant, smoothly undulating or planar plains made of glacis (pediments), duricrusted to various degrees (pediplains of the present study); (ii) the tabular sandstones of the southern Taoudenni basin intruded by dolerite sills best preserving old duricrusts topping

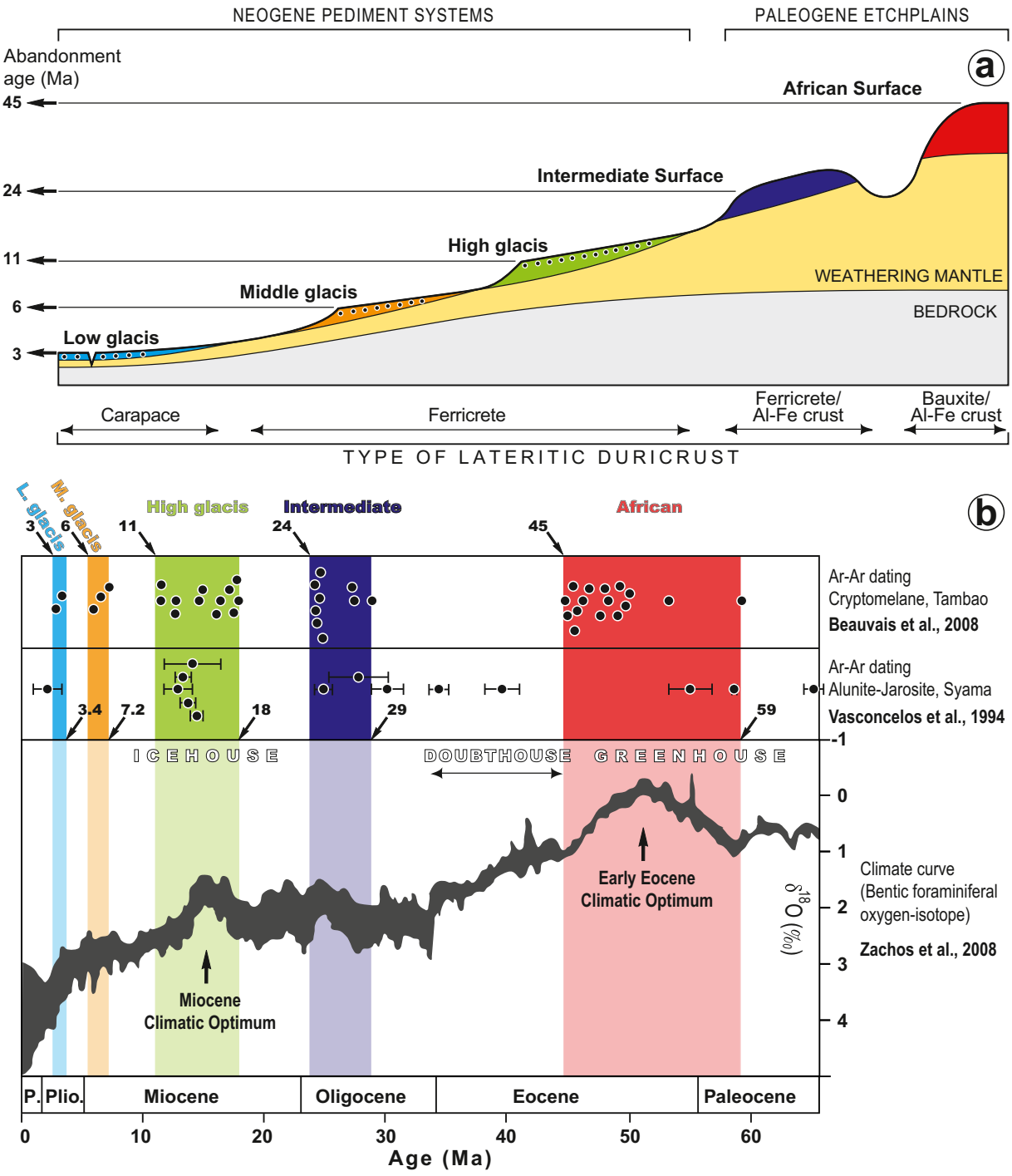

Fig. 5. (a) Schematic representation of the West African morphoclimatic sequence of relict lateritic landforms. (b) Age constraints on the development and abandonment of each member of the sequence (modified after Beauvais and Chardon, 2013 and Chardon et al., 2016), along with the climate curve of Zachos et al. (2008). Cryptomelane ages were obtained in the weathering profiles of each term of the sequence at Tambao, Northeastern Burkina Faso (Beauvais et al., 2008; e.g., Fig. 3). Alunite and jarosite ages were obtained at Syama, Southwestern Mali (Vasconcelos et al., 1994; e.g., Fig. 3). Vertical colour bars are the main weathering periods of each level in the sequence, whereas intervening blank spaces are periods of dominant landform dissection and erosion.

thick weathering profiles (i.e., bauxitic and Intermediate surface remnants defined above) and (iii) hilly or mountainous terrains - typified by greenstone belts - preserving small relicts of the old bauxitic or Intermediate duricrusts and ferricrete-capped piedmont glacis (Fig. 4). She also mapped a latitudinal band of optimal duricrusting, coinciding with the Guinean and Soudanian climatic zones (Fig. 3). De Swardt (1964) proposed independently a comparable geomorphic stepping scheme of older/higher paleolandforms (i.e., bauxitic and/or Intermediate) versus younger/lower surfaces (i.e., glacis) in Nigeria. Daveau's regional scheme was refined by Michel (1978), who reported the main remnants of the bauxitic etchplain and drew attention onto relics of the Intermediate Surface in Sahel and Southwestern Sahara (Michel, 1977a). Only recently a preliminary landform-regolith provinces map was proposed by Chardon et al. (2018). But among the milestones in our understanding of regional landform-regolith patterns, one may refer to Michel (1973a, 1977b) for the Senegambia drainage; Boulvert (2005) and

Mamedov et al. (2022) for Guinea; Grandin (1976) and Boulangé (1984) for Ivory Coast and Burkina Faso; Brückner (1957) and Hilton (1963) for Ghana; De Swardt (1964), Fölster (1969b) and Rohdenburg (1969) for Nigeria; Ségalen (1967), Fritsch (1978), Kadomura and Hori (1978) and Morin (1987, 1989) for Cameroon; Lévêque (1979a, 1979b) for Togo; Thomas (1978, 1980) for Sierra Leone and Fabre (2005) for the Sahara (Figs. 2 and 3). Topical reviews are also available on West African landforms and laterites (Tardy, 1997; Tardy and Roquin, 1998; Burke and Gunnell, 2008; Grandin, 2008; Grandin and Joly, 2008; Chardon et al., 2018).

3. Method

The landform-regolith map (Fig. 6) was produced by systematic manual geomorphic photointerpretation using the GoogleEarth™ software. The software allows for enhanced three-dimensional exploration of virtual landscapes combining the Shuttle Radar Topography Mission digital elevation model at 90 m resolution with an optimized, open access harmonized satellite image cover. Photointerpretation was initiated over regions surveyed by the author in the course of detailed ground work or mapping along regional itineraries in Bénin, Burkina Faso, Côte d'Ivoire, Western and Northern Guinea, Southwestern Mali, Southwestern Niger, Senegal, and Northwestern Mauritania (Fig. 3). The mapping protocol transposes to a regional scale the concept of detailed (1:50,000 to 1:200,000 scale) morpho-pedological mapping (Martin, 1966; Avenard et al., 1974; Avenard, 1977; Pèltre, 1977, 1979; Eschenbrenner, 1978; Lévêque, 1979a; Beaudou and Sayol, 1980; see Pédro and Kilian, 1986) by delimitating provinces with type-relief associations and *catena* i.e., the configuration of the regolith along slopes. Hereafter, such provinces are referred to as landform-regolith associations, mapped as landform-regolith units.

Within and outside the areas the author actually studied in the field, mapping combined photointerpretation and the available field-based documentation, which is specifically referred to in Table 1. Among these publications, one must point out the outstanding 1:200,000 and 1/500,000 scale morpho-pedological maps of Guinea by Boulvert (2003, 2005), which were key starting points of our work, particularly because they helped deciphering the intricacy of the Southeastern Guinean Rise (Figs. 2 and 6) and propagating mapping over the underexplored neighboring regions. The recent (Quaternary) landforms of the Sahara were not specifically studied in this work. Nor were the Sub-Saharan Quaternary alluvial terraces unless they have been specifically linked to the regional landform-regolith record. Definition of lateritic landform-regolith terms used below may be found in Thomas (1994), Eggleton et al. (2008) and more specifically in Chardon et al. (2018) for the West African context.

4. Landform-regolith associations: definitions and map patterns

4.1. Relict Paleogene Mantled Etchplains

Remnants of landscapes capped by either bauxitic duricrusts or Intermediate ferricretes topping a thick (> 50 m) weathering profile allowed defining three types of mantled etchplains that had a great regional extent. The oldest one is the Bauxitic Mantled Etchplain (i.e., the African Surface), mapped as a first landform-regolith association (Bx). Large Intermediate ferricrete-capped paleolandscape remnants are preserved in two main contexts. In the first context, Intermediate paleolandscapes and their weathering profiles comprises landform(s) and/or regolith inherited from the Bx etchplain. They constitute a mixed landform-regolith association grouped under the Composite Bauxitic-Intermediate Mantled Etchplain (BxInt). In the second context, devoid of bauxitic landforms or regolith remnants, pristine Intermediate duricrust-capped weathering mantles underline flat landscapes of regional extent. These occurrences were mapped as the Intermediate Mantled Etchplain sensus stricto (Int, IntS).

4.1.1. Bauxitic Mantled Etchplain (Bx)

This landform-regolith association refers to a low-relief (<80 m), multiconvex landscape, capped by bauxitic duricrusts and underlain by a thick (typically >80 m) weathering profile (Fig. 7a). The typical wavelength of the bauxitic landscape is of 2–4 km, attesting to a ramified drainage network at the time the etchplain was functional. Limited dissection of the mapped Bx etchplain took place along that same paleodrainage network, which is rarely entrenched beyond the base of the bauxitic weathering profile (Fig. 7a).

The petrography of bauxites is spatially variable, depending on the lithology of the bedrock, their depth in the weathering profile and their geomorphic setting (Boulangé, 1984; Mamedov et al., 2011, 2021, 2022; Sawadogo et al., 2020). Among the capping duricrusts, a very common type is the breccia-like facies (Fig. 8a). The most spectacular is the pisolithic facies found on lower hillslopes (Fig. 8b) that represents geochemically evolved (senile) Fe-enriched bauxites (Boulangé, 1984) also called metabauxites (Tardy, 1997). The weathering profile is very rich in Kaolinite (e.g., Fig. 8e) and generally dominated by a saprolitic horizon.

The Bx etchplain is preserved in the Fouta Djalon and its western and eastern piedmonts, as well as in parts of the Mandingue and Banfora Plateaus (Figs. 2, 6 and 9). In the highest, Northeasternmost part of the Fouta Djalon, relict bauxitic landscapes are found on both sides of sandstone escarpments (Fig. 6). This led Michel (1973a, 1978) to speculate on the preservation of a Triassic "Gondwana" and a Cretaceous "post-Gondwana" surfaces (King, 1962) above the Eocene etchplain. Nonetheless, he also acknowledged that two bauxitic etchplains separated by an escarpment (e.g., the Eocene African and the "post-Gondwana" surfaces) were connected by gentle and smooth bauxite-capped slopes laterally replacing the escarpment (Michel, 1973a, 1978). A given etchplain can therefore comprise escarpments or more generally residual topography it could not level (Burke and Gunnell, 2008). Besides, the gentle western piedmont slope of the Fouta Djalon preserves a continuous bauxite cover from 1400 m elevation to the coast over a 250 km distance (Chardon et al., 2006; Figs. 6 and 9). There is no documented petrographic contrast in the capping bauxitic duricrusts as a function of elevation either. In any case, a Triassic bauxitic etchplain is precluded because it would cut Jurassic sills (Chardon et al., 2006). Furthermore, apatite fission track thermochronology indicate >1.5 km of denudation over the Fouta Djalon in the Early Cretaceous (Wildman et al., 2022). A paleomagnetic study by Théveniaut (2012) in Léro, Northeastern Guinea (Figs. 2 and 6), indicates that a > 30 m-thick section of the saprolitic weathering profile underlying the landscape carved in the Bx etchplain is 70–80 Ma-old. The age of this saprolite located 200 m under the bauxite caps shows that the Bx etchplain is underlain by a very thick weathering profile that was already functional in the Late Cretaceous. Bauxitization of alluvial channels filled with bauxite pebbles in the Sangaredi mining district on the western slope of the Fouta Djalon (Mamedov et al., 2011; see also Chardon et al., 2006) would also be consistent with a single long-lived (Cretaceous- Eocene) bauxitic etchplain.

Outside its mapped remnants, relics of the Bx etchplain occupy most hills of the BxInt relics (see below) West of longitude 0° and South of latitude 16°N (Fig. 6). More generally, numerous small (km-size or less), unmapped relics of the Bx etchplain are scattered South of the Sahelian zone (Beauvais and Chardon, 2013; Grimaud et al., 2018; Fig. 3). The Bx etchplain therefore occupied the map area from the Guinea Gulf coast to at least 16°N (Fig. 6). To summarize, the Bx etchplain formed over Northwestern Africa over a protracted period of time, starting in the Late Cretaceous (>70 Ma) and until the Eocene (ca. 45 Ma; Fig. 5b). No earlier landforms appear to have survived in Northwestern Africa, although bauxitic etchplanation could not rectify some reliefs such as Mount Mali (Michel, 1973a) and several sandstone escarpments in the Fouta Djalon (Figs. 2 and 6).

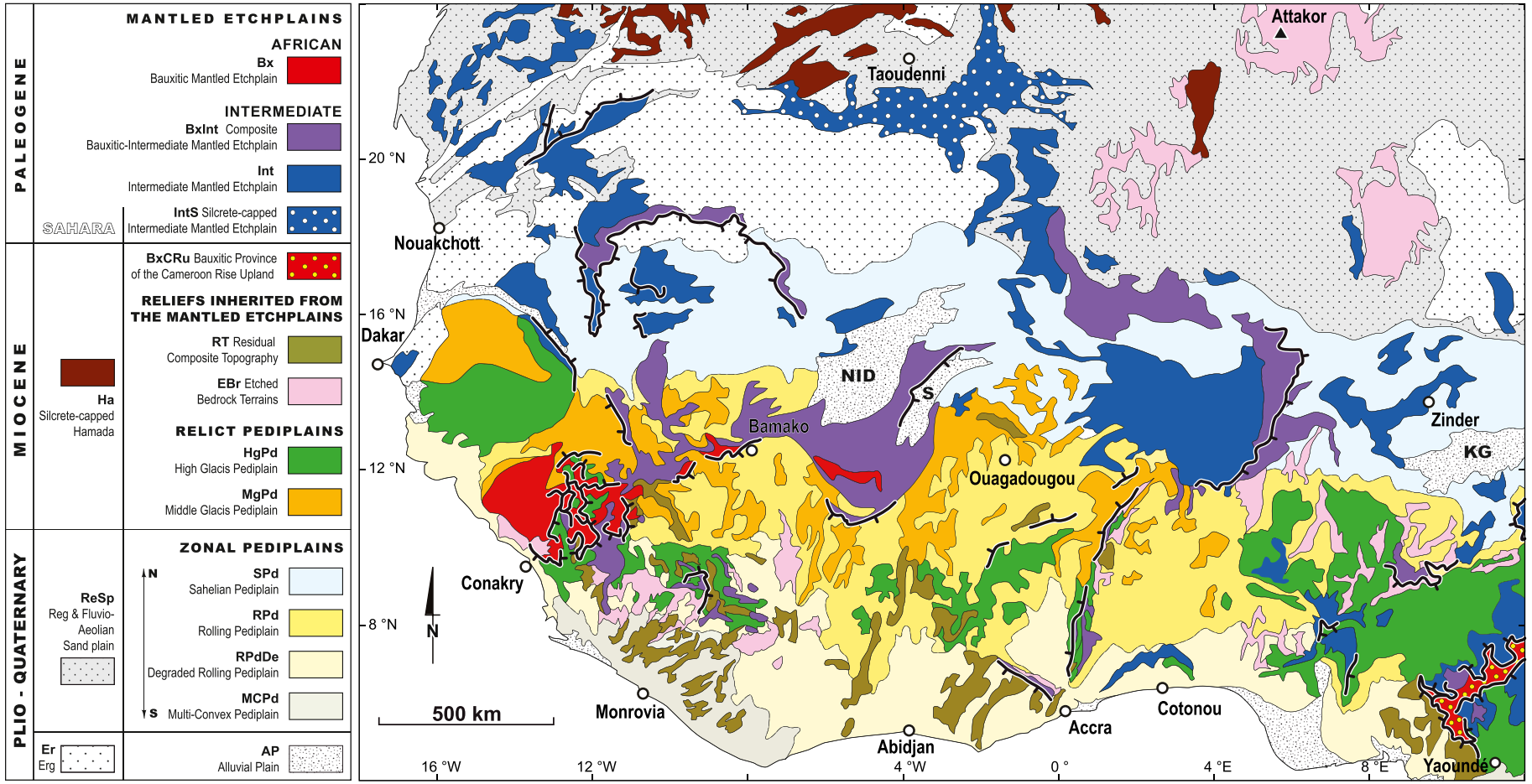

Fig. 6. Landform-regolith map of Northwestern Africa. Escarpments are drawn as thick ticked black lines. NID: Niger internal delta; S: Sourou delta; KG: K-Gana River delta.

Table 1
Works on the Northwestern African landforms and regolith, with indication of their relevance to the landform-regolith associations of Fig. 6. See Figs. 2 and 3 for locations.

Reference	Map unit(s)	Area, comments and keywords
de Chételat, 1938[a]	Bx	Fouta Djalon western piedmont, Guinea
Michel, 1973a[a]	Bx, BxInt	Fouta Djalon, Mandingue Plateau, Guinea, SW Mali
Mamedov et al., 2010	Bx, BxInt	Map of bauxitic plateaus & Aluminum prospects, Guinea
Mamedov et al., 2011	Bx	Sangaredi deposit, western piedmont of the Fouta Djalon, Guinea
Chardon et al., 2006	Bx	Fouta Djalon and its piedmonts, Guinea
Mamedov et al., 2020 Mamedov et al., 2021 Mamedov et al., 2022	Bx, BxInt	Fouta Djalon and its piedmonts, Mandingue Plateau, Guinea, Mali
Boulvert, 2003[a] Boulvert, 2005[a]	Bx, BxInt, RT, EBr, HgPd, MgPd, RPd	Morpho-pedological maps of Guinea at 1:200,000 and 1:500,000 scale
Daveau and Michel, 1969	Bx, Int	Tagant, SW Mauritania
Michel, 1977a Michel, 1977b[a]	Bx, Int	Mauritania, W Mali
Bravard, 1976	BxInt	E of Tagant, S Mauritania
Thomas, 1978	BxInt, EBr, HgPd, RPd	Sierra Leone
Jodot, 1933	BxInt	Bauxites petrography, Niger inland delta area
Chardon et al., 2016	BxInt, Int	Niger inland delta area, Iullemmeden basin
Bourdeau, 1991	Bx, BxInt	Duricrusts mapping and geochemistry SW Mali
Cornet, 1943[b]	BxInt, Int	Tilemsi, Mali
Daveau, 1959	BxInt	Bandiagara Plateau, Mali
Daveau, 1960	BxInt, Bx	Banfora Plateau, W Burkina Faso, S Mali
De Swardt, 1956 De Swardt, 1964[a]	BxInt, Int, RPd	N Nigeria
Boulangé and Eschenbrenner, 1971 Valeton and Beissner, 1986[a] Valeton, 1991 Becker, 1992 Zeese et al., 1994	BxInt	Jos Plateau, Nigeria
Zeese, 1983	BxInt, RPd	Jos Plateau and its piedmont, NE Nigeria
Hieronymous, 1972 Hieronymous, 1973	BxCRu	Bauxites, Cameroon Rise, Cameroon
Morin, 1987 Morin, 1989[a]	BxCRu	Cameroon Rise, Cameroon
Momo Nouazi et al., 2016 Momo Nouazi et al., 2020	BxCRu	Cameroon Rise Neogene bauxites, W Cameroon
Schwarz, 1997	BxCRu	Cameroon Rise bauxites and ferricretes, Nigeria
Fritsch, 1978	BxInt, Int, HgPd	Adamaoua plateau (E of Cameroon Rise), Cameroon
Michel, 1959 Michel, 1973a[a]	Int	S and E Senegal
Nahon, 1971 Nahon et al., 1977a Nahon, 1986[a]	Int	Weathering profiles, W Senegal
Lappartient and Nahon, 1970	Int	Weathering profiles, *Continental Terminal*, E Senegal
Nahon et al., 1973 Nahon et al., 1977b Nahon, 1980[a]	Int, SPd	Intermediate duricrusts, W Senegal, W Mauritania
Radier, 1959[b]	Int	Gourma - Tilemsi area, E Mali
Beaudet et al., 1981a Beaudet et al., 1981b	Int	Gourma, Bandiagara Plateau, Tilemsi, Mali
Hubert, 1908[b] de Chételat, 1928[b] Pougnet, 1949[b] Réformatsky, 1935[b] Dresch and Rougerie, 1960 Greigert, 1966 Gavaud, 1977 Beaudet et al., 1977	Int, BxInt	Weathering profiles capping the *Continental Terminal*, pre-*Continental Terminal* bauxites, SW Niger, N Bénin
Gavaud and Boulet, 1967	Int, SPd	S Niger
Fabre et al., 1996 Fabre, 2005[a]	IntS, Int, Ha	Western Sahara
Du Preez, 1956	Int, RPd, RPdDe	Nigeria
Kogbe, 1978	Int, BxInt	NW Nigeria
Zeese, 1991	Int, BxInt	NE Nigeria
Schnell, 1946[b] Schnell, 1948[b]	RT	Geomorphology, duricrusts, Mont Nimba, SE Guinea
Leclerc et al., 1949[b]	RT	Geormorphology, Mont Nimba, SE Guinea
Leclerc et al., 1955	RT	Geology, geomorphology, Mont Nimba, SE Guinea
Misra and Raucq, 1986	RT	BIF, supergene iron ores, Mont Nimba, SE Guinea
Pascual, 1988	RT	Bauxites, Mont Nimba, SE Guinea
Rougerie, 1961[b]	RT, HgPd	Geomorphology, eastern piedmont of the Simandou Range, E Guinea
Lamotte and Rougerie, 1952[b]	RT	Geomorphology, Simandou range and Mont Nimba, SE Guinea
White, 1973	RT	Geology, geomorphology, BIF, supergene iron ore, Wologizi Range (Mt Wuteve), Liberia
Gaskin, 1975	RT, BxInt	BIF, supergene iron ore, Sula greenstone belt, Central Sierra Leone
Faure and Volkoff, 1989	RT, RPd	NE Togo
Sawadogo et al., 2020[a]	RT, MgPd	Comprehensive landform-regolith associations, Central Burkina Faso
Eschenbrenner, 1969	RT	NE Côte d'Ivoire
Boulangé et al., 1973[a]	RT	Duricrusts systematics, West African morphoclimatic sequence, Côte d'Ivoire
Grandin, 1976[a]	RT, MgPd	Landform-regolith associations of the West African morphoclimatic sequence, mostly Côte d'Ivoire
Boulangé, 1984[a] Boulangé, 1986 Boulangé and Millot, 1988	RT	Bauxite and Intermediate landform-regolith associations, Côte d'Ivoire and West Africa
Grandin and Joly, 2008	RT, MgPd, SPd	Relict pediment examples, Côte d'Ivoire, Burkina Faso
Beaudet and Coque, 1986	RT, MgPd, SPd	Burkina Faso
Avenard et al., 1974[a]	RT, RPd, RPdDe	Central Côte d'Ivoire
Avenard, 1973 Avenard, 1977	RT, RPdDe, BxInt	W Côte d'Ivoire, Man area
Meyer, 1992	RT	NE Togo
Jaeger, 1953[b] Daveau, 1971	EBr	Geomorphology, Mount Loma (Mt Bintumané), Sierra Leone
Thomas, 1965	EBr	Nigeria
Michel, 1969	HgPd, MgPd, SPd	S and E Senegal
Avenard, 1975	HgPd	Central Côte d'Ivoire
Bachelier, 1959	HgPd, MCPd	Catena, W Central Cameroon
Martin, 1966[a] Martin, 1967 Martin, 1970	HgPd, MCPd	W Central Cameroon
Yongué and Belinga, 1987	HgPd, MCPd	Intermediate ferricrete degradation, W Central Cameroon
Embrechts and Dedapper, 1987	HgPd, MCPd	W Central Cameroon
Kadomura and Hori, 1990[a]	HgPd, MCPd	Catena studies, W Central Cameroon

(*continued on next page*)

Table 1 (*continued*)

Reference	Map unit(s)	Area, comments and keywords
Fritsch, 1969	HgPd	Southern piedmont of Benue valley, N Cameroon
Michel, 1959	HgPd, MgPd, SPd	Senegal, SW Mali, S Mauritania
Michel, 1973a[a]	MgPd	Senegal, SW Mali
Beauvais et al., 1999 Beauvais et al., 2004	MgPd	Geophysical imaging of High and Middle glacis catena, E Senegal
Butt and Bristow, 2013	MgPd	Djelimagara area, SW Mali
Daveau et al., 1962[a] Bamba et al., 2002 Grimaud et al., 2015	MgPd	W Burkina Faso
Mensching, 1966	MgPd, SPd	Burkina Faso, Niger, Nigeria
Boulet, 1970	MgPd, SPd	N Burkina Faso
Sanfo et al., 1992 Sanfo et al., 1993	MgPd	N Burkina Faso
Ambrosi and Nahon, 1986	MgPd	Intermediate weathering profile petrology, NE Burkina Faso
Parisot et al., 1995	MgPd	NE Burkina Faso
Ouangrawa et al., 1996	MgPd	E Burkina Faso
Boeglin and Mazaltarim, 1989	MgPd	High glacis / Intermediate ferricrete petrology, SW Burkina Faso
Eschenbrenner and Grandin, 1970[a]	MgPd	E & NE Côte d'Ivoire, SW Burkina Faso
Teeuw, 2002	MgPd	N Côte d'Ivoire
Collinet, 1974[a] Beaudou and Sayol, 1980	MgPd, RPd	Catena studies, N Côte d'Ivoire
Eschenbrenner, 1988	MgPd, RPd	High & Middle glacis, iron nodules, Côte d'Ivoire
Arhin et al., 2015	MgPd	NW Ghana
Le Cocq, 1986	MgPd, RPd, EBr	NW Togo
Poss, 1996	MgPd, RPd	N Togo
Pélissier and Rougerie, 1953	RPd, MgPd, RT, BxInt	NE Guinea
Eschenbrenner, 1978[a]	RPd, RPdDe, EBr, RT	NW Côte d'Ivoire
Delvigne and Grandin, 1969	RPd	Central Côte d'Ivoire
Pèltre, 1977[a]	RPd	S Côte d'Ivoire
Bonvallot and Boulangé, 1970	RPd, RPdDe	S Central Côte d'Ivoire
Pèltre, 1979[a]	RPd, RPdDe	Central Côte d'Ivoire
Poss, 1982	RPd, HgPd	Central Côte d'Ivoire
Viennot, 1983	RPdDe, RT, BxInt	W Central Côte d'Ivoire
Hilton, 1963	RPd, RT	NE Ghana
Lévêque, 1979a Lévêque, 1979b[a]	RPd, RPdDe	Systematic catena study, Togo
Junge and Skowronek, 2007	RPd	Central Bénin
Heinrich, 1992	RPd, SPd	NE Nigeria
Fölster, 1969a Fölster, 1969b[a] Fölster et al., 1971a[a]	RPd, RPdDe	Systematic catena studies, SW Nigeria
Grandin and Hayward, 1975	RPdDe	Bauxitic, Intermediate and glacis relicts, Freetown Peninsula, Sierra Leone
Thomas et al., 1985 Thomas and Thorp, 1985 Teeuw, 1987 Teeuw, 1991	RPdDe	E Sierra Leone
Thomas and Thorp, 1980[a]	RPdDE, MCPd	E Sierra Leone
Bowden, 1987 Bowden, 1997	RPdDe	Piedmont of massifs rising above pediplain, SW Sierra Leone
Brückner, 1955[a] Brückner, 1957	RPdDe	S Ghana
Nye, 1954[a]	RPdDe	Catena study, SW Nigeria

Table 1 (*continued*)

Reference	Map unit(s)	Area, comments and keywords
Thomas, 1966 Burke and Durotoye, 1971	RPdDe	SW Nigeria
Moss, 1965	RPdDe, Int	Meso-Cenozoic sediments, SW Nigeria
Verheye and Pomel, 1984	MCPd, RPdDe	Coastal Côte d'Ivoire (Bauxite, Intermediate, High glacis relics)
Kadomura and Hori, 1978[a]	MCPd, HgPd, Int, BxInt	Zonation of landform-regolith associations, Cameroon
Temgoua et al., 2002 Bitom et al., 2003	MCPd	Intermediate ferricrete degradation and slope evolution, S Cameroon
Boulet et al., 1977 Boulet, 1978	SPd	N Soudanian and Sahelian zones
Chamard et al., 1978	SPd	Latest duricrust (Low glacis?), NE Burkina Faso
Leprun, 1977 Leprun, 1979	SPd, MGPD	Duricrust degradation (mostly High and Middle glacis), Soudanian zone
Villemur, 1967	Ha, IntS	Taoudenni area, N Mali
Capot-Rey, 1951[b]	EBr, Re	Iforas, W Mali
Büdel, 1955 Birot et al., 1955 Rognon, 1967 Beaudet et al., 1977 Büdel, 1982	EBr, Re	Hoggar
Dresch, 1961[b]	Re, IntS, Ha	Central and eastern Reguibat Rise
Dresch, 1959[b] Vogt and Black, 1963 Beaudet et al., 1977 Morel, 1981 Morel, 1985	Re, EBr	Aïr
Dewolf et al., 1972[b]	Re	Algeria, NW Mali
Fabre, 2005[a]	Re, Ha	Western Sahara

[a] Pioneering, seminal or exhaustive study of particular interest.
[b] Preliminary or exploratory work.

4.1.2. *Composite Bauxitic - Intermediate Mantled Etchplain (BxInt)*

Two types of BxInt associations are distinguished, those still comprising bauxite-capped hills and plateaus (type 1) and those devoid of bauxitic duricrust but re-using part of the weathering mantle of the Bx etchplain (type 2). Type 1 occurrences correspond to a composite, often convexo-concave landscape deriving from partial dissection of the Bx etchplain (Fig. 7b). It is almost continuously duricrusted, with remnant duricrusts of the bauxitic landscape on hilltops and Intermediate Al—Fe duricrusts and ferricretes derived from upper duricrusts on slopes (Michel, 1973a, 1978; Boulangé, 1984). That landscape is underlain by a thick (>80 m) and laterally continuous weathering profile. The space-time relationships between bauxites degradation and formation of the Intermediate duricrusts in such contexts are illustrated in Fig. 10. Mature (i.e., pisolithic) bauxites formed at the edge of a plateau pass downslope to a nodular Al—Fe duricrust underlain by a massive ferricrete and a carapace layer, which formed at the expense of the underlying saprolite by downward/downslope iron impregnation. This *catena* attests to a contribution of lateral mass transfers (especially in iron) from bauxites to duricrusting and weathering of the upper Intermediate landscape (Boulangé, 1984, 1986). Type 1 BxInt etchplain is preserved as a large continuous map unit from the Mandingue Plateau to the Banfora and Bandiagara Plateaus. Patches are preserved South of the Fouta Djalon, in the Southern Atakora Range and on the Jos Plateau, whereas smaller relics seat on mafic sills clusters of the Southeastern Guinean Rise, as well as on the upper piedmont of the Cameroon rise (Figs. 2, 3, 6, 9).

Type 2 occurrences of the BxInt etchplain are mainly found in the Iullemmeden basin, where they fringe the "Continental Terminal" Fm to the East and Northeast (Figs. 4 and 6). They correspond to a > 80 m thick kaolin layer developed from Late Cretaceous and Paleocene marine series and capped by the same, laterally continuous Intermediate ferricrete (see below) as that capping the nearby "Continental Terminal" Fm, which seals a planar paleolandscape of regional extent (Chardon et al.,

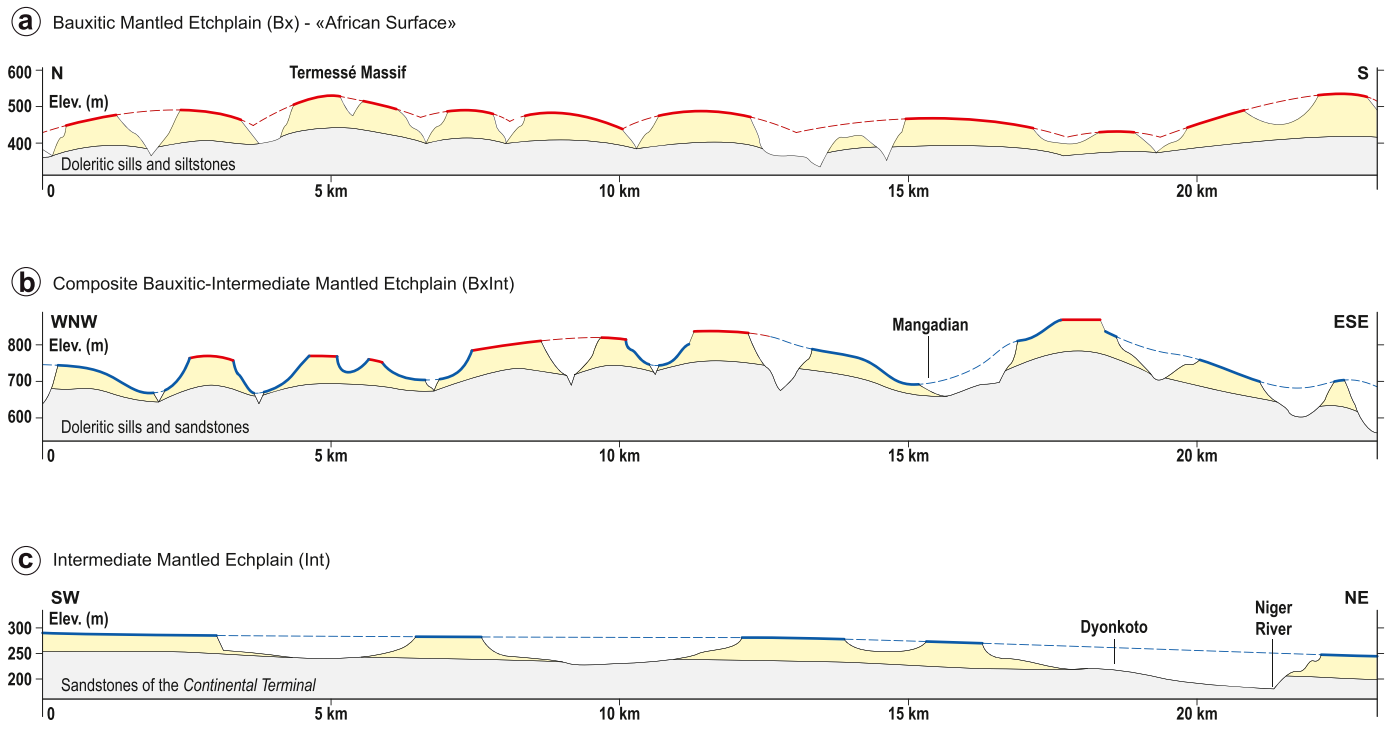

Fig. 7. Simplified cross-sections illustrating the landform-regolith associations of relict Paleogene etchplains. Duricrusts are schematized as thick colored lines; weathering mantles are in yellow, geological substrate in grey. (a) Bauxitic Mantled Etchplain (Bx), western piedmont of the Fouta Djalon, Northwestern Guinea. Termessé Massif coordinates: 11.4928°N/13.4017°W. (b) Composite Bauxitic-Intermediate Mantled Etchplain (BxInt), Northeastern Guinea. Mangadian village coordinates: 11.8311°N/9.8812°W. (c) Intermediate Mantled Etchplain (Int), Southwestern Niger. Dyonkoto village coordinates: 13.6177°N/1.8428°E. The vertical scale is slightly dilated in (c). (For interpretation of the references to colour in this figure legend, the reader is referred to the web version of this article.)

2016; Fig. 9b). Pisolithic bauxitic duricrust fragments systematically found on the kaolin near the base of the "Continental Terminal" Fm indicate that the kaolin was topped by bauxitic duricrusts before burial under the "Continental Terminal" Fm (Hubert, 1908; Pougnet, 1949; Greigert, 1966; Gavaud, 1977; Chardon et al., 2016). Type 2 occurrences of the BxInt etchplain therefore correspond to a weathering profile formed under the Bx etchplain that was later reworked and ultimately capped by an Intermediate ferricrete (Fig. 9B). Fieldwork in Mauritania (Daveau and Michel, 1969) attests to the preservation of comparable remnants of the composite etchplain above the Hodh escarpment and in the Tagant (Figs. 2, 6 and 9a).

4.1.3. *Intermediate Mantled Etchplain (Int, IntS)*

Large relicts of the Intermediate Mantled Etchplain (Int) are preserved (i) in the western Sahara and Sahel (West of 8°W), (ii) in a large girdle stretching from the Taoudenni area to the Zinder area and encompassing the Iullemmeden basin, (iii) in the Lower Niger River bend area and (iv) on the northern and southern piedmonts of the Cameroon Rise (Figs. 2, 6 and 9). These relics represent a ferricrete-capped planar landscape underlain by a > 60 m-thick weathering profile (Figs. 7c, 8f, 9). Lower slopes of the BxInt etchplain and the entire Int etchplain are capped by a distinctive class of ferricretes i.e., the "Intermediate ferricrete". They are typically nodular or alveolar, kaolinite- and quartz-rich, hematitic and goethitic (Fig. 8a and b). Kaolinite-goethite mix set the typical violet/purple colour of most Intermediate ferricretes, which also display goethite-rich yellowish ferriargilans (Fig. 8b). Following the comprehensive study of Nahon (1976), Intermediate ferricretes have become a reference case for ferruginous lateritic profile development (Nahon et al., 1977a; Nahon and Millot, 1977; Nahon, 1986; Thomas, 1994).

Relics of the Int etchplain are generally more dissected than those of the BxInt etchplain. Intermediate ferricretes of the Atlantic Sahara show evidence for partial replacement by calcareous crusts (calcretes), which increases northward (Nahon et al., 1977b; Nahon, 1980; Michel, 1977a). In the Sahelian zone and particularly in the Sahara (Fig. 3), Intermediate ferricretes become dismantled to various degrees and spread as sheets of blocks and nodules, especially on felsic or iron-poor bedrock and on the sandstone tablelands of the Tagant and Adrar (Figs. 2 and 6). In most parts of the Western Sahara, these nodules represent a significant component of the regs (Michel, 1977b, 1978; Fabre, 2005). But the Intermediate weathering profile has been preserved under most regs, as seen in mining pits and drill holes commonly revealing a > 100 m thick saprolite (e.g., Bronner, 1992; Fig. 4). In the Tanezrouft, South and East of Taoudenni, the Intermediate ferricrete sealing the northwestern digitation of the Cenozoic Iullemmeden basin passes laterally to a ferruginous silcrete armoring a large veneer of the etchplain (see Fabre et al., 1996; Figs. 2 and 6). This veneer defines the Silcrete-capped Intermediate Mantled Etchplain map unit (IntS), interpreted by Fabre et al. (1996) as sealing Cretaceous series under the ergs of the Majabat Al Koubra (Figs. 2, 4 and 6).

4.1.4. *Age and regional significance of the post-bauxitic mantled etchplain*

The BxInt, Int and IntS map units collectively define a single long-lived etchplain eventually capped by Intermediate-type ferricretes or ferruginous silcretes. The spatial variability of that etchplain is consistent with protracted and uneven erosion and weathering of the Bx etchplain after ca. 45 Ma, which ended by a period of duricrusting between 29 and 24 Ma according to Ar—Ar dating (Fig. 5). This timing is confirmed independently in several contexts. For instance, on the Jos Plateau (Fig. 2), the BxInt etchplain is preserved on Paleocene volcano-sediments (Boulangé and Eschenbrenner, 1971; Valeton and Beissner, 1986; Valeton, 1991; Becker, 1992) and sealed by a 27 Ma lava flow (Zeese et al., 1994). The ferruginous silcrete caping the etchplain (IntS) tops weathered sediments bearing 30 Ma old glauconites (K—Ar date; Fabre et al., 1996) and, along with the Intermediate ferricretes of northern Mauritania and Western Sahara, is overlain by Aquitanian

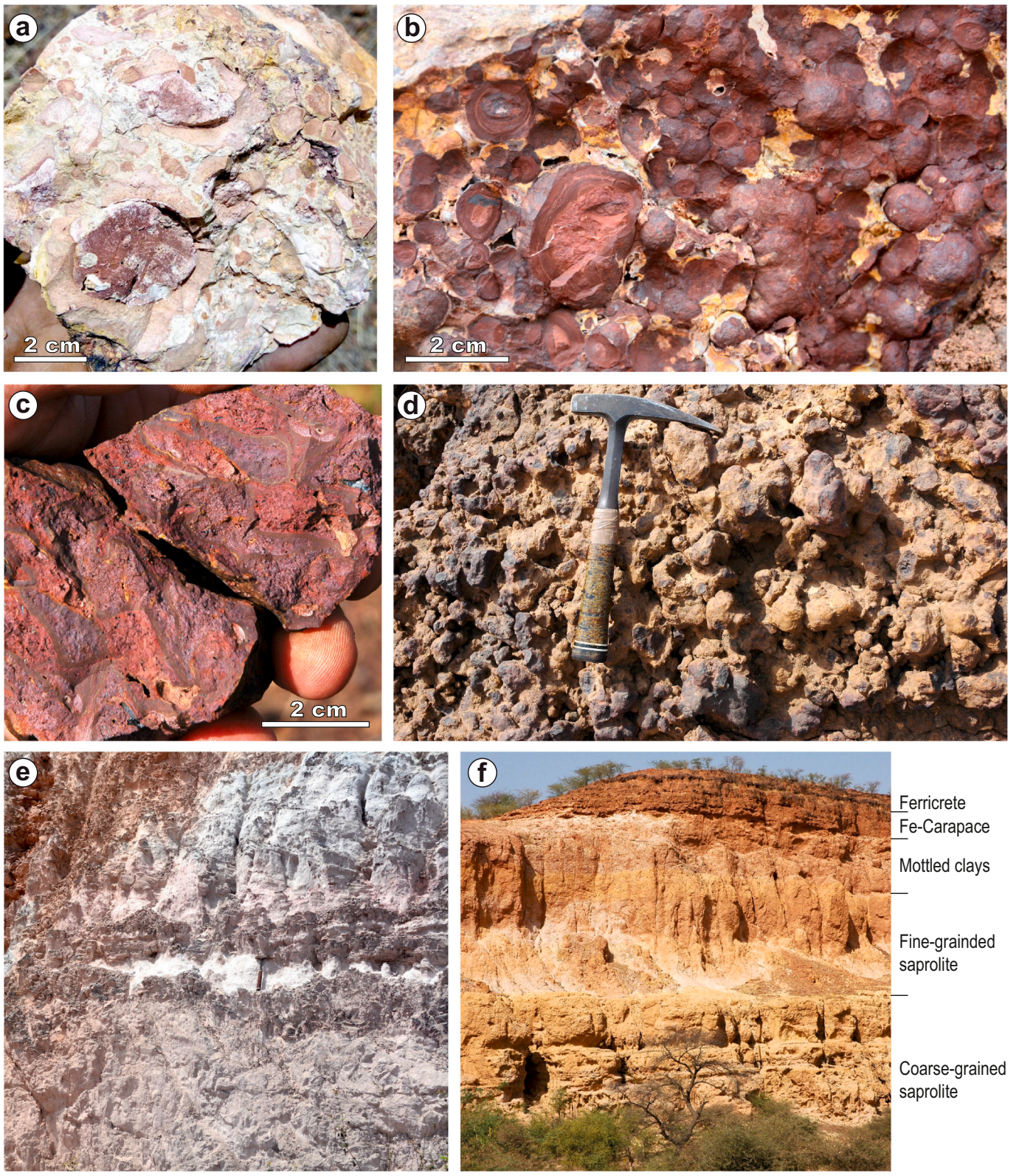

Fig. 8. Type-duricrusts and weathering profiles of the Paleogene mantled etchplains (Bx, Int, BxInt). (a) Breccia-like bauxite, Kongoussi area, Central Burkina Faso (courtesy of B. Sawadogo). Brownish patches are litho-relics. (b) Pisolithic Fe-bauxite, near Timbo, Guinea. (c) Intermediate ferricrete, Sansanding area, Southwestern Mali. Violet kaolinite-goethite rich nodules hosting relict quartz grains and fringed by goethitic aureoles in a hematite-bearing matrix. (d) Nodular Intermediate ferricrete, near Sémmé, Eastern Senegal. (e) Kaolin (saprolite) under the bauxitic - Intermediate duricrusts transition, Bondoukou area, Northeastern Côte d'Ivoire (quarry of Fig. 10). (f) Weathering profile of the Intermediate Mantled Etchplain (Int) developed on Paleogene siltstones of the "Continental Terminal" Fm, Dallol Bosso River valley (Lower Azaouak valley; Fig. 2), Southwestern Niger. The cliff is 60 m high. (For interpretation of the references to colour in this figure legend, the reader is referred to the web version of this article.)

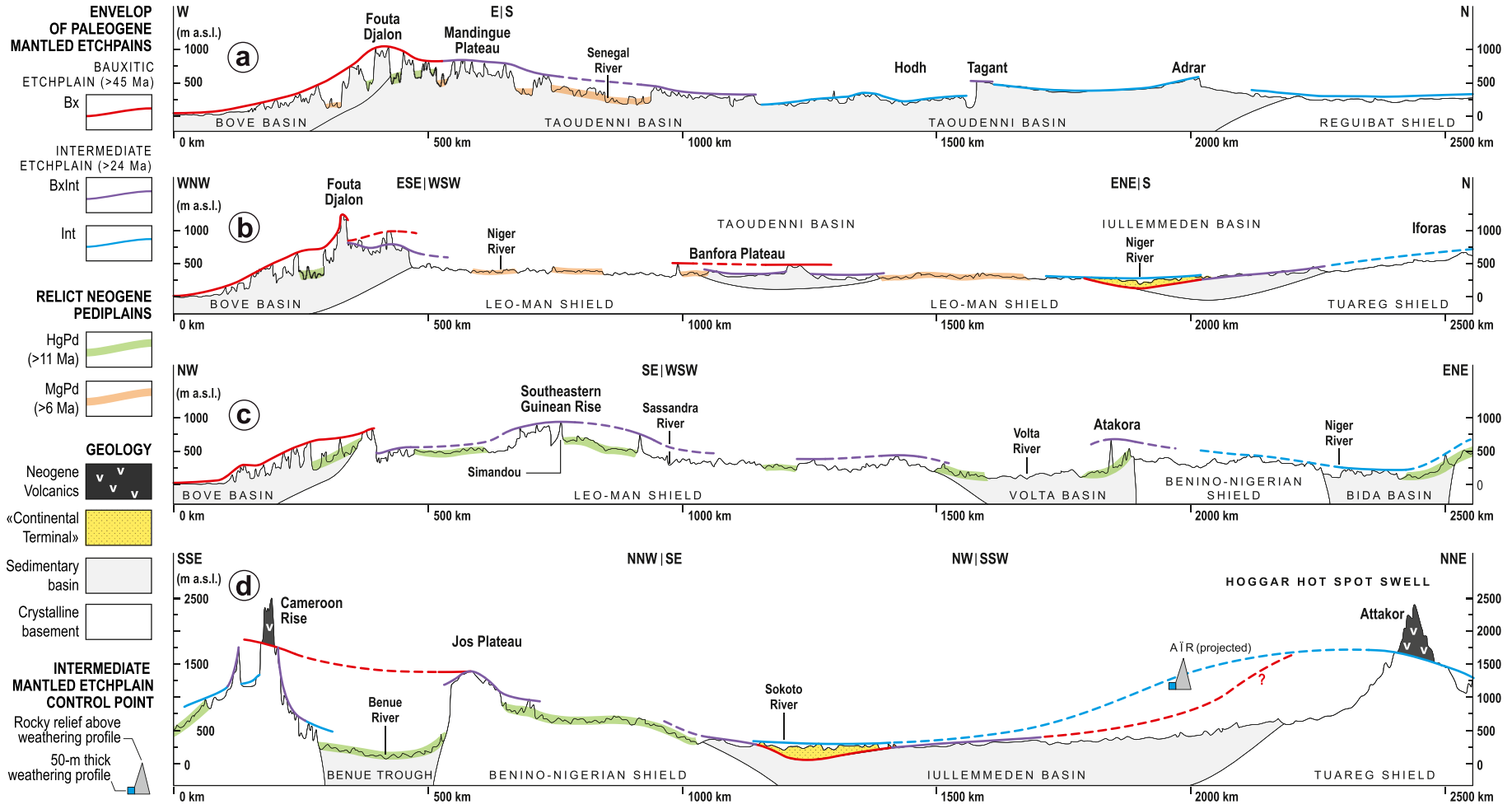

Fig. 9. Regional cross-sections illustrating the distribution of relict mantled etchplains and pediplains over northwestern Africa. The lines of section are located on Fig. 4.

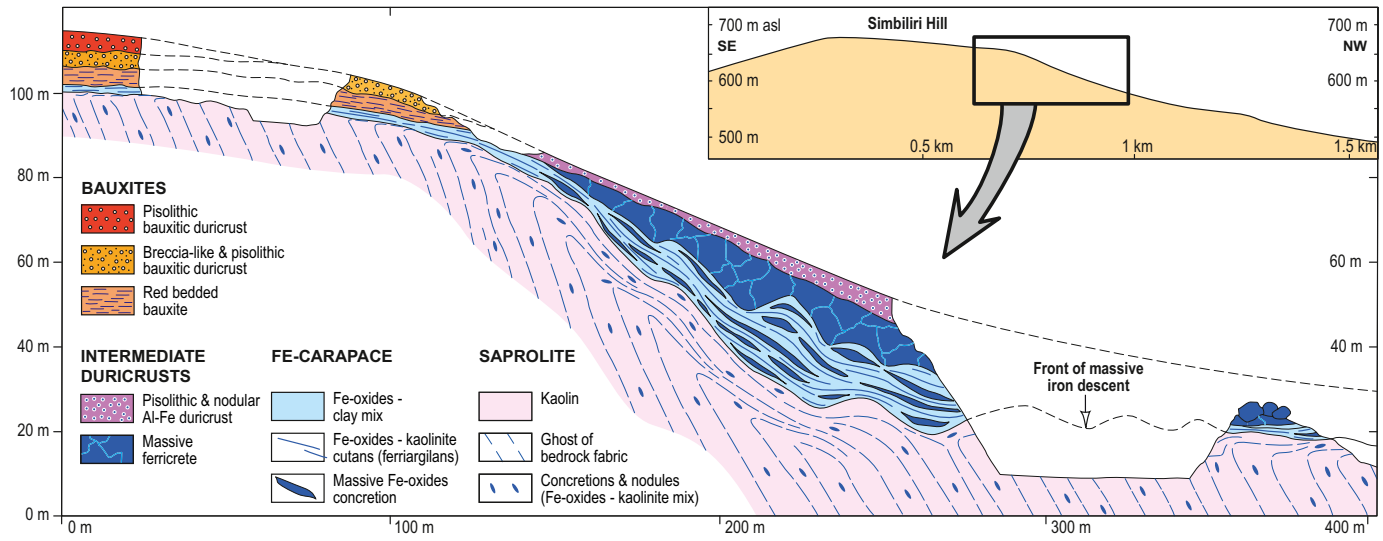

Fig. 10. Cross section of the *catena* at the transition between duricrusts of the Bauxitic Mantled Etchplain and those of the upper Intermediate landscape (Simbiliri quarry, Northeastern Côte d'Ivoire; coordinates of the top of section: 8.1122°N/2.9623°W). The inset shows the location of the cross-section on a topographic profile of the Simbiliri hill.

(23–20 Ma) lacustrine carbonates (see Fabre, 2005). The Intermediate weathering profile underlying most regs and ergs hosts kaolin and alum deposits scattered over the Western and Central Sahara (e.g., Antonovic et al., 1991; Lefranc, 1991; Bonhomme et al., 1996). The Tabelbala kaolin deposit located North of Taoudenni (outside the map of Fig. 6), which is also correlated with that of the Adrar remnant of the Intermediate etchplain (Figs. 2 and 6), provided a K—Ar Alunite age of 28 Ma (Bonhomme et al., 1996).

A kaolinic weathering profile affecting Oligocene fluvial sediments is preserved at >1500 m elevation under the basaltic traps of the Attakor range in the Hoggar massif (Rognon et al., 1983; Figs. 2 and 4). This profile correlates with that affecting the laterally equivalent "Continental Terminal" Fm in the Iullemmeden basin (Chardon et al., 2016; Fig. 8f), suggesting long-wavelength distortion and erosion of the Intermediate etchplain as a consequence of topographic growth of the Hoggar hot spot swell (Fig. 9d). The shape of the swell is further constrained by remnants of a > 50 m thick kaolinic weathering profile preserved in the Aïr massif (Vogt and Black, 1963; Beaudet et al., 1977; Fig. 2) on a bedrock with a youngest apatite (U—Th)/He exhumation age of 27 Ma (Rougier et al., 2013; Fig. 9d). Sheets of Intermediate-type ferricrete nodules spread over the peripheric piedmont of the Iforas basement also suggest that the massif results from barely stripping of the Intermediate Etchplain (e.g., Fabre, 2005; Figs. 2 and 6). Commencing Hoggar epeirogeny between ~38 and 29 Ma would have allowed for the deposition and preservation of the "Continental Terminal" Fm, especially in the Iullemmeden basin (Chardon et al., 2016). This led to the telescoping and merging of the Bx and Int etchplains into the composite BxInt etchplain at the margins of the basin (e.g., Fig. 9b and d). Moreover, the geomorphic setting of the Aïr weathering profile shows that the Intermediate Mantled Etchplain was studded with rocky reliefs of significant height (>350 m; Fig. 9d), whose low-relief top was sealed by a 35 Ma volcanic flow (Morel, 1985). Besides, the BxInt and Int etchplains comprise several sandstone escarpments (Figs. 6 and 9). Most small unmapped relics of bauxitic or Intermediate landforms scattered South of the Sahelian zone and West of 4°E are actually remnants of the BxInt etchplain (e.g., Grandin, 1976; Boulangé, 1984; Beauvais and Chardon, 2013; Grimaud et al., 2018; Sawadogo et al., 2020; e.g., Fig. 10).

To summarize, the Intermediate mantled etchplain (grouping BxInt, Int and IntS) occupied the entire surface of Northwestern Africa (Fig. 6). It was functional after 45 Ma and until the end of the Oligocene (24 Ma). Large parts of the Sahara are still underlain by part of its weathering mantle. The etchplain has been stripped off from the slopes of the Hoggar hotspot swell.

4.2. *Bauxitic Province of the Cameroon Rise upland (BxCRu)*

This province is defined as the crestal region of the Cameroon Rise surrounded by an escarpment system (Figs. 2 and 6). The upland slops down northwestward, with its highest topography (1800–3000 m a.s.l.) being made by volcanic edifices (i.e., the Cameroon Volcanic Line; Fig. 4) closest to its southeastern edge. Internal relief of the upland is complex, with an imbrication of steps and tablelands, but the salient patterns of landform-regolith associations may be summarized as follows after the exhaustive study of Morin (1987, 1989).

Earliest lava flows of the Cameroon Line (Early Eocene, 56–51 Ma; Moundi et al., 2007) erupted over a deeply weathered, low-relief landscape preserving a thick kaolinic weathering profile. These flows rework pebbles of bauxitic duricrust, suggesting the Bauxitic Mantled Etchplain is fossilized under the volcanics of the Cameroon Rise (Fig. 9d). Ubiquitous bauxitic duricrusts cap a variety of reliefs of the upland, but are mostly restrained to volcanic substrates. Three main bauxitic landform-regolith associations are distinguished: (i) primary bauxitic duricrusts capping plateaus and hills on the main interfluves, (ii) secondary bauxitic duricrusts cementing bauxite blocks spread on pediments and (iii) associations of coherent to loose colluvial bauxites and Al—Fe laterites caping multiconvex topographies. Ferruginous duricrusting has taken place on pediments preserved in the remaining parts of the upland, especially on granitic basement rocks. Bauxites are preserved on Paleogene volcanic rocks and on Miocene flows as young as 14 Ma (e.g., Momo Nouazi et al., 2020).

There is a need to reappraise the relationships between the detailed landform-regolith associations of Morin (1989) and specific volcanic units for which a growing geochronological data set has become available (e.g., Njonfang et al., 2011). Until then, one can only conclude that the Cameroon Rise upland is a remnant of the Bauxitic Mantled Etchplain, covered by Paleogene and Neogene volcanics that have undergone lateritic bauxitization in the Late Miocene (14–6 Ma). Oligocene (?) / Neogene bauxitization may be attributed to (i) very high rainfalls on the Cameroon Rise, which acted as an orographic attractor to northeastward-directed Atlantic moisture fluxes and (ii) the high sensitivity of freshly erupted ignimbrites and basalts to enhanced lateritic weathering (Ségalen, 1967; Fritsch, 1978; Morin, 1989; Burke and Gunnell, 2008). High-elevation Miocene bauxitization could tentatively be correlated with the main weathering period of the High glacis

system i.e., during the Miocene climatic optimum (Fig. 5; see also Schwarz, 1997).

4.3. Reliefs inherited from the mantled etchplains

4.3.1. Residual Composite Topography (RT)

This landform-regolith association corresponds to topographic massifs up to several hundreds of meters high that are topped by relics of Paleogene etchplains (Fig. 6). These massifs have a differentiated relief resulting from a punctuated dissection history of the etchplains and preserve relics of ferricrete-capped piedmont pediments of the High and/or Middle glacis systems (Fig. 11a and b). RT terrains coincide with Paleoproterozoic greenstone belts and supracrustal slivers hosted by Archean granitoids (Figs. 4 and 6), which are made of rocks prone to duricrusting such as mafic volcanics, intermediate to felsic volcanosediments and banded iron formations (BIF). Numerous small unmappable RT units are scattered South of the Sahelian zone (e.g., Beauvais and Chardon, 2013; Figs. 2 and 6).

In RT piedmont contexts, glacis ferricretes are dominantly Fe-oxide-cemented conglomerates made of clasts of bauxitic and Intermediate duricrusts, Fe-nodules and quartz fragments taken in a matrix of reworked saprolite and Fe-nodules (Fig. 12). Debris- and mud flow are common facies of glacis covers (Fig. 12a). Intermediate ferricretes and the nodules / concretions formed in kaolinic mantles underlying Bauxites and Intermediate duricrusts (e.g., Fig. 10) are the dominant sources for the clasts in glacis detrital ferricretes (e.g., Sawadogo et al., 2020; Fig. 12a). Glacis ferricretes on distal parts of piedmonts are still detrital but finer-grained, as are the ferricretes capping the pediplains described below. Such ferricretes can easily be mistaken for duricrusts derived from a saprolite seating on its parental bedrock (Chardon et al., 2018) as are those in which advanced iron impregnation obliterates conglomerate textures (Fig. 12a). The thickness of the weathering profiles developed under High and Middle glacis ferricretes rarely exceed 15 and 5 m, respectively.

BIF-bearing supracrustal belts forming RT units host two of the highest summits of the Guinean Rise (i.e., Mount Nimba at 1752 m a.s.l. and the Simandou at 1658 m a.s.l.; Fig. 2). These massifs generally culminate above their surrounding plains by >800 m. Their crests and uppermost slopes are capped by cangas (i.e., ferricretes made of oxidized (weathered) BIF fragments cemented by Fe-oxydes) preserving patches of bauxites on non-BIF bedrocks in depressions of the crestal regions (Fig. 11b; e.g., Pascual, 1988). The massifs are flanked by relics of wide concave pediments of high (>400–500 m) vertical amplitude. These pediments are sealed by Intermediate ferricretes topping a > 30 m thick kaolinic weathering profile, laterally correlating with remnants of the Int etchplain (Fig; 11b). This shows that bauxite-capped BIF RT massifs formed mountains above the Intermediate Mantled Etchplain.

In rain forest environments i.e., towards the coastal regions of Sierra Leone and Liberia, as well as in Westernmost Cameroon (Figs. 3 and 6), RT massifs have generally a lower height above the plains. Their duricrusts and part of their underlying regolith appear to have been degraded under rainforest climatic conditions. This resulted, at least in some areas, in the exhumation of bedrock structural ridges that are flanked by piedmonts with thick, mostly unconsolidated *catena* (e.g., Birchall et al., 1980; van Mourik et al., 1980).

4.3.2. Etched Bedrock relief (EBr)

This map unit refers principally to groups of bare granitic or gneissic reliefs emerging from the plains. Such reliefs characterize most of the basement of the Iforas, Aïr and Hoggar massifs (Capot-Rey, 1951; Rognon, 1967; Morel, 1985; Figs. 3 and 6). Mappable occurrences are mostly fields of inselbergs, whalebacks and tors that are generally separated by sandy pediments (e.g., Fig. 11c). In Sub-Sahelian West Africa, the amplitude of inselberg reliefs can exceed 500 m (e.g., Fig. 11c). Two main clusters have been mapped south of 16°N, in the Southeastern Guinean Rise, and in Nigeria (Figs. 3 and 6). The Mounts Loma constitute an EBr unit hosting the culminating point of the Guinean Rise (1948 m a.s.l. at Bitumané Peak; Figs. 2 and 6). That summit is even capped by what appears to be a remnant of Intermediate ferricrete formed on a thin dolerite sill (Jaeger, 1953; Daveau, 1971).

The morphogenesis of granitic inselbergs, whalebacks and tors is controlled by a variety of geological and morphoclimatic factors (Thomas, 1994). Nonetheless, the generation of vast and dense fields of such landforms, especially if they are several hundreds of meters high, must somehow involve exhumation of the lower front of a very thick weathering profile (Ollier, 1960) i.e., typically that of a mantled etchplain. This is suggested by spectacular cliff exposures along escarpments of the eastern piedmont of the Fouta Djalon (Figs. 2 and 6), which show >400 m high bauxite-capped inselbergs in the process of being stripped of their weathering mantle. Although the relief of the original weathering front is generally amplified by erosion beyond stripping of the sole mantled etchplain (Thomas, 1994), we therefore consider EBr remnants as reliefs inherited from the Paleogene etchplains.

As seen above, the crystalline reliefs of the Tuareg shield (Aïr, Iforas and Hoggar; Figs. 2 and 6) are inherited from the stripping of the Int etchplain (e.g., Fig. 9b and d). The sub-Saharan distribution of EBr units has probably several causes (petrographic, geomorphologic). Nonetheless, the EBr cluster fringing the continental divide on the uppermost Atlantic slope of the Southeastern Guinean rise (Figs. 2 and 6) could result from enhanced erosion along the uppermost reaches of the short Atlantic drainages. Small patches of etched granitic bedrock, and, more commonly, individual inselbergs, are scattered over the plains of Sub-Saharan West Africa (e.g., Grimaud et al., 2018) and over the Sahara outside the Tuareg shield (e.g., Dresch, 1959).

Bare sandstones exposed inland Conakry, around the Volta basin and along the northern flank of the Benue valley have also been mapped as EBr landform-regolith associations (Figs. 2-4 and 6). They would have been exhumed by essentially the same processes as granitic terrains, although the resulting landforms would be more specific to sandstones (e.g., Boulvert, 2005).

4.4. Pediplains

The remaining part of Sub-Saharan West Africa devoid of alluvial cover consists of pediplains (Fig. 6). Pediplain landform-regolith associations are of two types. The first type corresponds to relict pediplains of the ferricrete-capped High and Middle glacis systems (HgPd, MgPd). The second type corresponds to a regional, Sub-Saharan pediplain resulting from the degradation of the Middle glacis Pediplain. This pediplain is divided in four bands based on latitudinal (i.e., zonal) contrasts in landform-regolith associations (SPd, RPd, RPdDe, MCPd). Development of the pediplains mostly consisted in stripping the Paleogene mantled etchplains and, in some areas, beyond the etchplains' regolith mantles i.e., by eroding the underlying bedrock. All the map units defined in the preceding sections are therefore relictual landform-regolith associations that survived the installation of pediplains. The pediplains described below are all studded with relics of these older landform-regolith associations too small to be mapped at the scale of Fig. 6.

4.4.1. Relict pediplains

4.4.1.1. High glacis Pediplain (HgPd). The High glacis pediplain is preserved on both platform sedimentary cover and crystalline basement, forming a girdle of four main patches i.e., (i) the southern Senegalo-Mauritanian basin, (ii) the Fouta Djalon area and Southeastern Guinean Rise, (iii) the Volta basin and its surroundings and (iv) most of Nigerian lowlands (Figs. 2-4, 6 and 9). The typical occurrence (Fig. 13a) is a very-low local relief (<15 m), duricrusted rolling plain of 3–5 km wavelength, with a distinctive bee-nest shape drainage map pattern. The thickness of the weathering profile does not exceed relief amplitude. The

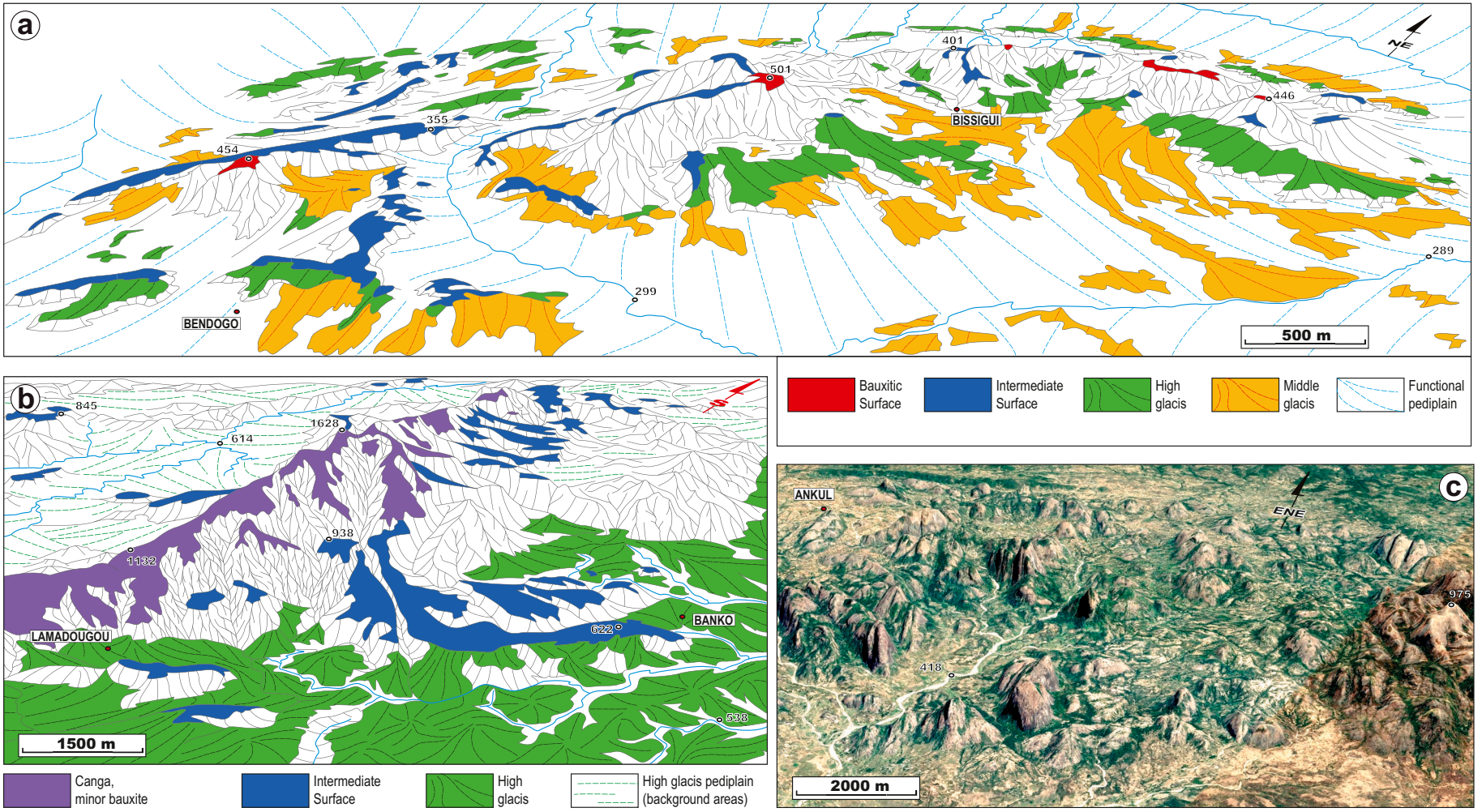

Fig. 11. Aerial views of composite landform-regolith associations draping reliefs inherited from the Paleogene mantled etchplains. (a) Residual Composite Topography (RT) of the Goren greenstone belt, Central Burkina Faso (Figs. 3 and 6). Terrains in white are mostly active erosional landforms. The functional pediplain corresponds in this case to the Sahelian Pediplain (SPd). Total width of the view: 14 km; Bissigui village coordinates: 13.1405°N/1.2415°W. (b) Residual Composite Topography (RT) of a BIF bearing supracrustal belt (Southern Simandou range, Eastern Guinea; Figs. 2 and 9c). Steep terrains in white are mostly erosional. The displayed segment of the range is ~17 km long; Banko village coordinates: 8.5457°N/8.9750°W. (c) GoogleEarth™ view of the Ankul area, Central Nigeria, showing a granitic inselberg field typical of Etched Bedrock Terrains (EBr). Total width of the view: 19 km; Ankul village coordinates: 9.3827°N/7.9647°E; © 2022 Maxare Technologies. Spot heights in meters. Vertical exaggeration is x 2.5 in (a) and x 2 in (b) and (c).

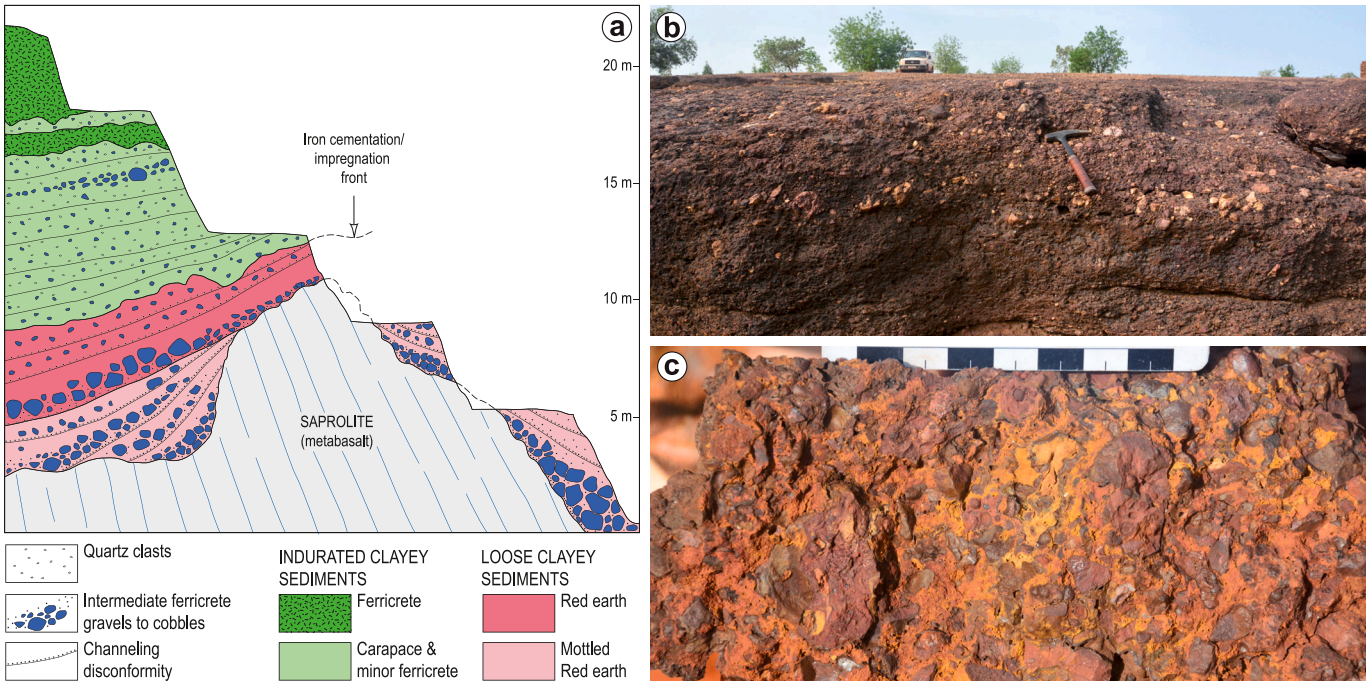

Fig. 12. Illustrations of relict Neogene piedmont pediment material (High and Middle glacis) such as found in Residual Composite Topography (RT) terrains or around small isolated massifs in relict and zonal pediplain environments. (a) Sketch roadcut section through stacked debris flows of a High glacis relic (Bondoukou area, Northeastern Côte d'Ivoire; coordinates: 8.18709°N/2.93752°W). Sediments are reworked weathering profiles filling up gullies >10 m deep. Sedimentologic structures are erased up-section as duricrusting increases, so that the topping ferricrete has no recognizable detrital character (comparable to that of Fig. 13a). (b) Middle glacis conglomeratic ferricrete, Kongoussi area, Goren greenstone belt, Central Burkina Faso. Light-colored clasts are bauxites and darker cobbles are Intermediate ferricretes and Fe-nodules. The matrix is a cemented gravel of Fe-nodules. (c) High glacis conglomeratic ferricrete. Gravels (mostly angular) are pink bauxites (locally pisolithic) and Intermediate ferricretes and Fe-nodules, cemented by a mix of kaolinite-rich clays and Fe-oxydes (same glacis relic as in (a) but 5 km farther to the North; scale bar in cm). (For interpretation of the references to colour in this figure legend, the reader is referred to the web version of this article.)

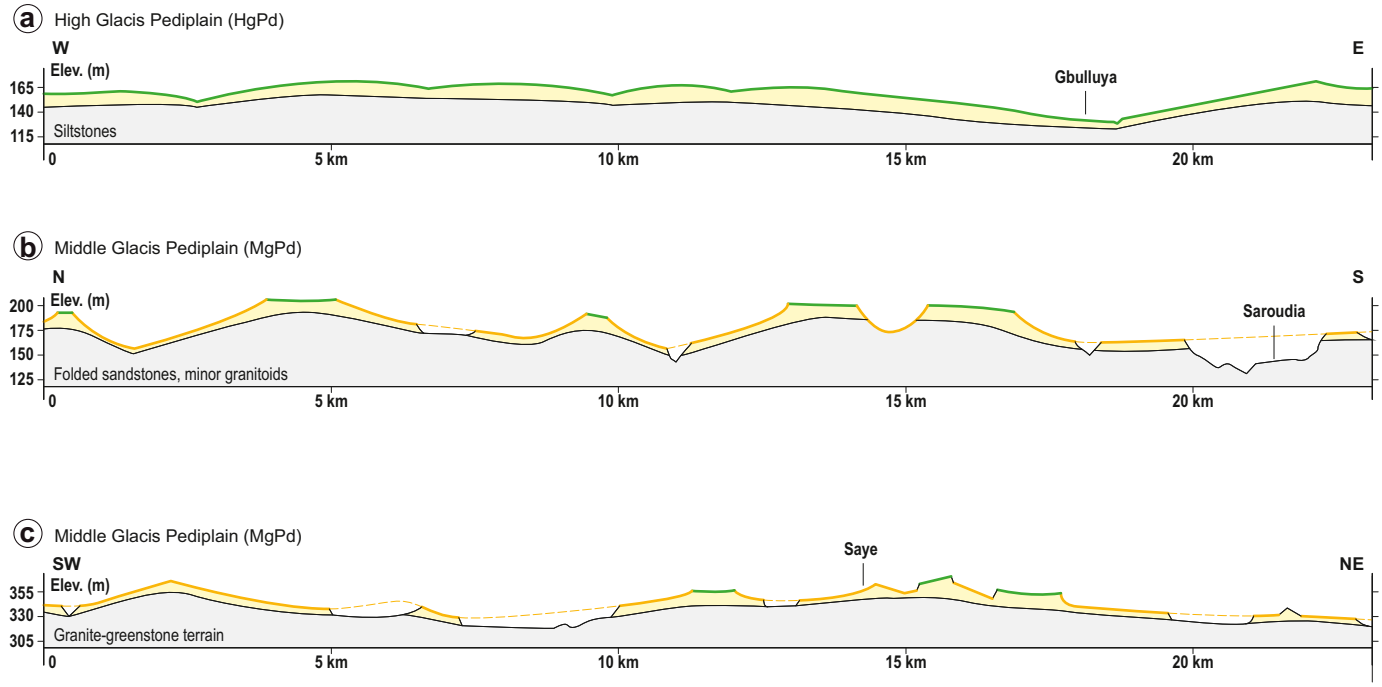

Fig. 13. Simplified cross-sections illustrating the landform-regolith associations of relict Neogene pediplains. Duricrusts are schematized as thick colored lines (green: High glacis; orange: Middle glacis); weathering mantles in yellow; geological substrate in grey. (a) High glacis pediplain (HgPd), North-Central Ghana. Gbulluya village coordinates: 9.4865°N/1.0126°W. (b) Middle glacis pediplain (MgPd), Southeasternmost Senegal. Saroudia village coordinates: 12.5227°N/11.5780°W. (c) Middle glacis pediplain (MgPd), Northwestern Burkina Faso. Saye village coordinates: 13.3021°N/2.2399°W. (For interpretation of the references to colour in this figure legend, the reader is referred to the web version of this article.)

capping ferricrete is at best a few meters thick, generally detrital, alveolar or globular (Fig. 14a). It is a cemented mix of gravel, sand and silts with visible Fe-oxides fragments and nodules or quartz clasts at depth. In high plain contexts, especially in the vicinity of older landform-regolith relics such as in the Guinean highlands (e.g., Boulvert, 2005), the HgPd is a convexo-concave pediplain with hills preserving Intermediate ferricretes. This configuration also applies to the HgPd remnant South of the Cameroon Rise (Martin, 1970; Yongué and Belinga, 1987), where High glacis are being degraded under the rain forest environment (Embrechts and Dedapper, 1987; Kadomura and Hori, 1990).

In Nigeria, duricrusting of the High glacis pediplain decreases eastward (Figs. 2 and 6). Ferricrete caps are almost absent in the Benue valley except along its southern piedmont i.e., close to relicts of the Intermediate Etchplain (Fritsch, 1969). This is attributed to the rain shadow effect exerted by the Cameroon Rise on Atlantic and equatorial moisture fluxes that would have prevented weathering of its hinterland (Ségalen, 1967; Fritsch, 1978; Morin, 1989). The lack of sufficient duricrusting allowed for a greater dissection of the High glacis Pediplain in some regions of the Benue valley (e.g., Michel, 1973b).

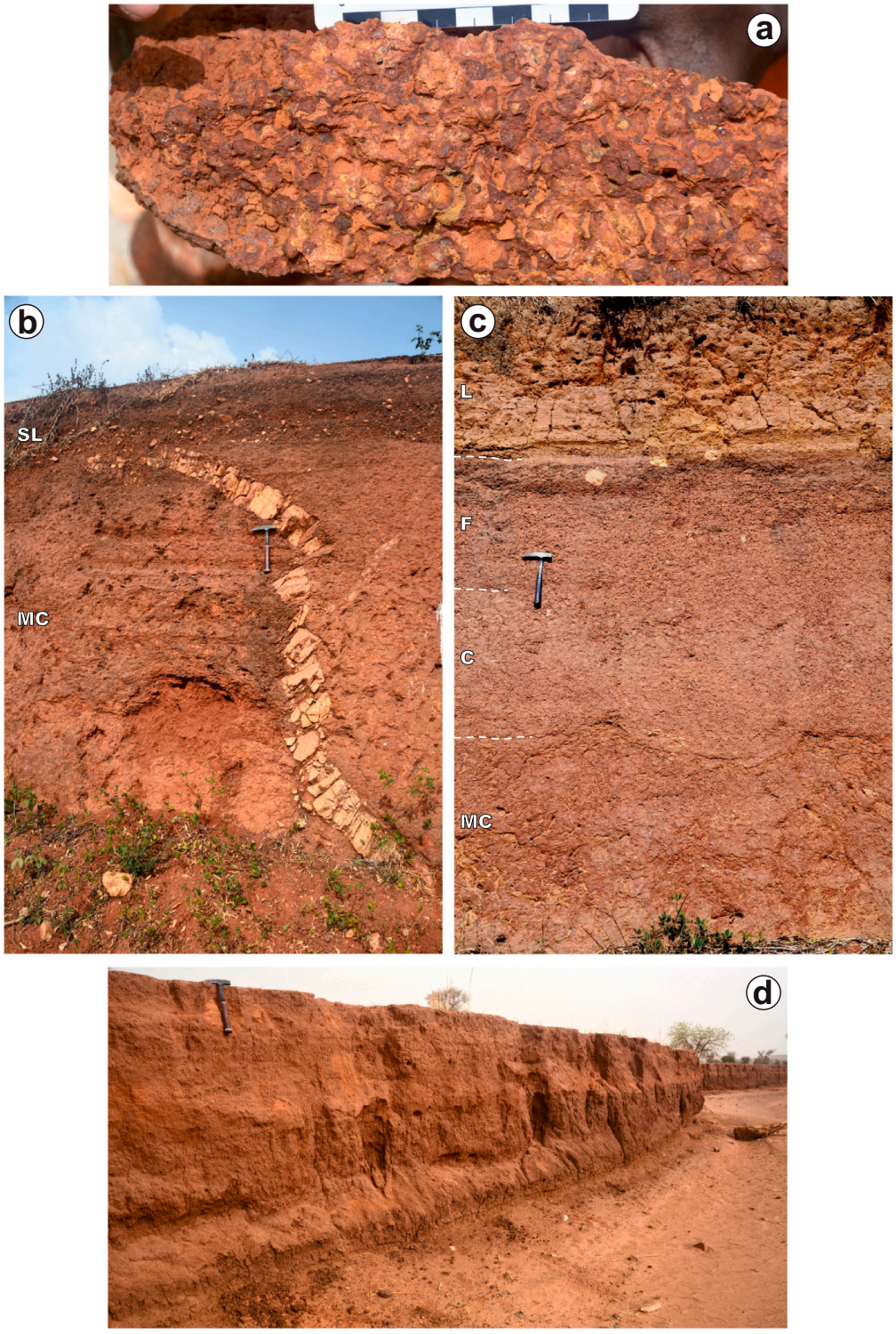

Fig. 14. Illustration of selected types of pediplains regolith. (a) Alveolar ferricrete typical of the High and Middle glacis as found in relict pediplains (HgPd, MgPd), the Rolling Pediplain (RPd) or the Sahelian Pediplain (SPd). Example is taken from a High glacis interfluve in the Madiani area, Northwestern Côte d'Ivoire (scale bar in cm). (b)-(c) Stone lines of the Degraded Rolling Pediplain (RPdDe) in Southeastern Côte d'Ivoire. (b) Quartz dike feeding a stone line near Akoupé. MC: mottled clays; SL: stone line. (c) Section of a hill apex near Bonahoin. MC: mottled clays; C: Fe-Carapace; F: ferricrete; L: loam. The stone line encompasses horizons C and F. Only large quartz clasts are visible in the gravel given the intensity of iron impregnation. (d) Streamcut through fine-grained sediments of the Sahelian Pediplain (SPd), Kongoussi area, Burkina Faso. The granitic bedrock locally crops out at the base of section, where it is converted into a smectite-rich arene bearing carbonate nodules. See Fig. 15 for the location of the various types of regolith in the catena of the zonal pediplains.

4.4.1.2. Middle glacis Pediplain (MgPd). The Middle glacis pediplain results from partial dissection of the High glacis pediplain. It is a composite, multi-concave and almost fully duricrusted pediplain, whose interfluves are made of relictual plateaus of the ferricrete-capped High glacis pediplain (Fig. 13b and c). The weathering profile underlying the pediplain is that of the High glacis stage that has been only locally weakly rectified downslope by Middle glacis erosion. The Middle glacis ferricretes are Fe-oxide cemented gravel or sand covers generally less than a meter-thick. These duricrusts are comparable to those of the HgPd and are typically globular or alveolar (e.g., Fig. 14a). Weathering fringes a few decimeters-thick generally formed by reactivation / deepening of the High glacis weathering profile under downslope portions of Middle glacis (Eschenbrenner and Grandin, 1970). The pediplain has a relief amplitude of 15 to 30 m and its lower parts are locally dissected and occupied by Low glacis and/or alluvial plains (e.g., Fig. 13b and c). The Middle glacis Pediplain typifies the Soudanian duricrusted landscape (Grandin and Joly, 2008; Fig. 3) and is particularly well preserved on Paleoproterozoic greenstone terrains, where it is studded with small relictual massifs carrying relics of the Paleogene etchplain(s) and inselbergs (Daveau et al., 1962; Michel, 1969; Eschenbrenner and Grandin, 1970; Michel, 1973a; Grimaud et al., 2015). No mappable remnants of the pediplain are found East of 4°E, although Middle glacis installation appears to have contributed in some areas to the dissection of the High glacis Pediplain (Ségalen, 1967; Fritsch, 1969, 1978; Michel, 1973b).

4.4.1.3. Regional significance of the relict pediplains. At the time they were functional, both the High and Middle glacis relict pediplains were connected to the glacis draping the piedmonts of the relictual massifs (RT units mostly; Fig. 11A and B). Both pediplains are preserved in current savannas (the Guinean and Soudanian zones; Figs. 3 and 6), which appear to have been propitious to optimal morphogenesis, duricrusting and preservation of the two paleo-pediment systems. Their preservation from stripping is due to their ferricrete caps (Grimaud et al., 2015). HgPd and MgPd associations are therefore quasi-fossil landform-regolith associations, dating back from the early Late Miocene (~11 Ma) and the Latest Miocene (~6 Ma), respectively, according to Ar—Ar dating (Fig. 5).

High and Middle glacis relics are not preserved north of the Sahelian zone (Fig. 3), except on some BIF reliefs of northwestern Mauritania, where ferricrete-capped glacis relics are stepped under an Int etchplain remnant (Nahon, 1976; Michel, 1977a). Over most of the Sahara, even if the High and Middle glacis systems may have developed, they did not have a decisive impact on the relief or the landform-regolith associations, for the very low regional Saharan relief was eventually leveled by regs that barely removed the Intermediate ferricrete.

4.4.2. Zonal Pediplains

Zonal pediplains occupy nearly 50% of the map area. Because they consist of the monotonous repetition of subdued hills, they are called rolling pediplains (Rohdenburg, 1969; Chardon et al., 2018). The generic term Rolling Pediplain (RPd) has been ascribed to the widest of the zonal pediplains, which results from only a slight modification of the Middle glacis pediplain. The Degraded Rolling Pediplain (RPdDe) and the Multi-Convex Pediplain (MCPd) may be seen as the Rolling Pediplain having been further degraded at lower latitudes (i.e., today's Forest zone; Figs. 3 and 6). Finally, the Sahelian Pediplain (SPd) results from a modification of the Rolling Pediplain at higher latitudes (Figs. 3 and 6). In the end, the latitudinal map pattern of zonal pediplain landform-regolith associations (Figs. 6 and 15) reflects the climatic zonation of morphopedological processes stressed out by Millot (1980, 1983) and accounted for by the model of Raunet (1985). Because they are still functional, and considering the ~6 Ma terminal age of the Middle glacis pediplain from which they derive (Fig. 5), one must consider zonal pediplains as Plio-Quaternary.

4.4.2.1. Rolling Pediplain (RPd). This landscape is directly inherited from the Middle glacis pediplain, with its interfluves capped by dismantled High glacis ferricretes (Fig. 15b). The slopes are rectilinear to slightly convexo-concave, which contrasts with those of the Middle glacis pediplain that are more systematically concave (Figs. 13b, c and 15b). Away from hill apexes, mottled clays are the most advanced products of weathering of the bedrock. Slopes are covered over most of their width by colluvial gravel and loam sheets indurated to various degrees (from unconsolidated up to become a carapace, and, more rarely a ferricrete) (Fig. 15b). These slope covers are generally referred to as latosols (Tardy, 1997). The gravel units are made of Fe-nodules and Fe-nodule fragments mostly reworked from the relict High glacis ferricrete, as well as quartz clasts. The main sources for the loam units are (i) material stripped off from the relict High glacis ferricrete and (mostly) its underlying weathering horizons and (ii) material having been brought up from under the colluvial cover by termites (reworked termite mounds) (Fölster, 1969a).

Stone lines are distinctive layers in the regolith composed of angular to subrounded fragments of quartz, Fe-duricrust and more rarely, bedrock, as well as Fe-nodules. Stone lines generally floor each gravel and loam colluvial unit. They are typical of the Rolling Pediplain (RPd) and its two southern derivatives (RPdDe, MCPd) (Nye, 1954; Brückner, 1955; Fölster, 1969b; Rohdenburg, 1969; Lévêque, 1979b; Teeuw, 1987). The deepest of the stone lines rests atop the mottled clays, and locally atop deeper weathering horizons where the mottled horizon has been eroded away by slope processes. Basal stone lines are seen to be fed by dismantled quartz dikes as well as the High glacis ferricrete (e.g., Fig. 14b). Gravel dominates the slope material of the Rolling Pediplain, but the proportion of loam and loamy colluvial units increases southward. The drainage network is slightly entrenched under a scarplet cutting the lower indurated portions of slopes. Current solid fluxes to river beds are dominated by colluvial slope material (Fig. 15b).

The southern and northern boundaries of the Rolling Pediplain corresponds to the disappearance of the High glacis ferricrete relics on interfluves. Its limits mimic the isohyet pattern, in particular its southern boundary that coincides with the invagination of the 1250 mm/yr curve marking the forest-savanna boundary in Côte d'Ivoire (Avenard et al., 1974; Pèltre, 1977; Figs. 3 and 6).

4.4.2.2. Degraded Rolling Pediplain (RPdDe). This map unit occupies a 100 to 200 km wide strip south of the Rolling Pediplain (Fig. 6). Its hill tops are pronouncedly convex as a consequence of removal of the High glacis ferricrete relics, so that the pediplain has become strictly convexo-convave (Fig. 15d). While the Fe-carapace inherited from the High glacis can still be locally preserved on few hilltops, a new carapace and even a ferricrete can develop under hill apexes at the expense of the lowermost colluvial cover, including the basal stone line (Fig. 14c) especially on non-granitic basement. Hills are in this case cored by an apparently comprehensive weathering profile although the saprolite and the mottled clay horizons underlying the basal stone line are essentially inherited from earlier stage(s) of weathering. Active solid fluxes to river beds are provided by both colluvial slope cover material and the upper horizons of the weathering profile (Fig. 15c).

4.4.2.3. Multi-Convex Pediplain (MCPd). The northern boundary of this map unit is transitional with the RPdDe unit. The two occurrences are (i) the coastal regions of Sierra Leone and Liberia and (ii) Southwestern Cameroon (Figs. 3 and 6). In the latter case, instead of deriving from the degradation of the Middle Glacis pediplain, the Multi-Convex Pediplain derives from the High glacis pediplain, with relict Intermediate ferricretes on hill tops. The Multi-Convex Pediplain consists of pronouncedly convex hills separated by flat-bottom valleys (Fig. 15d). Hills are blanketed by continuous colluvial mantles made dominantly of loam material. Multi-convex pediplains are called half orange landscapes on the basis of their hills cross-sectional pattern (e.g., Thomas, 1994; Fig. 15d).

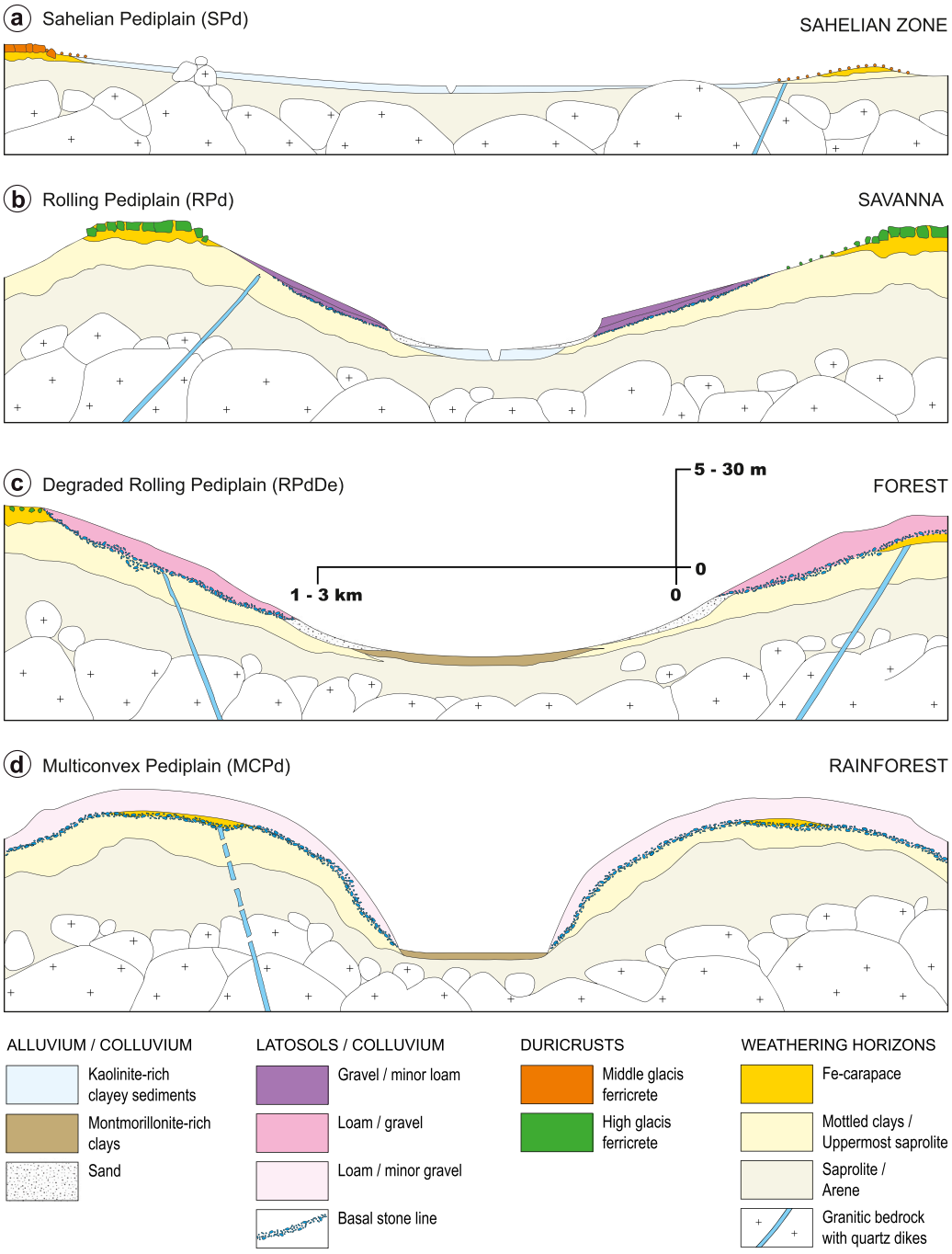

Fig. 15. Schematic catena cross-sections of the Late Neogene zonal pediplains, modified from the diagram concept of Raunet (1985). (a) Sahelian Pediplain (SPd). (b) Rolling Pediplain (RPd). (c) Degraded Rolling Pediplain (RPdDe). (d) Multiconvex Pediplain (MCPd). Only the basal stone lines are shown. The various sedimentary units that constitute the colluviums cannot be shown at this scale. See text for further explanations.

Hills are more systematically cored by the composite weathering profile that started to develop in the Degraded Rolling Pediplain (Kadomura and Hori, 1978, 1990). Current solid fluxes to the river beds are exclusively made of loam cover material.

4.4.2.4. Slope processes of the zonal pediplains under savanna and forest environments. Systematic logging allowed Fölster (1969a, 1969b) to document at least 3 erosional/deposition phases of slope pedimentation in the southern RPd and in the RPdDe (see also Burke and Durotoye, 1971). Each pedimentation phase was generally followed by a weathering phase (mostly cementation) of the gravel/loam material emplaced by pedimentation, with an impact on the underlying weathering profile (Fölster et al., 1971a). Detailed accounts of recent to active slope dynamics of the RPdDe unit in Sierra Leone were provided by Teeuw (1987, 1991) through the study of stone line systems. The RPdDe colluvial mantles were also investigated through attempted correlations with radiocarbon-dated Holocene (<12,500 yr BP) alluvial terraces (e.g., Burke et al., 1971; Thomas and Thorp, 1980, 1985; Hall et al., 1985; Teeuw, 1987). The prevailing view is nonetheless that stone line-bounded colluvial units would sign semi-arid or arid climate incursions in the humid tropics (Thomas and Thorp, 1992). In particular, stratigraphy, human artifacts chronology and radiocarbon dating in the colluvial mantles of the Multi-Convex Pediplain would argue for a major arid phase between 20,000 and 12,000 yr BP (e.g., Kadomura and Hori,

1990). That phase was ascribed to the last glacial maximum (LGM), which brought the desert front at today's outer forest zone and saw the installation of the so-called Ogolian dune fields over the Sahelian zone (Michel, 1973a, 1980; Thomas and Thorp, 1992; Figs. 3 and 6). The Holocene paleoenvironmental colluvial record of the Multi-Convex Pediplain is richly documented i.e., post-LGM reforestation (12–9 Ka BP), period of closed forests (9–3 Ka BP) and finally aridification and anthropogenic forest degradation (3–1 Ka BP and forward) (Kadomura and Hori, 1990).

4.4.2.5. Sahelian Pediplain (SPd). The Sahelian pediplain occupies a 200–300 km wide corridor between the Savanna belt and the Sahara (i.e., mostly the Sahelian zone; Figs. 3 and 6). The northern limit of the Sahelian pediplain is not always clear cut, with pediments grading into flat regs. The Sahelian pediplain has a very-low relief. It is made of straight and nearly flat pediments commonly >10 km wide (Fig. 15a). Pediments are covered by a detrital blanket rarely exceeding a few meters in thickness (Fig. 14d). This blanket consists of unconsolidated kaolinite-rich loam sheets separated by gravels of Fe-nodules and sub-rounded quartz or bedrock fragments. The pediplain is actively resurfaced at each rainy season by sheetflood processes. The fossil Ogolian dunes and the southernmost functional Saharan dunes contribute to the sand fraction of the material being spread on the pediplain (e.g., Michel, 1973a; Chamard and Courel, 1980).

Besides Int relics, the scarce residual reliefs of the Sahelian pediplain are mostly inselbergs. Relict ferricrete-capped Middle glacis plateaus a few meters high are preserved near the southern margin of the Sahelian zone. On the piedmonts of such residual reliefs, a carapace cementing gravels of the Low glacis is seen to underlay the pediment sedimentary layer (Sanfo et al., 1992; Sawadogo et al., 2020). Away from these piedmonts, the pediment sedimentary layer rests directly on weakly decomposed bedrock (Figs. 14d and 15a). But in various areas, Sahelian pedimentation (and, farther North, reg functioning) does not appear to have stripped off the relictual Intermediate weathering mantle. The 3.3–2.9 Ma age of the Low glacis ferricrete at Tambao (Beauvais et al., 2008) provides a weathering milestone in the history of the Sahelian Pediplain, which may be considered as the continuation of the Low glacis pedimentation cycle (e.g., Michel, 1969, 1973a). Besides, Sahelian pedimentation would have started as early as 6 Ma i.e., after duricrusting and abandonment of the Middle glacis system (Fig. 5).

4.4.2.6. Zonal pediplains: synthesis. Zonal pediplains have evolved over the Plio-Quaternary and should therefore have undergone a long and potentially complex history. Only part of their Late Quaternary landform-regolith record has been deciphered so far, mainly based on radiocarbon dating. Until further insights are provided by other dating means, one may however address global trends in the pediplains evolution.

Zonal pediplains rectified the landforms of the Middle glacis pediplain mostly by slope processes i.e., pedimentation, mostly outside domains of weathering-prone lithologies preserving duricrusted landform-regolith associations (Bx, BxInt, Int, RT, HgPd, MgPd; Fig. 6). Pedimentation took place at the expense of Middle glacis stage regolith mantles that had reached a state of pedoclimatic disequilibrium (Boulet et al., 1997) around 6 Ma i.e., the last main regional duricrusting episode in West Africa. Slope indeed had to adapt to cooler and dryer Pliocene-Quaternary climate (e.g., deMenocal, 2004; Senut et al., 2009). Pedoclimatic disequilibrium enhanced hydro-pedological processes that concurred to ferricretes disaggregation and loosening of underlying weathering mantles (Boulet et al., 1977; Chauvel et al., 1977; Leprun, 1977). Towards the arid tropics and the Sahara, enhanced loosening of the regolith favored extreme mechanical planation by Sahelian pediments and desert regs (SPd and ReSp map units) (Millot, 1980, Millot, 1983). Under seasonally dry climate(s) of the savannas and the outer forest (RPd, RPdDe), moderate or intermittent loosening of the regolith led to episodic remobilization and cementation of slope material (Fölster, 1969b). By contrast, perhumid forest environments (MCPd) favored regolith regeneration by enhanced weathering and bioturbation (Boulet et al., 1997). This contributed to produce and maintain loamy covers closer to dynamic equilibrium that could keep a more reliable recent (Holocene) paleoenvironmental record.

4.5. Saharan landform-regolith associations and alluvial plains

4.5.1. Silcrete-Capped Hamada (Ha)

Hamadas are very large sedimentary veneers a few meters thick that unconformably overly the duricrusted remnants of the Intermediate Mantled Etchplain (see Fabre, 2005). They mostly consist of continental carbonates hosting a large proportion of aeolian sand. The series are silicified, particularly up-section, which formed a protective duricrust (silcrete). Hamadas are interpreted as sebkras or swamps of regional extent (Fabre, 2005). Their carbonates provided an Aquitanian (23–20 Ma) gastropod fauna (Jodot and Rouaix, 1957; Villemur, 1967; see Fabre, 2005).

4.5.2. Saharan silicifications: age and origin

The present work suggests that silicification of the Intermediate Etchplain in the Sahara (IntS) took place in the Late Oligocene (30–23 Ma). That of the Hamadas would be loosely dated as post-Aquitanian (<20 Ma). Only Fabre et al. (1996) and Fabre (2005) have addressed the geological context and significance of these duricrusts in our map area (Fig. 6) since the first exploratory study of Saharan silicifications (Auzel and Cailleux, 1949). A comparable morpho-climatic context of silicification would be that of Southeastern Kuwait, where Khalaf et al. (2020) argued for a groundwater table origin for the silcretes (chert horizons) due to climate cooling in the Oligocene or Miocene.

4.5.3. Reg and Fluvio-aeolian Sand Plain (ReSp), Erg (Er)

These map units refer to topics that are beyond the scope of the present study. They represent landform-regolith associations that are still functional and archetypical of the desert environments (Fig. 6). In particular, the ReSp unit is the end product of a long, slow and very limited post-Early Miocene (i.e., post-Hamadas) morphogenesis, for which only the Late Quaternary is reasonably deciphered (e.g., Fabre, 2005 for topical aspects of the recent geological evolution the Western Sahara). Anyhow, preservation of the Oligocene Intermediate etchplain throughout the Sahelian and Saharan domains outside the Hoggar swell argues for negligible erosion or relief creation since ~24 Ma (Figs. 6 and 16).

4.5.4. Alluvial plain (AP)

Besides coastal, deltaic and estuarian occurrences, this map unit refers to three main active inland deltas (Fig. 6). That of the K-Gana river, in the East (Fig. 6), represents the uppermost part of a deltaic system fringing the northwestern shore of Lake Chad. The two others are the Niger and Sourou inland deltas, which are inferred to have installed during aridification of the LGM (Jacobberger, 1987 and references therein; Fig. 6). Their formation was also considered within the framework of regional slope modification due to the growth of the Hoggar swell (Grimaud et al., 2014; Chardon et al., 2016).

5. Interpretation of the regional landform-regolith patterns

5.1. Pre-Pliocene pan-tropical landform-regolith associations: continental and global climatic proxies

5.1.1. Paleogene mantled etchplains

The Bauxitic Mantled Etchplain results from protracted, very intense lateritic weathering initiated in the Late Cretaceous. The etchplain must have extended north of the Tagant (Michel, 1977b; Figs. 2 and 6), but it could have been stripped off there before installation of the Intermediate

Mantled Etchplain. But the Intermediate kaolinic regolith mantles of the Sahara could as well be in part inherited from the late Cretaceous to Eocene weathering that took place under the Bauxitic Etchplain. This would be consistent with the numerous inselberg studding the Reguibat shield that dominate Intermediate ferricrete remnants.

The Bauxitic Mantled Etchplain started to be dissected after ~45 Ma. It is interpreted as Pan-African (Valeton, 1991), with remnants found up to central Chad (Koro, ~16°N), in western and northern Central Africa, as well as along the eastern edge of the Southern African plateau, from Tanzania to South Africa (see also De Putter and Ruffet, 2020). But, among other considerations, the formation of post-Eocene bauxites on the Cameroon Rise due to specific morphoclimatic conditions led Tardy and Roquin (1998) to suspect Neogene bauxites among the central and southern African occurrences. In any case, stratigraphic and geochronological dating attest to the development and preservation of Early- to Mid-Eocene lateritic bauxites on the shields of Northern Africa, India and South America (Prasad, 1983, see also Bárdossy and Aleva, 1990; Vasconcelos et al., 2015; Bonnet et al., 2016; Jean et al., 2019) and precisely in relation with conspicuous relict etchplains. The world's Eocene bauxitic mantled etchplains are ubiquitous proxies of the Early Eocene climatic optimum at the end of the last greenhouse period that started in the Late Cretaceous (e.g., Fig. 5b).

The Early- to Mid-Eocene lateritic bauxitic event typifies biostasy (Erhardt, 1955) i.e., a period of particularly hot/wet climate leading to extreme chemical weathering that enhances production and storage of thick regolith mantles under forest-protected soils and favors solute riverine exports to the ocean (see Fairbridge and Finkl, 1980). Accordingly, biostasy favors estuarian and marine chemical sedimentation. In Northwestern Africa, this led to typical carbonate deposits in epicontinental seas and rifted margin basins during the Early- and Mid-Eocene (e.g., Millot, 1970; Bennett and Rusk, 2002), and more specifically to basic chemical sedimentary associations of chert, flint, phosphate, dolomite, glauconite and montmorillonite, with attapulgite as the dominant clay mineral (Millot, 1970).

The Intermediate Mantled Etchplain marks a major period of weathering and regolith production too. Its massive and distinctive

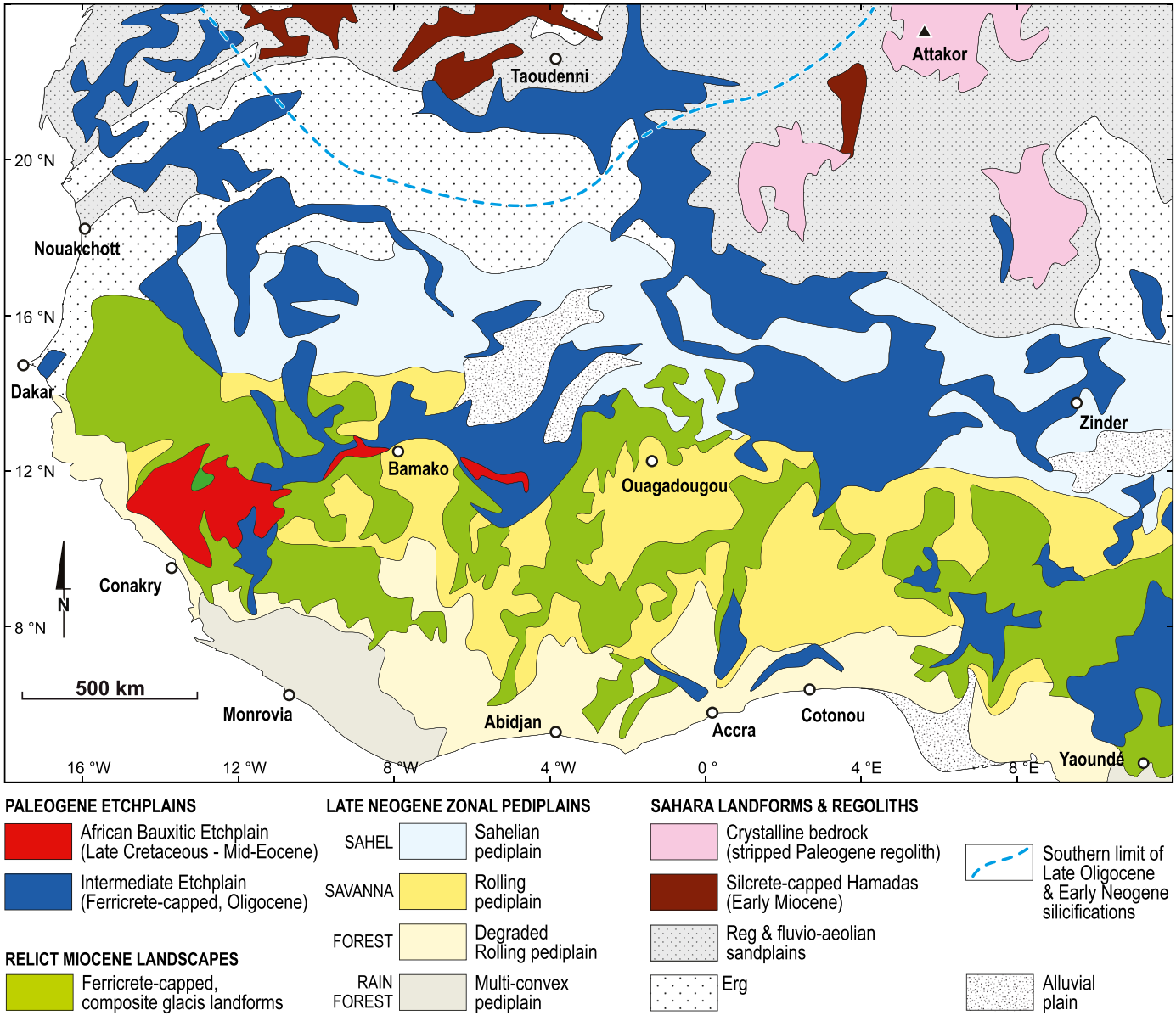

Fig. 16. Synthetic landform-regolith map of Northwestern Africa (simplified from Fig. 6). In particular, large Residual Composite Topography units (RT) and the relict pediplains (HgPd, MgPd; Fig. 6) have been grouped as "Relict Miocene landscapes", whereas Sub-Saharan Etched Bedrock Terrains (EBr; Fig. 6) and small southern RT units were included in the pediplains hosting them.

capping ferricrete, cemented mostly in the Late Oligocene (29–24 Ma), reflects significant relative accumulation of iron, because it formed also outside the influence of inherited bauxitic regolith (e.g., Fig. 8f). Reconnaissance photointerpretation beyond the boundaries of our map as well as bibliographic sources point to numerous and/or vast remnants of the Intermediate Mantled Etchplain between ~4 and 22°N up to the shoulders of the east African rift system (e.g., De Swardt, 1964; Schwarz, 1994; Boulvert, 1996; Guillocheau et al., 2015; Simon, 2015). In fact, most of the laterites mapped north of the equator in Central Africa appear to derive from the Intermediate ferricretes (Beauvais, 1991, 2009; Beauvais and Roquin, 1996; Temgoua et al., 2002; Bitom et al., 2003; Fig. 1b).

An etchplain comparable in every way to the West African Intermediate Etchplain is documented over Western Peninsular India, which weathered mostly at 32–22 Ma (Jean et al., 2019). Old etchplains of cratonic South America also keep record of intense Oligocene weathering at least between 35 and 31 Ma, following Eocene weathering (e.g., Vasconcelos and de Carmo, 2018), suggesting a Paleogene etchplain configuration comparable to that documented in Africa and India. The world's Intermediate mantled etchplains sign intense rock weathering during the "doubthouse" climatic period (Fig. 5b). In particular, Intermediate iron accumulation would have required protracted humid climate with a long dry season (Nahon, 1986) to occupy the intertropical belt, especially in the late Oligocene (30–24 Ma).

5.1.2. Miocene Pediplains

The High and Middle glacis pediplains formed over Sub–Saharan West Africa and possibly over the future Sahara. The High glacis ferricrete and its underlying weathering profile reflect moderate weathering intensities, with much less kaolinite content than the mantled etchplains (Grandin, 2008). East of our map area (Fig. 6), a duricrusted pediment system comparable to the High glacis has been documented downslope relict landform-regolith associations we attribute to the Intermediate Mantled Etchplain (Pallister, 1956; De Swardt, 1964; McFarlane, 1976; Boulvert, 1996; Guillocheau et al., 2015). The High glacis pediplain attests to the prolonged installation of a dry climate propitious to mechanical erosion in the inner tropics during the Early Miocene. Its weathering and duricrusting (18–11 Ma) required seasonally dry/humid climate during the Miocene climatic optimum (Fig. 5b). Along with the bauxitic and Intermediate etchplains, the High glacis system has been tentatively correlated by Grandin and Thiry (1983) among Africa, India and South America. Correlation at least with India would be validated by the documentation by Jean et al. (2019) of a post-Intermediate, regional lateritic pediment system weathered at 14–11 Ma. Development of the Middle glacis pediplain relates to a last durable incursion of semi-arid climate propitious to mechanical erosion in the inner tropics between 11 and 7 Ma (Fig. 5b), which could have accompanied the onset of desertification in the Sahara at ~8–7 Ma (see Senut et al., 2009). Installation of seasonally dry climate at the Miocene-Pliocene boundary (7.2–5.8 Ma; Beauvais et al., 2008; Fig.5b) allowed for a last phase of limited ferruginous weathering and duricrusting over Sub-Saharan West Africa.

After the "doubthouse" period and abandonment of the Intermediate Etchplain (Fig. 5b), installation of pedimentation and shorter/lower intensity weathering periods from the Early Miocene onward would sign rhexistasy (Erhardt, 1955) i.e., a rupture with the biostatic regime, by which cooler/dryer climate enhances mechanical erosion of the regolith mantles that are not protected by the rainforest vegetation cover anymore and therefore exported through the river systems (see Fairbridge and Finkl, 1980). That rupture would indeed be attested to by increasing solid sedimentary fluxes to the African equatorial rifted margin basins after the Oligocene (Grimaud et al., 2018). But rock uplift, particularly in the Hoggar swell, would also be a major erosional source for those fluxes (Grimaud et al., 2018).

5.1.3. Preservation factors

As early pointed out by Daveau (1962) and Michel (1973a, 1978), the map pattern attests to the first-order structural and lithological control exerted by tabular sandstones and dolerite sills on the preservation of mantled etchplains (Figs. 4, 6 and 9). A comparable control is exerted by dolerite sills and greenstones on the preservation of Residual Composite Topopography map units (RT, Figs. 4 and 6). Weathering-prone lithologies (mafics and volcano-sediments, mostly) indeed favor iron-rich protective duricrusts that better resist erosion, as opposed to weaker, less iron-rich duricrusts developed on, for instance, granitic rocks. Tabular sandstones tend to form erosional scarps and escarpments protecting the sandstones and their regolith cover from further erosion. An additional reason for the exceptional preservation of the bauxitic etchplain in Western Guinea could be that the area remained at equatorial latitudes from the Early Cretaceous to the Eocene (Fig. 1c). This would have ensured renewal or maintenance of thick weathering mantles since the late Cretaceous and ultimate formation of massive duricrusts that protected the etchplain from later destruction.

The preservation pattern of the High glacis Pediplain was dictated by the same structural and lithological factors that favored preservation of the mantled etchplains (e.g., Figs. 4 and 6). But, for the High glacis ferricrete recycles mostly Intermediate duricrusts, the High glacis pediplain is also well preserved around the etchplain remnants or clusters thereof because it is where it is best duricrusted (e.g., Guinean Rise; Fig. 6). For the same reason, the preservation pattern of the Middle glacis pediplain is lithologically controlled (greenstones / mafic rocks; Figs. 4 and 6), its ferricrete cover being mostly dependent on that of the High glacis forming its interfluves (e.g., Fig. 13b and c).

The distribution of Paleogene and Miocene relict landform-regolith associations does not appear to vary among the main drainage basins. Nonetheless, a dense girdle of relict landform-regolith associations occupies the Upper Niger River watershed region in the Fouta Djalon, the Southeastern Guinean Rise and the Mandingue plateau (Figs. 2 and 6). But the watershed has probably been pinned down there as a consequence of the litho-structural control exerted by the tabular sandstones and dolerite sills on the preservation of duricrusted paleolandscapes (Figs. 2, 4 and 6; see also Chardon et al., 2016).

5.2. Plio-quaternary pediplains: record of climatic zonation of the inner tropics

The zonal pediplains reflect installation of a latitudinal climatic zonation over Sub-Saharan West Africa after the Miocene (Fig. 16). They evolved by adapting their slopes and *catena* to the overall southward tendency from arid to perhumid climate. Migration, dilation or retraction of latitudinal bio-climatic bands must have occurred since 6 Ma, such as during the LMG. It is why *catena* are polyphased and composite, because they are partly inherited from past distortions of the regional climatic zones. The latitudinal zonation of the functional pediplain is expected to extend eastward across Central and Eastern Africa in accordance with the continental-scale bio-climatic zonation (White, 1986). Further work is needed to actually constrain this pattern, by starting with field-based documentation such as the works of Fölster (1964), Fölster et al. (1971b) and Kadomura and Hori (1990).

5.3. Etchplains and pediplains: overlaps in the terminology

Development of the pediplains did not remove everywhere the entire regolith mantles of the Paleogene etchplains. For instance, the High glacis Pediplain (HgPd), especially in the Southeastern Guinean Rise, preserves Intermediate ferricretes on its interfluves and, therefore, the original Intermediate weathering mantle underneath. This is also the case for the High glacis Pediplain and the Multi-Convex Pediplain SE of the Cameroon Rise (e.g., Fig. 6). More generally, within ~200 km from the coast, the Plio-Quaternary pediplains may exhibit thick weathering mantles exceeding the local relief amplitude, such as in SE Nigeria

(Thomas, 1966). Tens of meters-thick kaolinitic weathering mantles also underlay hills of Southern Côte d'Ivoire. These may be interpreted as remnants of the Intermediate weathering mantle that were not leveled by pedimentation because the Intermediate etchplain tends to merge with the pediplains at sea level near the coast (Grimaud et al., 2014; see also Grandin, 1976; e.g., Figs. 6 and 16). A comparable telescoping pattern is seen in the Sahelian and Saharan zones outside the Hoggar swell, where the Intermediate ferricrete is ubiquitous or barely eroded, so that the Sahelian Pediplain and the regs may be underlain by Intermediate kaolinic regolith (e.g., Fig. 17a).

Portions of the pediplains preserving Paleogene regolith mantle may therefore be described as partially stripped etchplains (Thomas, 1989a). In order to emphasize the rupture in the surface processes between (i) Late Cretaceous-Paleogene morphogenesis, which led to the formation of the two etchplains by intense weathering and (ii) installation of pedimentation and moderate to weak weathering afterwards, the term pediplain is preferred here to name the Neogene low-relief landscapes. Despite locally thick weathering mantles under these landscapes, part of which may be inherited, this terminology aims to emphasize mechanical slope processes (pedimentation) under cooler / dryer Neogene climates as primary landscape shaping agents.

5.4. The legacy of Paleogene weathering and applied geology

Besides the considerable size of their relics, the inheritance of Paleogene etchplains in today's landform-regolith associations is of prime importance. Most of the local relief produced in Northwestern Africa since the end of the Oligocene was indeed cut into the etchplains weathering mantle by pedimentation and the original Paleogene regolith constitutes considerable volumes of the residual massifs (RT units and smaller occurrences) studding the pediplains (Chardon et al., 2018; Sawadogo et al., 2020). The original stock of iron and associated elements extracted by intense protracted Paleogene weathering and accumulated in bauxitic and Intermediate regolith was also the main source for ferricretes and latosols of the Neogene pediplains, either by recycling of duricrust fragments or downslope solute transfers (Maignien, 1956, 1966; Grandin, 1976; Sawadogo et al., 2020).

Remnants of the West African Paleogene mantled etchplains are known and exploited for their supergene economic potential in Fe, Al and Mn (e.g., White, 1973; Gaskin, 1975; Grandin, 1976; Misra and Raucq, 1986; Mamedov et al., 2021, 2022). Providing favorable bedrock compositions, remnants of the Paleogene mantled etchplains should typically host supergene concentrations in Ti, Zr, V, Nb, Cr, Sb, Sn, W,

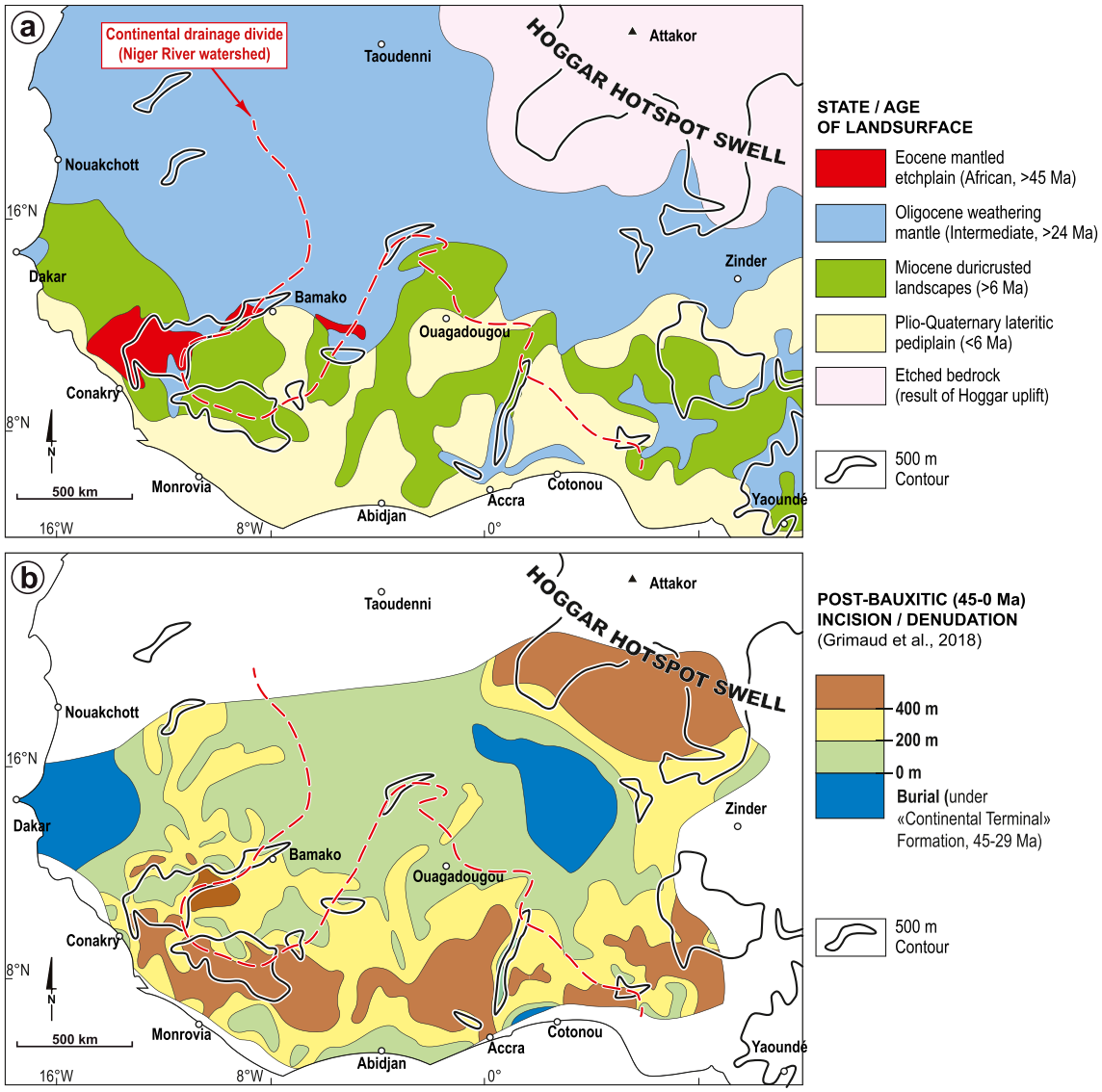

Fig. 17. (a) Northwestern Africa's landsurface state/age summary map (synthetized after Fig. 16). (b) Corresponding erosion map calibrated from incision measurements of the Eocene Bauxitic Mantled Etchpain (modified after Grimaud et al., 2018).

Th, Hf and rare earth elements (Sawadogo et al., 2020). This great economic potential is still to be investigated systematically.

Pediments constitute a challenge for interpreting the geochemical soil surveys undertaken for the purpose of mineral exploration. Indeed, contrary to mantled etchplains, pediment covers are detrital i.e., they have been transported downslope. Hence, such covers have generally no clear genetic link with the bedrock or the saprolite they overlay (Chardon et al., 2018). Caution is therefore required in planning and interpreting geochemical soil surveys in the Miocene duricrusted landscapes (complex terrain hosting various relict pediments), the Sahelian Pediplain and, by extension, Saharan regs (Fig. 16). In particular, one would have to use the landform-regolith mapping chart and geomorphological exploration guides implemented by Sawadogo et al. (2020) for lateritic pediment terrains. Mineral exploration in zonal pediplains (Fig. 16) should be simpler. Indeed, the maximum transportation distance of regolith on pediments in such contexts cannot exceed the distance between hill apexes and the next river drain (e.g., Fig. 15b to 15d). A soil geochemical anomaly may therefore be easily sourced upslope.

5.5. Long-term landform-regolith evolution processes and large-scale denudation scheme

5.5.1. Landsurface age map

To the very first order, the landsurface of Northwestern Africa may be described by 5 map units reflecting its overall age and long-term denudation pattern (Fig. 17a). The first unit groups the remnants of the African bauxitic etchplain. The second and most widespread unit comprises areas preserving the Intermediate Oligocene etchplain or part of its weathering mantle. It occupies the entire Saharan and Sahelian domain outside the Hoggar swell and smaller Sub-Sahelian patches of favorable lithologies. This unit therefore characterizes a landsurface having undergone negligible (<100 m) denudation since the Oligocene. The Hoggar swell corresponds to bedrock etched from its Intermediate weathering mantle. Relict Miocene duricrusted landscapes occupy Sub-Saharan patches of weathering-prone lithologies where the Oligocene etchplain was partly dissected. Finally, the functional lateritic pediplain characterizes a Sub-Sahelian domain in which Pre-Pliocene landform-regolith associations have been mostly stripped off (Fig. 17a) and where the lateritic covers are being reworked by slope processes.

The simplified map pattern (Fig. 17a) is somehow consistent with the denudation map obtained by Grimaud et al. (2018) from the differential elevation between the reconstructed Bauxitic Mantled Etchplain and todays topography (Fig. 17b). Comparison between the two maps would indeed suggest that the post-Oligocene installation of pediment systems in the Guinean and Soudanian zones of savannas focused denudation in that latitudinal band (Fig. 17b). But that denudation band may also reflect rock uplift along the marginal upwarp inherited from Cretaceous rifting of the Equatorial Atlantic Ocean (Grimaud et al., 2018). This chicken-and-egg problem is not solved yet. In any case, one has to consider denudational isostatic uplift produced by the sole erosional unloading of the lithosphere that attained 250 m on the marginal upwarp and >700 m on the upper flank of the Hoggar swell over the past 45 Ma (Chardon et al., 2016). To summarize, Cenozoic erosion over Northwestern Africa focused on the Hoggar swell. Low erosion (200–400 m) took place along a Sub-Sahelian ribbon of low rock uplift on which dryer post-Oligocene climate(s) and/or denudational isostasy may have favored denudation. The remaining surface of Northwestern Africa underwent very-low or limited erosion (<200 m) since the Eocene.

5.5.2. Long-term landform-regolith evolution model

The landform-regolith pattern of Northwestern Africa (Figs. 6 and 16) is a patchwork resulting from periods of regolith production and landscape stabilization and periods of unevenly distributed regolith stripping and landscape dissection. Spatial variability of both regolith production by weathering and regolith stripping by mechanical erosion was controlled to the first-order by lithological variations of the bedrock. The two main periods of regolith production, supergene iron accumulation and landscape stabilization relate to the Bauxitic etchplain, elaborated from the Late Cretaceous to the Mid-Eocene and the Intermediate etchplain, formed during the Oligocene. Dryer Miocene climate favored stripping of Paleogene etchplains by pedimentation, particularly on felsic lithologies. That period was punctuated by two lasting incursions of seasonally humid climate (Mid-Miocene climatic optimum and End-Miocene) allowing for duricrusting and therefore partial protection of the relief so generated. The Plio-Quaternary sees the remaining landsurface made mostly of felsic lithologies adapting its slopes to the modern latitudinal climatic zonation of the inner tropics. One has therefore to consider both (i) paleo-climatic periods and ruptures (Büdel, 1982) and (ii) bedrock contrasts (Thomas, 1989b, 2012) as the main factors having concurred to produce the composite landform-regolith pattern of Northwestern Africa.

Paleogene etchplains encompassed escarpments and reliefs (e.g., Fig. 9), whereas relict Miocene pediplains are distributed over the map area and encompass a wide elevation range and several escarpments (Figs. 2 and 6). Besides, intensive inventories have shown that the Intermediate etchplain and the two Miocene pediment systems, at the time they were functional, each graded to local base levels separated by bedrock contrast-controlled static knickzones of the river network (Grimaud et al., 2014, see also Tricart, 1958). In other words, and as early stressed by De Swardt (1964) and Rohdenburg (1969), escarpments and knickzones do not separate stepped diachronous landsurfaces (i.e., higher/older versus lower/younger); they compartmentalize base level domains of contrasted elevation bearing contemporaneous landforms and catena. Slow uneven erosion throughout those stepped drainage networks resulted in the long-term denudation and landform-regolith patterns of Northwestern Africa (Figs. 16 and 17). A neglected but first-order factor having driven slow uneven river entrenchment through the cratonic landscapes is ultimately the very long-term post-Early Eocene eustatic sea-level fall (Peulvast et al., 2008). Epeirogenic movements must have distorted the Paleogene etchplains and even enhanced erosion as suggested by the Hoggar swell case (Chardon et al., 2016). Miocene pediplains must have been affected too by epeirogeny, though to a lesser degree because they are younger. But the cause (mantle- versus erosion-driven), tempo and magnitude of epeirogeny, as well as its true contribution to the denudation scheme, still need to be assessed.

5.5.3. Implications for continental erosion models

In order to model erosion over the Sub-Saharan portion of the region, which is typical of the cratonic geosystem, one should take into account the landform-regolith maps of Figs. 6 or 16 that are also erosion and weathering susceptibility maps. In other words, mass transfers though West African landscapes and *catena* and therefore mechanical and chemical erosion will be compartmentalized among domains of landform-regolith units. The first domain corresponds to the Plio-Quaternary zonal pediplains, whose landforms and *catena* tend towards pedoclimatic equilibrium. The second domain corresponds to the Paleogene etchplains and the relict Miocene landscapes (Fig. 16), whose landforms and catena are mostly fossil (in state of pedoclimatic disequilibrium), composite or both. Each erosional domain would be characterized by a specific relief, groundwater flow and hydrogeochemical regime, which is ultimately governed by the configuration of the landform-regolith associations.

The functional zonal pediplains eroded very slowly over the late Neogene (<2 m/My; Grimaud et al., 2015, see also Braucher et al., 1998). They are fundamentally hillslope processes-controlled. A type-half interfluve soil-mantled hillslope model (e.g., Bovy et al., 2016) would therefore be pertinent to simulate solid and solute fluxes to rivers by considering negligible river intrenchment rates. Etchplain terrains and Miocene relict landscapes eroded slowly during the late Neogene (2–12 m/My; Beauvais and Chardon, 2013; Grimaud et al., 2014). They

are made of low-sloping, fossil duricrust-capped surfaces separated by steeper slopes providing access to (relict) regolith available to mechanical erosion. Erosion proceeds essentially by duricrust dissection by drainage network growth (Grimaud et al., 2015). Pertinent erosion models would therefore have to combine (i) very subdued river incision and hillslope diffusion (e.g., Braun and Willett, 2013) with (ii) a soil-mantled hillslope model somehow able to simulate elements fluxes through thick and mostly inherited regolith mantles.

6. Discussion

6.1. Epeirogeny, mega-geomorphology and the definition of "paleo-planation surfaces"

Long (x100 km) and very-long (x1000 km) wavelength topographic massifs of Africa are considered as uplifts (i.e., swells; e.g., Fig. 1a) produced by mantle convection after the African plate slowed down its northward displacement at the onset of Alpine collision at ca. 30 Ma (Burke, 1996; Burke et al., 2003). This model led to a redefinition of the African Surface, which would encompass the current topography of the continent and be the end-result of mantle-driven deformation and correlative erosion of an originally flat, sea-level elevation, 100 Ma-old landsurface (Burke and Gunnell, 2008). This Cenozoic all-swell growth model prompted the use of reconstructed "planation surfaces" (paleo-etchplains and pediplains) as epeirogenic deformation gauges i.e., long-wavelength paleo-topographic deformation markers and/or successive steps of staircases carved on the slopes of growing reliefs (e.g., Guillocheau et al., 2015, 2018; Picart et al., 2020; see, in particular, Egbogah, 1975, Boulangé and Millot, 1988 and Burke and Gunnell, 2008 for West Africa). The present study, by systematically tying geomorphic analysis to catena inventories and regolith dating on a regional scale, allows for a critical evaluation of such a model and its corollary approaches of long-term shield morphogenesis.

The definition of swells having grown during the Late Cenozoic is problematic, as illustrated in Northwestern Africa. The so-called "Dakar swell" and "Leo swell" (SW of Ouagadougou) of Burke and Gunnell (2008) do not exist in the topography. The staircase distribution model of the West African morphoclimatic sequence on the northern flank of the "Fouta Djallon swell" claimed by these authors (i.e., the massif formed by the Fouta Djalon and the southeastern Guinean rise) is not attested either (Figs. 2, 9 and 6; see also Grimaud et al., 2014; Chardon et al., 2018). Finally, there is no geological evidence to support the Cenozoic growth of that latter massif, nor for the "South-West Nigeria swell" (i.e., massif west of the Niger-Benue confluence) or the "Jos swell" claimed by the authors (Figs. 2 and 5). Besides, the occurrence of late Cenozoic volcanic clusters does not attest to recent uplift at their emplacement as implied by Burke (1996).

Paleogene etchplains, and particularly the 70–45 Ma Bauxitic Mantled Etchplain that would correspond to the originally flat African surface of Burke and Gunnell (2008), were never flat, nor at sea level except at the coast (Chardon et al., 2016). Indeed, the Paleogene etchplains still encompass the entire regional elevation range and were drained down to interior base levels (lakes) or, most commonly, to the marine base-level while they were functional. In other words, a long or very-long wavelength topography at the time the Paleogene etchplains and Neogene pediplains were functional must have existed. Thus, ancient etchplains and pediplains cannot be used as direct passive epeirogenic deformation markers because their pre-deformation shape cannot be assessed. Furthermore, whatever the mantle-driven epeirogenic component of the current topography, a significant part (up to >30%) of the Cenozoic surface uplift/burial has to be due to denudational/depositional isostasy (Chardon et al., 2016). The current long-wavelength geometry of paleo-etchplains or pediplains therefore accounts for only part of the epeirogeny they have undergone and for an unknown but certainly subdued mantle component thereof.

The present work shows that paleo-etchplains and paleo-pediplains functioned over the differentiated, complexly stepped topography of Northwestern Africa (e.g., Fig. 9). Besides, most steps in the current topography (knickzones and escarpments) already existed in the Paleogene landscapes (Grimaud et al., 2014). Another important outcome of the present work is the identification of a single, active and climatically zoned Plio-Quaternary pediplain at the scale of Sub-Saharan Northwestern Africa over ~10° of latitude and over almost the entirety of its elevation range. Without a systematic landform-regolith mapping approach, the use of escarpments in the topography to document staircase patterns of supposedly successive etchplains or pediplains is therefore inappropriate and misleading. So is the photointerpretation-assisted distinction of generations of pediplains over very large cratonic landsurfaces. Indeed, such generations of pediplains could represent climatic zones of vast functional pediplains.

To conclude, it therefore appears that the premises of the all-swell growth geomorphological approaches to African topography are biased. They indeed imply landform and denudation patterns dictated by unsubstantiated epeirogenic pulses (see alo, for instance, Summerfield, 1985; van der Beek et al., 2002). The present work shows that African landform-regolith patterns are fundamentally long-term climate-controlled and that the all-swell growth model is simplistic.

6.2. Low temperature thermochronology and geochronology of laterites: West African cautionary notes

The preservation of Early Cenozoic landform-regolith associations poses a sizable but largely ignored challenge to low temperature thermochronology (apatite fission track analysis and (U—Th)/He dating), which is commonly used on shields, especially to calibrate long-term denudation of divergent continental margins (Beauvais et al., 2016). In the case of Northwestern Africa, thermal inverse modeling of apatite data by Gouiza et al. (2019) predicts >2 km of late Neogene denudation over the Mauritanides belt, whilst it is still covered by extensive relicts of the Intermediate Mantled Etchplain (Figs. 4 and 6), which precludes post-Oligocene denudation. Likewise, km-scale Neogene and even Quaternary denudation is predicted over the western Reguibat Shield (Leprêtre et al., 2015; Gouiza et al., 2018), whereas the terrain is blanketed by very large veneers of the Oligocene Intermediate Mantled Etchplain and Early Miocene Hamadas (Figs. 4 and 6). Such systematic overestimates of late Cenozoic exhumation of shield terrains (e.g., Beauvais et al., 2016) cast doubts on the actual pertinence of low-temperature thermochronology in such contexts, especially once the samples have entered for the last time the partial annealing zone. Post-45 Ma denudation over the map area outside the Hoggar swell cannot exceed the relative height of Bauxitic Mantled Etchplain remnants i.e., the local relief of a few hundred meters at best (Beauvais and Chardon, 2013; Fig. 17b). Dated preserved landform-regolith associations should be used instead as temporal and spatial constraints to improve thermal inversion of apatite data (e.g., Wildman et al., 2019), especially for higher-sensitivity (U—Th)/He dating, as apatite fission track thermochronology would be mostly blind to slow shield denudation over few My-long periods, especially on the late cooling path of samples i.e., during their final way to the surface. Regional supergene albitization events of cratonic platforms up to 200 m depth produce secondary apatites, as documented under the Triassic (i.e., post-Variscan) erosional landsurface of Europe (Thiry et al., 2023). Such supergene alteration events must have been common worldwide and could indeed have taken place in Northwestern Africa (e.g., Bamba et al., 1997). One would therefore have to ensure that bedrock samples used for apatite thermochronology work did not undergo albitization (Thiry et al., 2023).

Installation of alternating seasonally humid or dry climates over Northwestern Africa after the Eocene allowed for the exceptional preservation of distinct and diachronous duricrust-capped weathering mantles that kept a reliable record of pristine datable supergene minerals such as cryptomelane (Beauvais et al., 2008). There is therefore a great potential in the region to refine the landform-regolith chronogram

and cross-calibrate Ar—Ar geochronology with (U—Th)/He dating of iron oxyhydroxides (e.g., Shuster et al., 2005) and electron paramagnetic resonance dating of kaolinite (Balan et al., 2005; Allard et al., 2018). On shields where equatorial humid to perhumid climate maintained over the Cenozoic such as in South America (Tardy et al., 1991), prolonged duricrust degradation and regolith mantle reorganization took place in landscapes tending towards multi-convex pediplains (e.g., Boulet et al., 1997). In such contexts, geochronological dating of landform-regolith associations becomes tricky even though weathering periods are documented by geochronology in long-lived individual regolith mantles (e.g., Vasconcelos et al., 2015; Vasconcelos and de Carmo, 2018; Mathian et al., 2019; Heller et al., 2022). But the obtained age-frequency patterns reflect preservation biases instead of paleo-weathering intensities, with sometimes little or no memory of Pre-Late Neogene weathering periods. If preserved, old ages relate to crystal(s) that are not anymore in equilibrium with their surrounding supergene phases. Furthermore, the configuration of the regolith mantle hosting the dated phase(s) and its geomorphic setting have long been reorganized since crystallization age. Old ages interpretation is therefore not straightforward in terms of paleo-geomorphology, paleo--weathering or climate. Caution is further required to interpret ages of supergene minerals that (re)crystallized during the Neogene in older reworked regolith mantles unless a detailed investigation of their petrographic context is undertaken.

7. Conclusions

(1) The distribution of landform-regolith associations at the scale of Northwestern Africa constitutes a composite record of long-term Cenozoic surface dynamics of a type-tropical cratonic geosystem. This record reveals the primary control of long-term climate variability, spatial climatic zonation and geological substrate composition on landform-regolith evolution processes, from the landscape to the continental scale.

(2) Four main pan-tropical relict landform-regolith associations occupy nearly half of today's landsurface. Thick relict Paleogene regolith mantles of etchplains mark the imprint of (i) Late Cretaceous - Mid Eocene greenhouse that formed bauxites at the Early Eocene thermal maximum and (ii) Late Oligocene, seasonally humid climate that formed massive iron duricrusts. Development of two successive duricrust-capped pediment systems signs change to dry erosional climate during the Early Miocene and Late Miocene, and a return to weathering-prone, seasonally dry climate around the Miocene climatic optimum (18–11 Ma) and at the End-Miocene (7–6 Ma). Finally, development of a latitudinally zoned pediplain since the early Pliocene reflects installation of the modern climatic zonation of the tropics in Northwestern Africa from hyper-arid, in the North, to per-humid, in the South.

(3) The unevenness of slow, Cenozoic regional erosion was primarily controlled by the contrasting weathering susceptibility of bedrock lithologies and the compartmentalization of the drainage network into elevation domains separated by steps in the topography. The inheritance of Paleogene regolith mantles and duricrusts is patent in all younger landform-regolith associations, which essentially recycle regolith and elements initially accumulated by Paleogene weathering. Paleogene weathering must have led to major unsuspected supergene ore deposits and mineral exploration strategies must be adapted to the systematics of landform-regolith associations.

(4) The current susceptibility of the cratonic landsurface to weathering and erosion should be partitioned among (i) the functional zoned pediplain, which tends towards pedoclimatic equilibrium and (ii) Pre-Pliocene relict landform-regolith associations, which are essentially fossil.

(5) Ancient etchplains and pediplains are not reliable long-wavelength topographic gauges of mantle-driven epeirogeny because (i) they were not originally flat nor near sea-level elevation and (ii) erosional/depositional isostasy produced a significant part of today's topography. Staircase patterns of successive etchplains or pediplains inferred to result from positive epeirogenic pulses are invalid. Therefore, the cause, tempo and magnitude of epeirogeny and its contribution to today's African topography remain to be deciphered.

(6) Landform-regolith patterns question the ability of low-temperature thermochronology to accurately document final rock exhumation paths in cratonic contexts. Caution is required in interpreting the petrographic, geomorphic and climatic settings of geochronological ages of regolith minerals in morphoclimatic contexts less favorable than Northwestern Africa to the preservation of landform-regolith associations.

Declaration of Competing Interest

The author declares that he has no known competing financial interests or personal relationships that could have appeared to influence the work reported in this paper.

Data availability

The data and observations supporting the study are provided on the maps, cross-sections and other illustrations of the article, as well as in the cited literature.

Acknowledgments

My involvement in tropical geomorphology that eventually led to this contribution owes much to Georges Grandin and Bruno Boulangé, who introduced me to West African laterites and landforms through an initiatory field trip and lively discussions. I am indebted to Gérard Hérail and Fabrice Colin for having made this endeavor possible and acknowledge fruitful collaboration through the years with Anicet Beauvais, Ousmane Bamba, Delphine Rouby, Jean-Louis Grimaud and Benjamin Sawadogo. Frédéric Christophoul and Julien Berger kindly helped with GIS. Jean-Paul Liégeois and André Pouclet are thanked for sharing documentation on the Tuareg shield. Funding for much of this work was provided by TopoAfrica (ANR-08-BLAN-572 0247-02), WAXI 2 and WAXI 3 (AMIRA project P934A) and TotalEnergies (TS^2P project). This is a contribution of the JEAI FasoLith, supported by the IRD. It aims to pay tribute to the field scientists, cited or involuntarily omitted, who contributed to decipher the amazing landform-regolith patterns of Northwestern Africa. Michael F. Thomas, Médard Thiry and an anonymous referee are thanked for their constructive comments on the manuscript.

References

Allard, T., Gautheron, C., Bressan Riffel, S., Balan, E., Soares, B.F., Pinna-Jamme, R., Derycke, A., Morin, G., Bueno, G.T., do Nascimento, N., 2018. Combined dating of goethites and kaolinites from ferruginous duricrusts. Deciphering the Late Neogene erosion history of Central Amazonia. Chem. Geol. 479, 136–150. https://doi.org/10.1016/j.chemgeo.2018.01.004.

Ambrosi, J.P., Nahon, D., 1986. Petrological and geochemical differentiation of lateritic iron crust profiles. Chem. Geol. 57, 371–393. https://doi.org/10.1016/0009-2541(86)90059-8.

Antonovic, A., Strojkovic, M., Radulovic, P., Pesic, D., 1991. Kaolinic clay and quartzose sandstones - the chief mineral materials in the Central Sahara. In: Geology of Libya. Elsevier, pp. 2697–2702.

Arhin, E., Jenkin, G.R.T., Cunningham, D., Nude, P., 2015. Regolith mapping of deeply weathered terrain in savannah regions of the Birimian Lawra Greenstone Belt, Ghana. J. Geochem. Explor. 159, 194–207. https://doi.org/10.1016/j.gexplo.2015.09.008.

Auzel, M., Cailleux, A., 1949. Silicifications nord-sahariennes. Bull. Soc. Géol. Fr. S5-XIX, 553–559. https://doi.org/10.2113/gssgfbull.S5-XIX.7-9.553.

Avenard, J.M., 1973. Évolution géomorphologique Quaternaire dans le centre-ouest de la Côte d'Ivoire. Rev. Géomor. Dyn. XXII 145–160. https://doi.org/10.3406/geo.1970.19802.

Avenard, J.M., 1975. Géomorphologie et répartition des formations végétales dans la région du Foro-Foro (Nord de Bouaké). Rapport ORSTOM, Adopodoumé. https://www.documentation.ird.fr/hor/fdi:07690.

Avenard, J.M., 1977. Cartographie géomorphologique dans l'Ouest de la Côte d'Ivoire. Not. Expl. ORSTOM 71, 1–99. https://www.documentation.ird.fr/hor/fdi:09001.

Avenard, J.M., Bonvallot, J., Latham, M., Renard-Dugerdil, M., Richard, J., 1974. Aspects du contact forêt-savane dans le centre et l'ouest de la Côte d'Ivoire. Étude descriptive. Trav. Doc. ORSTOM 35, 1–235. https://www.documentation.ird.fr/hor/fdi:06945.
Bachelier, G., 1959. Étude pédologique des sols de Yaoundé. Contribution à l'étude de la pédogenèse des sols ferralitiques. Agron. Trop. XIV, 279–306. https://www.documentation.ird.fr/hor/fdi:18029.
Balan, E., Allard, T., Fritsch, E., Sélo, M., Falguères, C., Chabaux, F., Pierret, M.-C., Calas, G., 2005. Formation and evolution of lateritic profiles in the middle Amazon basin: insights from radiation-induced defects in kaolinite. Geochim. Cosmochim. Acta 69, 2193–2204. https://doi.org/10.1016/j.gca.2004.10.028.
Bamba, O., Beziat, D., Bourges, F., Debat, P., Lompo, M., Parizot, J.-C., Tollon, F., 1997. Nouveau type de gisement aurifère dans les ceintures de roches vertes birimiennes du Burkina Faso: les albitites de Larafella. J. Afr. Earth Sci. 25, 369–381. https://doi.org/10.1016/S0899-5362(97)00110-3.
Bamba, O., Parisot, J.-C., Grandin, G., Beauvais, A., 2002. Ferricrete genesis and supergene gold behaviour in Burkina Faso, West Africa. Geochem. Explor. Environ. Anal. 2, 3–13. https://doi.org/10.1144/1467-787302-001.
Bárdossy, G., Aleva, G.J.J., 1990. Lateritic Bauxites, Developments in Economic Geology. Elsevier, Amsterdam.
Beaudet, G., Coque, R., 1986. Les modelés cuirassés des savanes du Burkina Faso. Rev. Géogr. Phys. Géol. Dyn. 27, 213–224.
Beaudet, G., Coque, R., Michel, P., Rognon, P., 1977. Altérations tropicales et accumulations ferrugineuses entre la vallée du Niger et les massifs centraux sahariens (Aïr et Hoggar). Z. Geomorph. N.F. 21, 297–322.
Beaudet, G., Coque, R., Michel, P., Rognon, P., 1981a. Reliefs cuirassés et évolution géomorphologique des régions orientales du Mali. 1. La région du Tilemsi et la Vallée du Niger de Taoussa à Gao. Z. Geomorph. N.F. 38, 38–62.
Beaudet, G., Coque, R., Michel, P., Rognon, P., 1981b. Reliefs cuirassés et évolution géomorphologique des régions orientales du Mali. 2. Le Gourma et le plateau de Bandiagara, son contact avec le Macina. Z. Geomorph. N.F. 38, 63–85.
Beaudou, A.G., Sayol, R., 1980. Étude pédologique de la région de Boundiali–Korhogo (Côte d'Ivoire). Cartographie et typologie sommaire des sols à 1/200 000. Not. Expl. ORSTOM 84, 1–47. https://horizon.documentation.ird.fr/exl-doc/pleins_textes/pleins_textes_5/notexp/10054.pdf.
Beauvais, A., 1991. Paléoclimats et dynamique d'un paysage cuirassé du Centrafrique. Morphologie, pétrologie et géochimie (Ph.D. thesis).. Université de Poitiers, Poitiers https://www.documentation.ird.fr/hor/fdi:35558.
Beauvais, A., 2009. Ferricrete biochemical degradation on the rainforest–savannas boundary of Central African Republic. Geoderma 150, 379–388. https://doi.org/10.1016/j.geoderma.2009.02.023.
Beauvais, A., Chardon, D., 2013. Modes, tempo, and spatial variability of Cenozoic cratonic denudation: the West African example. Geochem. Geophys. Geosyst. 14, 1590–1608. https://doi.org/10.1002/ggge.20093.
Beauvais, A., Roquin, C., 1996. Petrological differentiation patterns and geomorphic distribution of ferricretes in Central Africa. Geoderma 73, 63–82. https://doi.org/10.1016/0016-7061(96)00041-9.
Beauvais, A., Ritz, M., Parisot, J.-C., Dukhan, M., Bantsimba, C., 1999. Analysis of poorly stratified lateritic terrains overlying a granitic bedrock in West Africa, using 2-D electrical resistivity tomography. Earth Planet. Sci. Lett. 173, 413–424. https://doi.org/10.1016/S0012-821X(99)00245-9.
Beauvais, A., Ritz, M., Parisot, J.-C., Bantsimba, C., Dukhan, M., 2004. Combined ERT and GPR methods for investigating two-stepped lateritic weathering systems. Geoderma 119, 121–132. https://doi.org/10.1016/j.geoderma.2003.06.001.
Beauvais, A., Ruffet, G., Henocque, O., Colin, F., 2008. Chemical and physical erosion rhythms of the West African Cenozoic morphogenesis: the ^{39}Ar-^{40}Ar dating of supergene K-Mn oxides. J. Geophys. Res.-Earth Surf. 113, F4007. F04007. https://doi.org/10.1029/2008jf000996. F04007.
Beauvais, A., Bonnet, N.J., Chardon, D., Arnaud, N., Jayananda, M., 2016. Very long-term stability of passive margin escarpment constrained by ^{40} Ar/ ^{39} Ar dating of K-Mn oxides. Geology 44, 299–302. https://doi.org/10.1130/G37303.1.
Becker, A., 1992. A time-space model for the genesis of early Tertiary laterites from the Jos Plateau, Nigeria. J. Afr. Earth Sci. 15, 265–269. https://doi.org/10.1016/0899-5362(92)90073-l.
Bennett, K.C., Rusk, D., 2002. Regional 2D seismic interpretation and exploration potential of offshore Deepwater Sierra Leone and Liberia, West Africa. Lead. Edge 21, 1118–1124. https://doi.org/10.1190/1.1523743.
Birchall, C.J., Bleeker, P., Cusani-Visconti, C., 1980. Land Systems Map of Sierra Leone at 1:500,000 Scale. Land Ressources Survey Project. FAO, Freetown.
Birot, P., Capot-Rey, R., Dresch, J., 1955. Recherches morphologiques dans le Sahara central. Trav. Inst. Rech. Sahar. 13, 13–74.
Bitom, D., Volkoff, B., Abossolo-Angue, M., 2003. Evolution and alteration in situ of a massive iron duricrust in Central Africa. J. Afr. Earth Sci. 37, 89–101. https://doi.org/10.1016/s0899-5362(03)00044-7.
Boeglin, J.L., Mazaltarim, D., 1989. Géochimie, degrés d'évolution et lithodépendance des cuirasses ferrugineuses de la région de Gaoua au Burkina Faso. Sci. Géol. Bull. 42, 27–44. https://doi.org/10.3406/sgeol.1989.1810.
Bonhomme, M., Fabre, J., Monod, T., Lécorché, J.P., Lamarche, J.P., Dos Santos, R.P., Aprahamian, J., Demenjeon, J.C., 1996. Lentilles d'argile kaolinique dans le Paleozoïque inférieur de Tabelbala (Sahara occidental algérien) et de Chinguetti (Adrar de Mauritanie). Mém. Serv. Géol. Alg. 8, 237–247.
Bonnet, N.J., Beauvais, A., Arnaud, N., Chardon, D., Jayananda, M., 2016. Cenozoic lateritic weathering and erosion history of Peninsular India from 40Ar/39Ar dating of supergene K–Mn oxides. Chem. Geol. 446, 33–53. https://doi.org/10.1016/j.chemgeo.2016.04.018.
Bonvallot, J., Boulangé, B., 1970. Note sur le relief et son évolution dans la région de Bongouanou (Côte d'Ivoire). Cah. ORSTOM Sér. Géol. 2, 171–183. https://www.documentation.ird.fr/hor/fdi:20683.
Boulangé, B., 1984. Les formations bauxitiques latéritiques de Côte d'Ivoire. Trav. Doc. ORSTOM 175, 1–342. https://www.documentation.ird.fr/hor/fdi:02941.
Boulangé, B., 1986. Relation between lateritic bauxitization and evolution of landscape. Trav. Int. Com. Stud. Bauxite, Alumina & Aliminum (ISCOBA) 16–17, 27–44. https://www.documentation.ird.fr/hor/fdi:29722.
Boulangé, B., Eschenbrenner, V., 1971. Note sur la présence de cuirasses témoins des niveaux bauxitiques et intermédiaires, plateau de Jos, Nigéria. Bull. Ass. Sén. Ét. Quat. Ouest Afr. 31, 83–92. https://www.documentation.ird.fr/hor/fdi:05412.
Boulangé, B., Millot, G., 1988. La distribution des bauxites sur le craton ouest-africain. Sci. Géol. Bull. 41, 113–123. https://doi.org/10.3406/sgeol.1988.1785.
Boulangé, B., Sigolo, J.B., Delvigne, J., 1973. Descriptions morphoscopiques, géochimiques et minéralogiques des faciès cuirassés des principaux niveaux géomorphologiques de Côte d'Ivoire. Cah. ORSTOM Sér. Géol. 5, 59–81. https://www.documentation.ird.fr/hor/fdi:19911.
Boulet, R., 1970. La géomorphologie et les principaux types de sols en Haute-Volta septentrionale. Cah. ORSTOM Sér. Pédol. 8, 245–271. https://www.documentation.ird.fr/hor/fdi:18412.
Boulet, R., 1978. Toposéquences de sols tropicaux en Haute-Volta. Équilibre et déséquilibre pédobioclimatique. Mém. ORSTOM 85, 1–274. https://www.documentation.ird.fr/hor/fdi:09233.
Boulet, R., Bocquier, G., Millot, G., 1977. Géochimie de la surface et formes du relief. I - Déséquilibre pédobioclimatique dans les couvertures pédologiques de l'Afrique tropicale de l'Ouest et son rôle dans l'aplanissement des reliefs. Sci. Géol. Bull. 30, 235–243. https://doi.org/10.3406/sgeol.1977.1519.
Boulet, R., Lucas, Y., Fritsch, E., Paquet, H., 1997. Geochemical processes in tropical landscapes: Role of the soil cover. In: Paquet, H., Clauer, N. (Eds.), Soils and Sediments. Mineralogy and Geochemistry. Springer-Verlag, Berlin Heidelberg, pp. 67–96.
Boulvert, Y., 1996. Étude géomorphologique de la République Centreafricaine : carte à 1/1 000 000 en deux feuilles ouest et est. Notices Explicatives ORSTOM, Paris. https://www.documentation.ird.fr/hor/fdi:010004014.
Boulvert, Y., 2003. Carte morphopédologique de la République de Guinée à 1/500 000, IRD Cartes et Notices. https://www.documentation.ird.fr/hor/fdi:010032368.
Boulvert, Y., 2005. Carte morphopédologique de la République de Guinée à 1/200 000 (CD-Rom). IRD Cartes et Notices, Bondy.
Bourdeau, A., 1991. Les bauxites du Mali. Géochimie et minéralogie (Ph.D. thesis). Université Louis Pasteur, Strasbourg, France.
Bovy, B., Braun, J., Demoulin, A., 2016. A new numerical framework for simulating the control of weather and climate on the evolution of soil-mantled hillslopes. Geomorphology 263, 99–112. https://doi.org/10.1016/j.geomorph.2016.03.016.
Bowden, D.J., 1987. On the composition and fabric of the footslope laterites (duricrusts) of the Sierra Leone, West Africa, and their geomorphological significance. Z. Geomorph. N.F. 64, 39–53.
Bowden, D.J., 1997. The geochemistry and development of lateritized footslope benches: The Kasewe Hills, Sierra Leone. Spec. Publ. Geol. Soc. 120, 295–305.
Brammer, H., 1956. A note on former pediment remnants in Haute Volta. Geogr. J. 122, 526–527.
Braucher, R., Colin, F., Brown, E.T., Bourlès, D.L., Bamba, O., Raisbeck, G.M., Yiou, F., Koud, J.M., 1998. African laterite dynamics using in situ-produced 10Be. Geochim. Cosmochim. Acta 62, 1501–1507. https://doi.org/10.1016/S0016-7037(98)00085-4.
Braun, J., Willett, S.D., 2013. A very efficient O(n), implicit and parallel method to solve the stream power equation governing fluvial incision and landscape evolution. Geomorphology 180–181, 170–179. https://doi.org/10.1016/j.geomorph.2012.10.008.
Bravard, Y., 1976. L'érosion dans le Dhar Ou Senn (Mauritanie du S.-E.). Rev. Géogr. Alp. 64, 311–326. https://doi.org/10.3406/rga.1976.2050.
Bronner, G., 1992. Structure et évolution d'un craton archéen. La dorsale Reguibat occidentale (Mauritanie). Tectonique et métallogénie des formations ferrifères. Doc. BRGM 201, 1–448.
Brückner, W., 1955. The mantle rock ("laterite") of the Gold Coast and its origin. Geol. Rundsch. 43, 307–327. https://doi.org/10.1007/BF01764011.
Brückner, W.D., 1957. Laterite and bauxite profiles of West Africa as an index of rhythmical climatic variations in the tropical belt. Eclogae Geol. Helv. 50, 239–256.
Büdel, J., 1955. Reliefgenerationen und plio-pleistozäner Klimawandel im Hoggar-Gebirge. Erkunde 9, 100–115. https://doi.org/10.3112/erdkunde.1955.02.03.
Büdel, J., 1982. Climatic Geomorphology. Princeton University Press, Princeton (N.J.).
Burke, K., 1996. The African plate. S. Afr. J. Geol. 99, 341–409.
Burke, K., Durotoye, B., 1971. Geomorphology and superficial deposits related to late Quaternary climatic variation in South-Western Nigeria. Z. Geomorph. N.F. 15, 430–444.
Burke, K., Gunnell, Y., 2008. The African erosion surface: a continental scale synthesis of geomorphology, tectonics, and environmental change over the past 180 million years. Geol. Soc. Am. Mem. 201, 1–66. https://doi.org/10.1130/2008.1201.
Burke, K., Durotoye, B., Whiteman, A.J., 1971. A dry phase south of the Sahara 20,000 years ago. W. Afr. J. Archeol. 1, 1–8.
Burke, K., MacGregor, D.S., Cameron, N.R., 2003. Africa's petroleum systems: four tectonic 'Aces' in the past 600 million years. Spec. Publ. Geol. Soc. 207, 21–60. https://doi.org/10.1144/GSL.SP.2003.207.3.
Butt, C.R.M., Bristow, A.P.J., 2013. Relief inversion in the geomorphological evolution of sub-Saharan West Africa. Geomorphology 185, 16–26. https://doi.org/10.1016/j.geomorph.2012.11.024.

Capot-Rey, R., 1951. Sur quelques formes de relief de l'Adrar des Ifogas. Trav. Inst. Rech. Sahar. 7, 193–199.
Chamard, C., Courel, M.F., 1980. De l'autochtonie des dépôts superficiels du Liptako nigéro-voltaïque. Rev. Géomor. Dyn. 30, 11–20.
Chamard, J.C., Courel, M.F., Pascual, J.F., 1978. La cuirasse gravillonnaire du Sahel nigéro-voltaïque. Trav. Doc. Géogr. Trop. 33, 259–286.
Chardon, D., Chevillotte, V., Beauvais, A., Grandin, G., Boulangé, B., 2006. Planation, bauxites and epeirogeny: one or two paleosurfaces on the West African margin? Geomorphology 82, 273–282. https://doi.org/10.1016/j.geomorph.2006.05.008.
Chardon, D., Grimaud, J.L., Rouby, D., Beauvais, A., Christophoul, F., 2016. Stabilization of large drainage basins over geological time scales: Cenozoic West Africa, hot spot swell growth, and the Niger River. Geochem. Geophys. Geosyst. 17, 1164–1181. https://doi.org/10.1002/2015gc006169.
Chardon, D., Grimaud, J.L., Beauvais, A., Bamba, O., 2018. West African lateritic pediments: Landform-regolith evolution processes and mineral exploration pitfalls. Earth-Sci. Rev. 179, 124–146. https://doi.org/10.1016/j.earscirev.2018.02.009.
Chauvel, A., Bocquier, G., Pédro, G., 1977. Géochimie de la surface et formes du relief III. Les mécanismes de la disjonction des constituants des couvertures ferrallitiques et l'origine de la zonalité des couvertures sableuses dans les régions intertropicales de l'Afrique de l'Ouest. Sci. Géol. Bull. 30, 255–263. https://doi.org/10.3406/sgeol.1977.1521.
Choubert, G., Faure-Muret, A., 1988. International Geological Map of Africa at 1: 5,000,000 Scale, third edition. Com. Geol. Map World/UNESCO, Paris.
Colin, F., Beauvais, A., Ruffet, G., Henocque, O., 2005. First Ar-40/Ar-39 geochronology of lateritic manganiferous pisolites: Implications for the Palaeogene history of a West African landscape. Earth Planet. Sci. Lett. 238, 172–188. https://doi.org/10.1016/j.epsl.2005.06.052.
Collinet, J., 1974. Compte-rendu d'une tournée dans le nord de la Côte d'Ivoire (18 avril au 14 mai 1974). Étude de quelques toposéquences représentatives des relations pédogenèse - morphogenèse dans la région de Boundiali, Rapport ORSTOM. https://www.documentation.ird.fr/hor/fdi:29260.
Cornet, A., 1943. La transgression crétacée-éocène à l'Ouest de l'Adrar des Iforas et les dépôts continentaux post-éocènes. Trav. Inst. Rech. Sahar. 2, 177–197.
Couvreur, T.L.P., Dauby, G., Blach-Overgaard, A., Deblauwe, V., Dessein, S., Droissart, V., Hardy, O.J., Harris, D.J., Janssens, S.B., Ley, A.C., Mackinder, B.A., Sonké, B., Sosef, M.S.M., Stévart, T., Svenning, J., Wieringa, J.J., Faye, A., Missoup, A.D., Tolley, K.A., Nicolas, V., Ntie, S., Fluteau, F., Robin, C., Guillocheau, F., Barboni, D., Sepulchre, P., 2021. Tectonics, climate and the diversification of the tropical African terrestrial flora and fauna. Biol. Rev. 96, 16–51. https://doi.org/10.1111/brv.12644.
Daveau, S., 1959. Recherches morphologiques sur la région de Bandiagara. Mém. Inst. Fr. Afr. Noire 56, 1–120.
Daveau, S., 1960. Les plateaux du Sud-Ouest de la Haute-Volta. Trav. Dép. Géogr. Fac. Lett. Sci. Hum. Dakar 7, 1–63.
Daveau, S., 1962. Principaux types de paysages morphologiques des plaines et plateaux soudanais dans l'Afrique de l'Ouest. Inf. Géogr. 26, 61–72. https://doi.org/10.3406/ingeo.1962.2136.
Daveau, S., 1971. Étude morphologique des Monts Loma. Mém. Inst. Fr. Afr. Noire 86, 24–60.
Daveau, S., Michel, P., 1969. Le relief du Tagant (Mauritanie). Rev. Géogr. Phys. Géol. Dyn. 11, 189–210.
Daveau, S., Lamotte, M., Rougerie, G., 1962. Cuirasses et chaines birrimiennes en Haute-Volta. Ann. Géogr. Fr. 387, 260–282. https://doi.org/10.3406/geo.1962.16250.
de Chételat, E., 1928. Notes d'un voyage géologique au Dahomey et en Haute Volta. Rev. Géogr. Phys. Géol. Dyn. I, 71–87.
de Chételat, E., 1938. Le modelé latéritique de l'Ouest de la Guinée française. Rev. Géogr. Phys. Géol. Dyn. XI 1–120.
De Putter, T., Ruffet, G., 2020. Supergene manganese ore records 75 Myr-long Campanian to Pleistocene geodynamic evolution and weathering history of the Central African Great Lakes Region – Tectonics drives, climate assists. Gondwana Res. 83, 96–117. https://doi.org/10.1016/j.gr.2020.01.021.
De Swardt, A.M.J., 1956. Recent erosion surfaces on the Jos Plateau. 3rd Int. W. Afr. Conf. 180–186.
De Swardt, A.M.J., 1964. Lateritisation and landscape development in parts of Equatorial Africa. Z. Geomorph. N.F. 8, 313–333.
Delvigne, J., Grandin, G., 1969. Étude des cycles morphogénétiques et tentative de chronologie paléoclimatique dans la région granitique de Toumodi, en Côte d'Ivoire. CR Acad. Sci. Paris 269, 1372–1375.
deMenocal, P.B., 2004. African climate change and faunal evolution during the Pliocene–Pleistocene. Earth Planet. Sci. Lett. 220, 3–24. https://doi.org/10.1016/S0012-821X(04)00003-2.
Dewolf, Y., Joly, F., Raynal, R., Rougerie, G., 1972. Premières observations sur une traversée du Sahara central. Bull. Ass. Géogr. Fr. 399, 190–211.
Doucouré, C.M., de Wit, M.J., 2003. Old inherited origin for the present near-bimodal topography of Africa. J. Afr. Earth Sci. 36, 371–388. https://doi.org/10.1016/S0899-5362(03)00019-8.
Dresch, J., 1959. Notes sur la géomorphologie de l'Aïr. Bull. Ass. Géogr. Fr. 280–281, 2–20.
Dresch, J., 1961. Plaines et "Eglab" de Mauritanie. Bull. Ass. Géogr. Fr. 299–300, 130–142.
Dresch, J., Rougerie, G., 1960. Observations morphologiques dans le Sahel du Niger. Rev. Géomorph. Dyn. 11, 49–58.
Du Preez, J.W., 1956. Origin, classification and distribution of Nigerian laterites. 3rd Int. W. Afr. Conf. 23–34.
Egbogah, E.O., 1975. Height distribution of West African bauxites as an index of Neogene tectonism. J. Nigerian Min. Geol. Metall. Soc. 10, 1–14.
Eggleton, R.A., Pain, C.F., Scott, K., 2008. Glossary of regolith terms. In: Scott, K., Pain, C.F. (Eds.), Regolith Science. Springer, CSIRO Publishing, Dordrecht, Collinwood, pp. 409–432.
Embrechts, J., Dedapper, M., 1987. Morphology and genesis of hillslope pediments in the Febe area (South-Cameroon). Catena 14, 31–43. https://doi.org/10.1016/s0341-8162(87)80004-8.
Erhardt, J., 1955. "Biostasie" and "rhexistasie". Esquisse d'une théorie sur le rôle de la pédogenèse en tant que phénomène géologique. CR Acad. Sci. Paris 241, 1218–1220.
Eschenbrenner, V., 1969. Étude géomorphologique et pédologique de la région de Tanda (Côte d'Ivoire). Rapport ORSTOM No. 4/69. https://www.documentation.ird.fr/hor/fdi:13603.
Eschenbrenner, V., 1978. Étude pédologique de la région d'Odienné (Côte d'Ivoire). Carte des paysages morphopédologiques, Feuille Odienné à 1/50 000. Not. Expl. ORSTOM 74, 1–123. https://www.documentation.ird.fr/hor/fdi:10004.
Eschenbrenner, V., 1988. Les glébules des sols de Côte d'Ivoire. Nature et origine en milieu ferrallitique, modalités de leur concentration, rôle des termites. Trav. Doc. ORSTOM 39, 1–780. https://www.documentation.ird.fr/hor/fdi:24932.
Eschenbrenner, V., Grandin, G., 1970. La séquence de cuirasses et ses différentiations entre Agnibiléfrou (Côte d'Ivoire) et Diébougou (Haute-Volta). Cah. ORSTOM Sér. Géol. 2, 205–246. https://www.documentation.ird.fr/hor/fdi:20685.
Fabre, J., 2005. Géologie du Sahara occidental et central. Tervuren Afr. Geosci. Coll. 108, 1–572. https://www.africamuseum.be/en/research/discover/publications/open-access/geology.
Fabre, J., Arnaud-Vanneau, A., Belhadj, Z., Monod, T., 1996. Évolution des terrains méso-cénozoïques d'une marge à l'autre du craton ouest africain, entre le Tanezrouft (Algérie) et l'Adrar de Mauritanie. Mém. Serv. Géol. Alg. 8, 187–229.
Fairbridge, R.W., Finkl, C.W., 1980. Cratonic erosional unconformities and peneplains. J. Geol. 88, 69–86. https://doi.org/10.1086/628474.
Faure, P., Volkoff, B., 1989. Les couvertures pédologiques polygénétiques des régions soudano-guinéennes de l'Afrique de l'Ouest. Caractères et organisation spatiale des sols du nord-est Togo sur socle granito- gneissique. In: Soltrop 89 : Actes du Premier Séminaire Franco-Africain de Pédologie Tropicale, Lomé, 6-12 Février 1989, (Colloques et Séminaires). ORSTOM, Paris, pp. 117–142. https://www.documentation.ird.fr/hor/fdi:27288.
Fölster, H., 1964. Morphogenese der südsudanesischen Pediplane. Z. Geomorph. N. F. 8, 393–423.
Fölster, H., 1969a. Late Quaternary erosion in SW-Nigeria. Bull. Ass. Sén. Ét. Quat. Ouest Afr. 21, 29–35.
Fölster, H., 1969b. Slope development in SW-Nigeria during late Pleistocene and Holocene. Göttinger Bodenkdl. Ber. 10, 3–56.
Fölster, H., Moshrefi, N., Ojenuga, A.G., 1971a. Ferralitic pedogenesis on metamorphic rocks, SW-Nigeria. Pédologie XXI,, 95–124.
Fölster, H., Kalk, E., Moshrefi, N., 1971b. Complex pedogenesis of ferrallitic savanna soils in South Sudan. Geoderma 6, 135–149. https://doi.org/10.1016/0016-7061(71)90030-.
Fritsch, P., 1969. Note préliminaire sur la morphologie du piedmont nord de l'Adamaoua dans la région de Kontcha. Ann. Fac. Sci. Cameroon 3, 101–111.
Fritsch, P., 1978. Chronologie relative des formations cuirassées et analyse géographique des facteurs de cuirassement au Cameroun. Trav. Doc. Géogr. Trop. 33, 114–132. https://www.persee.fr/doc/tlgpa_0249-647x_1978_num_2_1_874.
Gaskin, A.R.J., 1975. Investigation of the residual iron ores of Tonkolili district, Sierra Leone. Trans. Inst. Min. Metal. Sect. B B98–B119.
Gavaud, M., 1977. Les grands traits de la pédogenèse au Niger méridional. Trav. Doc. ORSTOM 76, 1–102. https://www.documentation.ird.fr/hor/fdi:09010.
Gavaud, M., Boulet, R., 1967. Carte pédologique de reconnaissance de la République du Niger à 1/500 000 (Niamey, Maradi, Zinder). https://horizon.documentation.ird.fr/exl-doc/pleins_textes/divers15-05/29233.pdf.
Gouiza, M., Bertotti, G., Andriessen, P.A.M., 2018. Mesozoic and Cenozoic thermal history of the Western Reguibat Shield (West African Craton). Terra Nova 30, 135–145. https://doi.org/10.1111/ter.12318.
Gouiza, M., Bertotti, G., Charton, R., Haimoudane, K., Dunkl, I., Anczkiewicz, A.A., 2019. New evidence of 'anomalous' vertical movements along the hinterland of the Atlantic NW African margin. J. Geophys. Res. Solid Earth 124, 13333–13353. https://doi.org/10.1029/2019JB017914.
Grandin, G., 1976. Aplanissements cuirassés et enrichissement des gisements de manganèse dans quelques régions d'Afrique de l'Ouest. Mém. ORSTOM 82, 1–276. https://www.documentation.ird.fr/hor/fdi:08271.
Grandin, G., 2008. Les cuirasses latéritiques - aluminisation et ferruginisation. In: Dewolf, Y., Bourrié, G. (Eds.), Les Formations Superficielles. Genèse - Typologie - Classification - Paysages et Environnements - Ressources et Risques. Ellipses, Paris, pp. 362–372.
Grandin, G., Hayward, D.F., 1975. Aplanissements cuirassés de la péninsule de Freetown (Sierra Leone). Cah. ORSTOM Sér. Géol. 7, 11–16. https://www.documentation.ird.fr/hor/fdi:20095.
Grandin, G., Joly, F., 2008. Glacis - Genèse, dynamique et formations corrélatives. In: Dewolf, Y., Bourrié, G. (Eds.), Les Formations Superficielles. Genèse - Typologie - Classification - Paysages et Environnements - Ressources et Risques. Ellipses, Paris, pp. 201–216.
Grandin, G., Thiry, M., 1983. Les grandes surfaces continentales tertiaires des régions chaudes. Succession des types d'altération. Cah. ORSTOM Sér. Géol. 13, 3–18. https://www.documentation.ird.fr/hor/fdi:03264.
Greigert, J., 1966. Description des formations crétacées et tertiaires du bassin des Iullemeden (Afrique occidentale). Publ. Dir. Min. Géol. Rép. Niger 2, 1–234.
Grimaud, J.L., Chardon, D., Beauvais, A., 2014. Very long-term incision dynamics of big rivers. Earth Planet. Sci. Lett. 405, 74–84. https://doi.org/10.1016/J.Epsl.2014.08.021.

Grimaud, J.-L., Chardon, D., Metelka, V., Beauvais, A., Bamba, O., 2015. Neogene cratonic erosion fluxes and landform evolution processes from regional regolith mapping (Burkina Faso, West Africa). Geomorphology 241, 315–330. https://doi.org/10.1016/j.geomorph.2015.04.006.
Grimaud, J.L., Rouby, D., Chardon, D., Beauvais, A., 2018. Cenozoic sediment budget of West Africa and the Niger delta. Basin Res. 30, 169–186. https://doi.org/10.1111/bre.12248.
Guillocheau, F., Chelalou, R., Linol, B., Dauteuil, O., Robin, C., Mvondo, F., Callec, Y., Colin, J.-P., 2015. Cenozoic landscape evolution in and around the Congo Basin: Contraints from sediments and planation surfaces. In: de Wit, M.J., Guillocheau, F., de Wit, M.C.J. (Eds.), Geology and Resource Potential of the Congo Basin. Springer-Verlag, Berlin Heidelberg, pp. 271–313.
Guillocheau, F., Simon, B., Baby, G., Bessin, P., Robin, C., Dauteuil, O., 2018. Planation surfaces as a record of mantle dynamics: the case example of Africa. Gondwana Res. 53, 82–98. https://doi.org/10.1016/j.gr.2017.05.015.
Gunnell, Y., 2003. Radiometric ages of laterites and constraints on long-term denudation rates in West Africa. Geology 31, 131–134. https://doi.org/10.1130/0091-7613(2003)031<0131:Raolac>2.0.Co;2.
Hall, A.M., Thomas, M.F., Thorp, M.B., 1985. Late Quaternary alluvial placer development in the humid tropics. The case of the Birim diamond placer, Ghana. J. Geol. Soc. 142, 777–787. https://doi.org/10.1144/gsjgs.142.5.0777.
Heinrich, J., 1992. Pediments in the Gongola basin, NE-Nigeria, development and recent morphodynamics. Z. Geomor. N. F. 91, 135–147.
Heller, B.M., Riffel, S.B., Allard, T., Morin, G., Roig, J.-Y., Couëffé, R., Aertgeerts, G., Derycke, A., Ansart, C., Pinna-Jamme, R., Gautheron, C., 2022. Reading the climate signals hidden in bauxite. Geochimica et Cosmochimica Acta 323, 40–73. https://doi.org/10.1016/j.gca.2022.02.01.
Hieronymous, B., 1972. Étude géologique de quelques types d'altérations dans l'Ouest du Cameroun. Ann. Fac. Sci. Cameroon 10, 39–68.
Hieronymous, B., 1973. Étude minéralogique et géochimique des formations bauxitiques de l'ouest du Cameroun. Cah. ORSTOM Sér. Géol. V 97–112. https://www.documentation.ird.fr/hor/fdi:19913.
Hilton, T.E., 1963. The geomorphology of North-Eastern Ghana. Z. Geomorph. N.F. 7, 308–325.
Hubert, H., 1908. Mission scientifique au Dahomey. Émile Larose Librairie-Éditeur, Paris. https://iris.univ-lille.fr/handle/1908/3038.
Jacobberger, P.A., 1987. Geomorphology of the upper Inland Niger Delta. J. Arid Environ. 13, 95–112. https://doi.org/10.1016/S0140-1963(18)31129-7.
Jaeger, P., 1953. Contribution à l'étude du modelé de la dorsale guinéenne. Les Monts Loma. Rev. Géomor. Dyn. IV, 105–113.
Jean, A., Beauvais, A., Chardon, D., Arnaud, N., Jayananda, M., Mathe, P.E., 2019. Weathering history and landscape evolution of Western Ghats (India) from 40Ar-39Ar Ar dating of supergene K–Mn oxides. J. Geol. Soc. 177, 523–536. https://doi.org/10.1144/jgs2019-048.
Jodot, P., 1933. Étude de quelques roches latéritiques de la vallée du Niger (Soudan occidental français). Bull. Soc. Géol. France 5 (III), 619–656.
Jodot, P., Rouaix, S., 1957. Découvertes de mollusques continentaux de l'Aquitanien et du Villafranchien au Sahara Mauritanien et soudanais. C.R. Som. Soc. Géol. Fr. 16, 375–377.
Junge, B., Skowronek, A., 2007. Genesis, properties, classification and assessment of soils in Central Benin, West Africa. Geoderma 139, 357–370. https://doi.org/10.1016/j.geoderma.2007.02.015.
Kadomura, H., Hori, N., 1978. Some notes on the landforms and superficial deposits in the forest and savanna zones of inland Cameroon. J. Geogr. 87, 349–367. https://doi.org/10.5026/jgeography.87.6_349.
Kadomura, H., Hori, N., 1990. Environmental implications of slope deposits in humid tropical Africa: evidence from Southern Cameroon and Western Kenya. Geogr. Rep. Tokyo Metrop. Univ. 25, 213–236. https://tokyo-metro-u.repo.nii.ac.jp/?action=pages_view_main&active_action=repository_view_main_item_detail&item_id=2875&item_no=1&page_id=30&block_id=164.
Khalaf, F.I., Thiry, M., Milnes, A., Alnaqi, R., 2020. Characterization of chert in the Dammam Formation (Eocene), Kuwait: Clues to groundwater silicification processes. J. Sediment. Res. 90, 297–312. https://doi.org/10.2110/jsr.2020.18.
King, L.C., 1948. On the ages of the African land-surfaces. Q. J. Geol. Soc. Lond. 104, 439–459.
King, L.C., 1962. The Morphology of the Earth. Oliver and Boyd, London, Edinburgh.
Kogbe, C.A., 1978. Origin and composition of the ferruginous oolites and laterites of Northwestern Nigeria. Geol. Rundsch. 67, 662–667.
Lamotte, M., Rougerie, G., 1952. Coexistence de trois types de modelé dans les chaînes quartzitiques du Nimba et du Simandou. Ann. Géogr. 61, 432–442. https://doi.org/10.3406/geo.1952.14001.
Lappartient, J.R., Nahon, D., 1970. Les formations cuirassées sur les grès argileux tertiaires du bassin sénégalo-mauritanien (bordures centrale et septentrionale). Ann. Fac. Sci. Marseille XLIV 213–227.
Le Cocq, A., 1986. Carte pédologique et carte des capacités agronomiques des sols à 1/100 000, Région de Bassar (Togo). Not. Expl. ORSTOM 102, 1–103. https://www.documentation.ird.fr/hor/fdi:31639.
Leclerc, J.C., Lamotte, M., Richard-Molard, J., 1949. Niveaux et cycles d'érosion dans le massif du Nimba. C.R. Acad. Sci. Paris 228, 1510–1512.
Leclerc, J.C., Richard-Molard, J., Lamotte, M., Rougerie, G., Portères, R., 1955. La chaîne du Nimba. Essai géographique. La réserve naturelle intégrale des Monts Nimba - Fasc. III. Mém. Inst. Fr. Afr. Noire 43, 1–171.
Lefranc, J.P., 1991. Alum deposits of Fezzan and the Sahara : their origin, distribution and importance. In: Geology of Lybia. Elsevier, pp. 2605–2618.
Leprêtre, R., Missenard, Y., Barbarand, J., Gautheron, C., Saddiqi, O., Pinna-Jamme, R., 2015. Postrift history of the eastern central Atlantic passive margin: insights from the Saharan region of South Morocco. J. Geophys. Res. Solid Earth 120, 4645–4666. https://doi.org/10.1002/2014JB011549.
Leprun, J.C., 1977. Géochimie de la surface et formes du relief. IV - La dégradation des cuirasses ferrigineuses. Étude et importance du phénomène en Afrique de l'Ouest. Sci. Géol. Bull. 30, 265–273. https://doi.org/10.3406/sgeol.1977.1522.
Leprun, J.C., 1979. Les cuirasses ferrugineuses des pays cristallins de l'Afrique occidentale sèche. Genèse, transformation, dégradation. Sci. Géol. Mém. 58, 1–224. https://www.persee.fr/doc/sgeol_0302-2684_1979_mon_58_1.
Lévêque, A., 1979a. Carte pédologique du Togo à 1/200 000. Socle granito-gneissique limité à l'ouest et au nord par les Monts Togo. Not. Expl. ORSTOM 82, 1–77. https://www.documentation.ird.fr/hor/fdi:01782.
Lévêque, A., 1979b. Pédogenèse sur le socle granito-gneissique du Togo. Différenciation des sols et remaniements superficiels. Trav. Doc. ORSTOM 108, 1–224. https://www.documentation.ird.fr/hor/fdi:09868.
Lihoreau, F., Sarr, R., Chardon, D., Boisserie, J.-R., Lebrun, R., Adnet, S., Martin, J.E., Pallas, L., Sambou, B., Tabuce, R., Thiam, M.M., Hautier, L., 2021. A fossil terrestrial fauna from Tobène (Senegal) provides a unique early Pliocene window in western Africa. Gondwana Res. 99, 21–35. https://doi.org/10.1016/j.gr.2021.06.013.
Maignien, R., 1956. De l'importance du lessivage oblique dans le cuirassement des sols en A.O.F. VIème Congrès de la Science du Sol, Paris 76, 463–467.
Maignien, R., 1966. Review of Research on Laterites, Natural Resources Research. UNESCO, Paris.
Mamedov, V.I., Bouféév, Y., Nikitine, Y., 2010. Carte gîtologique de la Guinée à 1/500 000. In: Ministère des Mines et de la Géologie, Géoprospect Ltd, Université d'États de Moscou M. Lomonossov, Conakry-Moscou.
Mamedov, V.I., Chausov, A.A., Kanishev, A.I., 2011. Formation Stages of the Unique Sangaredi Bauxite-Bearing Group, Futa Jallon-Mandingo Province, West Africa. Geol. Ore Deposits 53, 177–201. https://doi.org/10.1134/s1075701511030044.
Mamedov, V.I., Chausov, A.A., Okonov, E.A., Makarova, M.A., Boeva, N.M., 2020. The world's largest Fouta Djallon–Mandingo Bauxite Province (West Africa): Part I. Background. Geol. Ore Deposits 62, 163–176. https://doi.org/10.1134/S1075701520020026.
Mamedov, V.I., Makarova, M.A., Boeva, N.M., Vnuchkov, D.A., Bortnikov, N.S., 2021. The World's Largest Fouta Djallon–Mandingo Bauxite Province (West Africa): Part 2. The effect of Parent Rock Composition on the Abundance and Quality of Bauxites. Geol. Ore Deposits 63, 599–624. https://doi.org/10.1134/S1075701521050044.
Mamedov, V.I., Makarova, M.A., Zaitsev, V.A., 2022. The World's Largest Fouta Djallon–Mandingo Bauxite Province (West Africa): Part III. The Influence of Geomorphic Factors and the Age of Relief on the Spatial Distribution, Size, and Quality of Bauxite Deposits. Geol. Ore Deposits 64, 15–42. https://doi.org/10.1134/S1075701522090057.
Martin, D., 1966. Études pédologiques dans le Centre Cameroun (Nanga-Eboko à Bertoua). Mém. ORSTOM. Mém. ORSTOM 19, 1–162. https://www.documentation.ird.fr/hor/fdi:11474.
Martin, D., 1967. Géomorphologie et sols ferralitiques dans le Centre-Cameroun. Cah. ORSTOM Sér. Pédol. 2, 189–218. https://www.documentation.ird.fr/hor/fdi:18350.
Martin, D., 1970. Quelques aspects des zones de passage entre surfaces d'aplanissement du Centre-Cameroun. Cah. ORSTOM Sér. Pédol. VIII, 119–241. https://www.documentation.ird.fr/hor/fdi:18411.
Mathian, M., Aufort, J., Braun, J.-J., Riotte, J., Selo, M., Balan, E., Fritsch, E., Bhattacharya, S., Allard, T., 2019. Unraveling weathering episodes in Tertiary regoliths by kaolinite dating (Western Ghats, India). Gondwana Res. 69, 89–105. https://doi.org/10.1016/j.gr.2018.12.00.
McFarlane, M.J., 1976. Laterite and Landscape. Academic Press, London, New York.
Mensching, H., 1966. Flächenbildung in der Sudan-und Sahel-Zone (Ober-Volta und Niger). Z. Geomorph. N.F. 10, 1–29.
Meyer, B., 1992. A detailed soil differentiation of slopes with slight inclination in the Niamtougou plain in North-Togo. Z. Geomorph. N.F. 91, 124–134.
Michel, P., 1959. L'évolution géomorphologique des bassins du Sénégal et de la Haute-Gambie, ses rapports avec la prospection minière. Rev. Géomorph. Dyn. 10, 117–143.
Michel, P., 1969. Les grandes étapes de la morphogenèse dans les bassins des fleuves Sénégal et Gambie pendant le Quaternaire. Bull. Inst. Fr. Afr. Noire 31, 293–324.
Michel, P., 1973a. Les bassins des fleuves Sénégal et Gambie, étude géomorphologique. Mém. ORSTOM 63, 1–752. https://www.documentation.ird.fr/hor/fdi:06464.
Michel, P., 1973b. Recherches sur les cuirasses ferrugineuses en Afrique. 1- Mission au Cameroun. Bull. Ass. Sén. Ét. Quat. Ouest Afr. 39, 61–64.
Michel, P., 1977a. L'évolution géomorphologique de la Mauritanie méridionale et centrale. Problèmes des revêtements latéritiques, cuirasses ferrugineuses et croûtes calcaires. L'influence des variations du climat. Finisterra. Rev. Port. Geogr. 12, 5–27.
Michel, P., 1977b. Les modelés et dépôts du Sahara méridional et Sahel et du sud-ouest africain. Essai de comparaison. Rech. Géogr. Strasbourg 5, 5–39.
Michel, P., 1978. Cuirasses bauxitiques et ferrugineuses d'Afrique occidentale. Aperçu chronologique. Trav. Doc. Géogr. Trop. 33, 12–32.
Michel, P., 1980. The Southwestern Sahara margin: Sediments and climatic change during the recent Quaternary. Palaeoecol. Afr. 12, 297–314.
Millot, G., 1970. The Geology of Clays. Springer-Verlag, Berlin.
Millot, G., 1980. Les grands aplanissements des socles continentaux dans les pays subtropicaux, tropicaux et désertiques. Mém. h. sér. Soc. Géol. Fr. 10, 295–305.
Millot, G., 1983. Planation of continents by intertropical weathering and pedogenetic processes. IInd International Seminar on lateritisation processes, Sao Paulo, Brazil, July 4-12 1982, pp. 53–63.
Misra, A., Raucq, P., 1986. Itabirites et minerais de fer des Monts Nimba. Bull. Séances Acad. Roy. Sci. Outre-Mer 30, 285–301.
Momo Nouazi, M., Yemefack, M., Tematio, P., Beauvais, A., Ambrosi, J.-P., 2016. Distribution of duricrusted bauxites and laterites on the Bamiléké plateau (West

Cameroon): constraints from GIS mapping and geochemistry. Catena 140, 15–23. https://doi.org/10.1016/j.catena.2016.01.010.
Momo Nouazi, M., Beauvais, A., Tematio, P., Yemefack, M., 2020. Differentiated Neogene bauxitization of volcanic rocks (western Cameroon): morpho-geological constraints on chemical erosion. Catena 194, 104685. https://doi.org/10.1016/j.catena.2020.104685.
Morel, A., 1981. Formes, formations superficielles et variations climatiques récentes dans les massifs centraux de l'Aïr (Sud-Sahara). Palaeoecol. Afr. 13, 189–198.
Morel, A., 1985. Les hauts massifs de l'Aïr (Niger) et leurs piedmonts. Étude géomorphologique (Doctorat es Science thesis). Université Scientifique et Médicale de Grenoble, Grenoble, France.
Morin, S., 1987. Cuirasses et reliefs de l'ouest Cameroun. In: Séminaire Régional sur les Latérites : Sols, Matériaux, Minerais : Sessions 1 et 3, Douala (1986). ORSTOM, pp. 107–118. https://www.documentation.ird.fr/hor/fdi:25825.
Morin, S., 1989. Hautes terres et bassins de l'ouest camerounais. Étude géomorphologique (Doctorat es Science thesis). Université, Bordeaux III, Talence.
Moss, R.P., 1965. Slope development and soil morphology in a part of South-West Nigeria. J. Soil Sci. 16, 192–209. https://doi.org/10.1111/j.1365-2389.1965.tb01432.x.
Moundi, A., Wandji, P., Bardintzeff, J.-M., Ménard, J.-J., Okomo Atouba, L.C., Mouncherou, O.F., Reusser, É., Bellon, H., Tchoua, F.M., 2007. Les basaltes éocènes à affinité transitionnelle du plateau Bamoun, témoins d'un réservoir mantellique enrichi sous la ligne volcanique du Cameroun. C.R. Geoscience 339, 396–406. https://doi.org/10.1016/j.crte.2007.04.001.
Nahon, D., 1971. Genèse et évolution des cuirasses ferrugineuses quaternaires sur grès : exemple du massif de Ndias (Sénégal occidentale). Bull. Serv. Carte. géol. Als. Lorr. 14, 219–241. https://www.persee.fr/doc/sgeol_0037-2560_1971_num_24_4_1393.
Nahon, D., 1976. Cuirasses ferrugineuses et encroûtements calcaires au Sénégal occidental et en Mauritanie. Systèmes évolutifs : Géochimie, structures, relais et coexistence. Sci. Géol. Mém. 44, 1–221. https://www.persee.fr/doc/sgeol_0302-2684_1976_mon_44_1.
Nahon, D., 1980. Soil accumulations and climatic variations in Western Sahara. Palaeoecol. Afr. 12, 63–68.
Nahon, D., 1986. Evolution of iron crusts in tropical landscapes. In: Colman, S.M., Dethier, D.P. (Eds.), Rates of Chemical Weathering of Rocks and Minerals. Academic Press, Orlando, pp. 169–191.
Nahon, D., Millot, G., 1977. Géochimie de la surface et formes du relief V. Enfoncement géochimique des cuirasses ferrugineuses par épigénie du manteau d'altération des roches mères gréseuses. Influence sur le paysage. Sci. Géol. Bull. 30, 275–282. https://doi.org/10.3406/sgeol.1977.1523.
Nahon, D., Ruellan, A., Millot, G., 1973. Accumulations calcaires et ferrugineuses dans la marge occidentale du Sénégal, de la Mauritanie et du Maroc. Rapport sur la mission multidisciplinaire de janvier 1973. Bull. Ass. Sén. Ét. Quat. Ouest Afr. 39, 43–55.
Nahon, D., Janot, C., Karpoff, A.M., Paquet, H., Tardy, Y., 1977a. Mineralogy, petrography and structures of iron crusts (ferricretes) developed on sandstones in the western part of Senegal. Geoderma 19, 263–277. https://doi.org/10.1016/0016-7061(77)90069-6.
Nahon, D., Millot, G., Paquet, H., Ruellan, A., Tardy, Y., 1977b. Géochimie de la surface et formes du relief VII. Digestion et effacement des cuirasses ferrugineuses par des encroûtements calcaires en pays aride, Sahara de Mauritanie. Sci. Géol. Bull. 30, 289–296. https://doi.org/10.3406/sgeol.1977.1525.
Njonfang, E., Nono, A., Kamgang, P., Ngako, V., Tchoua, F.M., 2011. Cameroon Line alkaline magmatism (central Africa): a reappraisal. Geol. Soc. Am. Spec. Pap. 478, 173–191. https://doi.org/10.1130/2011.2478(09).
Nye, P.H., 1954. Some soil-forming processes in the humid tropics: I - a field study of a catena in the West African forest. J. Soil Sci. 5, 7–21. https://doi.org/10.1111/j.1365-2389.1954.tb02171.x.
Ollier, C.D., 1960. The inselbergs of Uganda. Z. Geomorph. N. F. 9, 285–304.
Ouangrawa, M., Grandin, G., Parisot, J.-C., Baras, E., 1996. Dispersion mécanique de l'or dans les matériaux de surface : exemple du site aurifère de Piéla (Burkina-Faso). Pangea 25, 25–40. https://www.documentation.ird.fr/hor/fdi:010009482.
Pain, C.F., 2008. Regolith description and mapping. In: Scott, K.M., Pain, C.F. (Eds.), Regolith Science. Springer, CSIRO Publishing, Dordrecht, Collinwood, pp. 281–305.
Pallister, J.W., 1956. Slope development in Buganda. Geogr. J. 122, 80–87. https://doi.org/10.2307/1791478.
Parisot, J.-C., Ventose, V., Grandin, G., Bourges, F., Debat, P., Tollon, F., Millot, L., 1995. Dynamique de l'or et d'autres minéraux lourds dans un profil d'altération cuirassé du Burkina Faso (Afrique de l'Ouest). Intérêt pour l'interprétation de la mise en place des matériaux constituant les cuirasses de haut-glacis. CR Acad. Sci. Paris 301, 295–302. https://www.documentation.ird.fr/hor/fdi:43155.
Pascual, J.F., 1988. Les sols actuels et les formations superficielles des crêtes nord-est du Nimba (Guinée). Contribution à l'étude géomorphologique du Quaternaire de la chaîne. Cah. ORSTOM Sér. Pédol. 24, 137–162. https://www.documentation.ird.fr/hor/fdi:27181.
Pédro, G., Kilian, J., 1986. Pedologic work and studies of physical environments carried out by French research organizations for the development of tropical regions. In: Seminar on French Agronomic Research in the Tropics, 15-16 May 1986, Washington. World Bank, pp. 5–65. https://horizon.documentation.ird.fr/exl-doc/pleins_textes/divers07/24239.pdf.
Pélissier, P., Rougerie, G., 1953. Problèmes morphologiques dans le bassin de Siguiri (Haut Niger). Bull. Inst. Fr. Afr. Noire 15, 1–47.
Pèltre, P., 1977. Le "V Baoulé" (Côte d'Ivoire centrale). Héritage géomorphologique et paléoclimatique dans le tracé du contact forêt - savane. Trav. Doc. ORSTOM 80, 1–198. https://www.documentation.ird.fr/hor/fdi:09307.
Pèltre, P., 1979. Carte des paysages géomorphologiques, Feuille Makono, 1/200 000. Not. Expl. ORSTOM. https://www.documentation.ird.fr/hor/fdi:09823.
Peulvast, J.-P., Claudino Sales, V., Bétard, F., Gunnell, Y., 2008. Low post-Cenomanian denudation depths across the Brazilian Northeast: implications for long-term landscape evolution at a transform continental margin. Glob. Planet. Chang. 62, 39–60. https://doi.org/10.1016/j.gloplacha.2007.11.005.
Picart, C., Dauteuil, O., Pickford, M., Owono, F.M., 2020. Cenozoic deformation of the south African plateau, Namibia: insights from planation surfaces. Geomorphology 350, 106922. https://doi.org/10.1016/j.geomorph.2019.106922.
Poss, R., 1982. Étude morphopédologique de la région de Katiola (Côte d'Ivoire). Not. Expl. ORSTOM 94, 1–142. https://www.documentation.ird.fr/hor/fdi:02387.
Poss, R., 1996. Étude morphopédologique du nord du Togo à 1/500 000. Not. Expl. ORSTOM 109, 1–143. https://www.documentation.ird.fr/hor/fdi:010005399.
Pougnet, R., 1949. Stratigraphie et identification des formations continentales du Moyen Niger et du Haut-Dahomey. Bull. Soc. Géol. Fr. 5 (XIX), 493–498. https://doi.org/10.2113/gssgfbull.S5-XIX.4-6.493.
Prasad, G., 1983. A review of the early Tertiary bauxite event in South America, Africa and India. J. Afr. Earth Sci. 1, 305–313.
Radier, H., 1959. Contribution à l'étude géologique du Soudan oriental. Deuxième partie : le bassin crétacé et tertiaire de Gao. Bull. Serv. Géol. Prosp. Min. A.O.F. 26 (2), 327–556.
Raunet, M., 1985. Bas-fonds et riziculture en Afrique. Approche structurale comparative. Agron. Trop. 40, 181–201. https://agritrop.cirad.fr/426885/.
Réformatsky, N., 1935. Quelques observations sur les latérites et les roches ferruginisées de l'ouest de la colonie du Niger français. Bull. Soc. Géol. Fr. 37, 575–589.
Retallack, G.J., 2010. Lateritization and bauxitization events. Econ. Geol. 105, 655–667. https://doi.org/10.2113/gsecongeo.105.3.655.
Rognon, P., 1967. Le Massif de l'Atakor et ses bordures. Étude géomorphologique. Éditions du CNRS, Paris.
Rognon, P., Gourinard, Y., Bandet, Y., Koeniguer, J.C., Delteildesneux, F., 1983. Précisions chronologiques sur l'évolution volcano-tectonique et géomorphologique de l'Atakor (Hoggar): Apport des données radiométriques (K/Ar) et paléobotaniques (bois fossiles). Bull. Soc. Géol. Fr. 25, 973–980. https://doi.org/10.2113/gssgfbull.S7-XXV.6.973.
Rohdenburg, H., 1969. Hangpedimentation and klimawechsel als wichtigste faktoren der flächen- und stufenbildung in den wechselfeuchten tropen an beispielen aus Westafrica, besonders aus dem schichtstufenland Südost-Nigerias. Göttinger Bodenkdl. Ber. 10, 57–133.
Rougerie, G., 1961. Modelés et dynamiques de savanes en Guinée orientale. Ét. Afr. 4, 24–50.
Rougier, S., Missenard, Y., Gautheron, C., Barbarand, J., Zeyen, H., Pinna, R., Liegeois, J. P., Bonin, B., Ouabadi, A., Derder, M.E., de Lamotte, D.F., 2013. Eocene exhumation of the Tuareg Shield (Sahara Desert, Africa). Geology 41, 615–618. https://doi.org/10.1130/g33731.1.
Sanfo, Z., Grandin, G., Parisot, J.-C., Pale, F., 1992. Aplanissements latéritisés anciens, glacis récents et indices d'or dans la région d'Aribinda (Burkina Faso). In: Schmitt, J. M., Gall, Q. (Eds.), Mineralogical and Geochemical Records of Paleoweathering. ENSPM Mém. Sci, Terre, Paris, pp. 15–30.
Sanfo, A., Colin, F., Delaune, M., Boulangé, B., Parisot, J.C., Bradley, R., Bratt, J., 1993. Gold: a useful tracer in sub-Sahelian laterites. Chem. Geol. 107, 323–326. https://doi.org/10.1016/0009-2541(93)90201-S.
Sawadogo, B., Bamba, O., Chardon, D., 2020. Landform-regolith mapping in the West African context. Ore Geol. Rev. 126, 103782 https://doi.org/10.1016/j.oregeorev.2020.103782.
Schnell, R., 1946. Note préliminaire sur les sols des Monts Niba (Afrique Occidentale française). CR Acad. Sci. Paris 222, 807–808.
Schnell, R., 1948. Le modelé des Monts Nimba (A.O.F) dans ses rapports avec les sols et l'évolution de la végétation. C.R. Acad. Sci. Paris 57, 213–218.
Schwarz, T., 1994. Ferricrete formation and relief inversion: an example from Central Sudan. Catena 21, 257–268. https://doi.org/10.1016/0341-8162(94)90016-7.
Schwarz, T., 1997. Distribution and genesis of bauxite on the Mambilla Plateau. SE Nigeria. Appl. Geochem. 12, 119–131. https://doi.org/10.1016/s0883-2927(96)00058-3.
Ségalen, P., 1967. Les sols et la géomorphologie du Cameroun. Cah. ORSTOM Sér. Pédol. 5, 137–187. https://www.documentation.ird.fr/hor/fdi:18349.
Senut, B., Pickford, M., Ségalen, L., 2009. Neogene desertification of Africa. C.R. Geoscience 341, 591–602. https://doi.org/10.1016/j.crte.2009.03.008.
Shuster, D.L., Vasconcelos, P.M., Heim, J.A., Farley, K.A., 2005. Weathering geochronology by (U-Th)/He dating of goethite. Geochim. Cosmochim. Acta 69, 659–673. https://doi.org/10.1016/j.gca.2004.07.028.
Simon, B., 2015. Rift du Lac Albert, Ouganda, Rift Est Africain : Déformation, érosion, sédimentation et bilan de matière depuis 17 Ma (Ph.D. thesis). Université de Rennes 1, Rennes. https://theses.hal.science/tel-01923327v1/file/SIMON_Brendan.pdf.
Summerfield, M.A., 1985. Plate tectonics and landscape development on the African continent. In: Morisawa, M., Hack, J.T. (Eds.), Tectonic Geomorphology. Allen & Unwin, Boston, pp. 27–51.
Tardy, Y., 1997. Petrology of Laterites and Tropical Soils. Balkema, Rotterdam.
Tardy, Y., Roquin, C., 1998. Dérive des continents, paléoclimats et altérations tropicales. Editions du BRGM, Orléans.
Tardy, Y., Kobilsek, B., Paquet, H., 1991. Mineralogical composition and geographical distribution of African and Brazilian periatlantic laterites. The influence of continental drift and tropical paleoclimates during the past 150 Myr and implications for India and Australia. J. Afr. Earth Sci. 12, 283–295. https://doi.org/10.1016/0899-5362(91)90077-c.
Teeuw, R.M., 1987. Variations in the composition of gravel layers across the landscape. Examples from Sierra Leone. Geo-Eco. Trop. 11, 151–169. https://www.geoecotrop.be/index.php?page=numero-11.

Teeuw, R.M., 1991. A catenary approach to the study of gravel layers and tropical landscape morphodynamics. Catena 18, 71–89. https://doi.org/10.1016/0341-8162(91)90008-L.
Teeuw, R.M., 2002. Regolith and diamond deposits around Tortiya, Ivory Coast, West Africa. Catena 49, 111–127. https://doi.org/10.1016/S0341-8162(02)00020-6.
Temgoua, É., Bitom, D., Bilong, P., Lucas, Y., Pfeifer, H.-R., 2002. Démantèlement des paysages cuirassés anciens en zones forestières tropicales d'Afrique centrale : formation d'accumulations ferrugineuses actuelles en bas de versant. C.R. Geoscience 334, 537–543. https://doi.org/10.1016/S1631-0713(02)01793-5.
Théveniaut, H., 2012. Recherches et applications du paléomagnétisme et du magnétisme des roches aux problématiques d'un service géologique national. Mémoire d'habilitation à diriger les recherches. Université d'Orléans, Orléans, France.
Thiry, M., Franke, C., Yao, K.F.E., Szuszkiewicz, A., Fàbrega, C., Jeleńska, M., Kądziałko-Hofmokl, M., Gurenko, A., Parcerisa, D., Sobczyk, A., Turniak, K., Aleksandrowski, P., 2023. Albitization and oxidation of Variscan granitoid rocks related to the post-Variscan paleosurface in the Sudetes (Bohemian Massif, SW Poland). Int. J. Earth Sci. 112, 951–980. https://doi.org/10.1007/s00531-022-02274-2.
Thomas, M.F., 1965. Some aspects of the geomorphology of domes and tors in Nigeria. Z. Geomorph. N.F. 9, 63–81.
Thomas, M.F., 1966. Some geomorphological implications of deep weathering patterns in crystalline rocks in Nigeria. Trans. Inst. Brit. Geogr. 40, 173–193. https://doi.org/10.2307/621576.
Thomas, M.F., 1978. Chemical denudation, lateritisation and landform development in Sierra Leone. Géo-Eco-Trop. 2, 243–264. https://www.geoecotrop.be/index.php?page=numero-2.
Thomas, M.F., 1980. Timescale of landform development on tropical shields - a study from Sierra Leone. In: Cullingford, R.A., Davidson, D.A., Lewin, J. (Eds.), Timescales in Geomorphology. John Wiley & Sons Ltd, pp. 333–354.
Thomas, M.F., 1988. Superficial deposits as resources for development — some implications for applied geomorphology. Scott. Geogr. Mag. 104, 72–83. https://doi.org/10.1080/00369228818736736.
Thomas, M.F., 1989a. The role of etch processes in landform development I. Etching concepts and their applications. Z. Geomorph. N.F. 33, 129–142. https://doi.org/10.1127/zfg/33/1989/129.
Thomas, M.F., 1989b. The role of etch processes in landform development II. Etching and the formation of relief. Z. Geomorph. N.F. 33, 257–274. https://doi.org/10.1127/zfg/33/1989/257.
Thomas, M.F., 1994. Geomorphology in the Tropics: A Study of Weathering and Denudation in Low Latitudes. Wiley & Sons, New York.
Thomas, M.F., 2012. Sources of geomorphological diversity in the tropics. Rev. Bras. Geomorfol. 12, 47–60. https://doi.org/10.20502/rbg.v12i0.258.
Thomas, M.F., Thorp, M.B., 1980. Some aspects of the geomorphological interpretation of Quaternary alluvial sediments in Sierra Leone. Z. Geomorph. N. F. 36, 140–161.
Thomas, M.F., Thorp, M.B., 1985. Environmental change and episodic etchplanation in the humid tropics of Sierra Leone: the Koidu etchplain. In: Douglas, J., Spencer, T. (Eds.), Environmental Change and Tropical Geomorphology. George Allen & Unwin, London, pp. 239–267.
Thomas, M.F., Thorp, M.B., 1992. Landscape dynamics and surface deposits arising from late Quaternary fluctuations in the forest-savanna boundary. In: Furley, P.A., Proctor, J., Ratter, J.A. (Eds.), Nature and Dynamics of Forest-Savanna Boundaries. Chapman & Hall, London, pp. 215–253.
Thomas, M.F., Thorp, M.B., Teeuw, R.M., 1985. Paleogeomorphology and the occurrence of diamondiferous placer deposits in Koidu, Sierra Leone. J. Geol. Soc. 142, 789–802. https://doi.org/10.1144/gsjgs.142.5.0789.
Tricart, J., 1958. Observations sur le façonnement des rapides des rivières intertropicales. Bull. Com. Trav. Hist. Sci. Sect. Géogr. LXXI, 289–313. https://gallica.bnf.fr/ark:/12148/bpt6k6267552z/f340.item.
Tricart, J., Michel, P., Vogt, J., 1957. Oscillations climatiques quaternaires en Afrique Occidentale. Vth INQUA Congress, Madrid-Barcelona, pp. 187–188.
Valeton, I., 1991. Bauxites and associated terrestrial sediments in Nigeria and their position in the bauxite belts of Africa. J. Afr. Earth Sci. 12, 297–310. https://doi.org/10.1016/0899-5362(91)90078-D.
Valeton, I., Beissner, H., 1986. Geochemistry and mineralogy of the Lower Tertiary in situ laterites of the Jos Plateau, Nigeria. J. Afr. Earth Sci. 5, 535–550.
van der Beek, P., Summerfield, M.A., Braun, J., Brown, R.W., Fleming, A., 2002. Modeling postbreakup landscape development and denudational history across the southeast African (Drakensberg Escarpment) margin. J. Geophys. Res. Solid Earth 107, 2351. https://doi.org/10.1029/2001JB000744.
van Mourik, D., Sao, D.K., Johnson, E.K., Harris, A.F., 1980. Land Systems of the Mano River Union Project Area of Liberia at 1:500,000 Scale, Map I. Land Resources Survey Project. FAO, Monrovia.
Vasconcelos, P.M., de Carmo, I.O., 2018. Calibrating denudation chronology through $^{40}Ar/^{39}Ar$ weathering geochronology. Earth-Sci. Rev. 179, 411–435. https://doi.org/10.1016/j.earscirev.2018.01.003.
Vasconcelos, P.M., Brimhall, G.H., Becker, T.A., Renne, P.R., 1994. Ar^{40}/Ar^{39} Analysis of supergene jarosite and alunite - Implications to the paleoweathering history of the Western USA and West-Africa. Geochim. Cosmochim. Acta 58, 401–420. https://doi.org/10.1016/0016-7037(94)90473-1.
Vasconcelos, P.M., Reich, M., Shuster, D.L., 2015. The paleoclimatic signatures of supergene metal deposits. Elements 11, 317–322. https://doi.org/10.2113/gselements.11.5.317.
Verheye, W., Pomel, R., 1984. Aspects géomorphologiques et stratigraphiques des niveaux indurés de la Basse Côte d'Ivoire. Z. Geomorph N. F. 28, 21–39.
Viennot, M., 1983. Étude pédologique de la région de Touba (Côte d'Ivoire). Not. Expl. ORSTOM 98, 1–91. https://www.documentation.ird.fr/hor/fdi:03049.
Villemur, J.R., 1967. Reconnaissance géologique et structurale du Nord du bassin de Taoudenni. Mém. BRGM 51, 1–152.
Vogt, J., 1959. Aspects de l'évolution morphologique récente de l'ouest africain. Ann. Géogr. Fr. 367, 193–206. https://doi.org/10.3406/geo.1959.16306.
Vogt, J., Black, R., 1963. Remarques sur la géomorphologie de l'Aïr. Bull. BRGM 1963, 1–29.
Vrielynck, B., Bouysse, P., 2003. The Changing Face of the Earth (with CD-Rom). Com. Geol. Map World/UNESCO, Paris.
White, R.W., 1973. Progressive metamorphism of iron-formation and associated rocks in the Wologizi Range, Liberia. U.S. Geol. Surv. Bull. 1302, 1–50.
White, F., 1986. La végétation de l'Afrique. ORSTOM, UNESCO, Paris.
Wildman, M., Webster, D., Brown, R., Chardon, D., Rouby, D., Ye, J., Huyghe, D., Dall'Asta, M., 2019. Long-term evolution of the West African transform margin: estimates of denudation from Benin using apatite thermochronology. J. Geol. Soc. 176, 97–114. https://doi.org/10.1144/jgs2018-078.
Wildman, M., Brown, R., Ye, J., Chardon, D., Rouby, D., Kouamelan, A.N., Dall'Asta, M., 2022. Contrasting thermal evolution of the West African Equatorial and Central Atlantic continental margins. Gondwana Res. 111, 249–264. https://doi.org/10.1016/j.gr.2022.08.010.
Ye, J., Chardon, D., Rouby, D., Guillocheau, F., Dall'asta, M., Ferry, J.N., Broucke, O., 2017. Paleogeographic and structural evolution of northwestern Africa and its Atlantic margins since the early Mesozoic. Geosphere 13, 1254–1284. https://doi.org/10.1130/GES01426.1.
Yongué, R., Belinga, S.M.E., 1987. Altération des gneisses migmatitiques de Yaoundé et le problème de la distribution du fer dans le paysage. In: Séminaire Régional Sur Les Latérites : Sols, Matériaux, Minerais. Douala (1986). ORSTOM, pp. 47–58. https://horizon.documentation.ird.fr/exl-doc/pleins_textes/pleins_textes_4/colloques/25821.pdf.
Zachos, J.C., Dickens, G.R., Zeebe, R.E., 2008. An early Cenozoic perspective on greenhouse warming and carbon-cycle dynamics. Nature 451, 279–283. https://doi.org/10.1038/nature06588.
Zeese, R., 1983. Reliefentwicklung in Nordost-Nigeria. Reliefgenerationen oder morphogenetische sequenzen. Z. Geomorph. N.F. 48, 225–234.
Zeese, R., 1991. Paleosols of different age in central and Northeast Nigeria. J. Afr. Earth Sci. 12, 311–318. https://doi.org/10.1016/0899-5362(91)90079-e.
Zeese, R., Schwertmann, U., Tietz, G.F., Jux, U., 1994. Mineralogy and stratigraphy of 3 deep lateritic profiles of the Jos Plateau (Central Nigeria). Catena 21, 195–214. https://doi.org/10.1016/0341-8162(94)90012-4.